

INFORMATION TO USERS

This manuscript has been reproduced from the microfilm master. UMI films the text directly from the original or copy submitted. Thus, some thesis and dissertation copies are in typewriter face, while others may be from any type of computer printer.

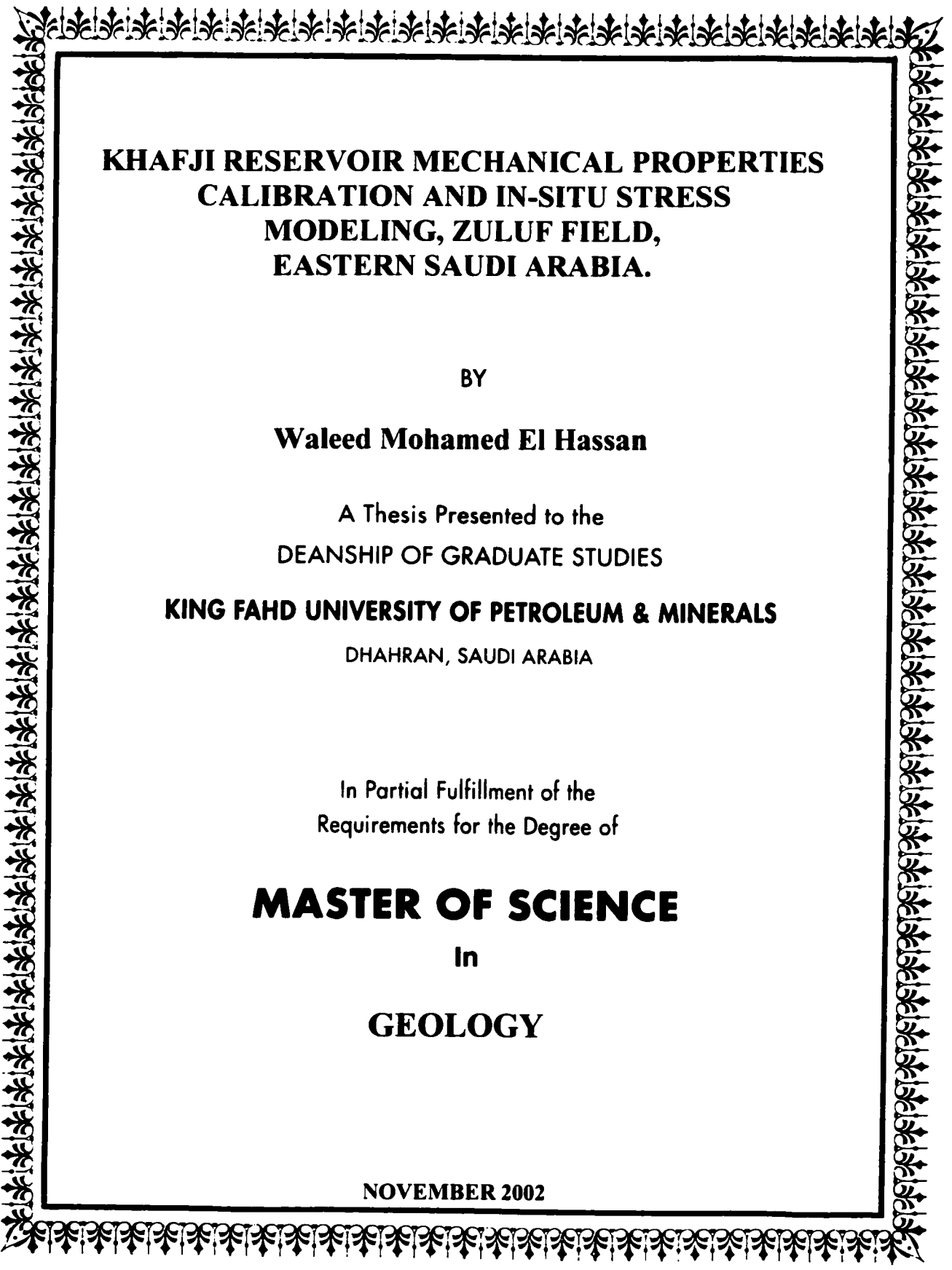
The quality of this reproduction is dependent upon the quality of the copy submitted. Broken or indistinct print, colored or poor quality illustrations and photographs, print bleedthrough, substandard margins, and improper alignment can adversely affect reproduction.

In the unlikely event that the author did not send UMI a complete manuscript and there are missing pages, these will be noted. Also, if unauthorized copyright material had to be removed, a note will indicate the deletion.

Oversize materials (e.g., maps, drawings, charts) are reproduced by sectioning the original, beginning at the upper left-hand corner and continuing from left to right in equal sections with small overlaps.

**ProQuest Information and Learning
300 North Zeeb Road, Ann Arbor, MI 48106-1346 USA
800-521-0600**

UMI[®]



**KHAFJI RESERVOIR MECHANICAL PROPERTIES
CALIBRATION AND IN-SITU STRESS
MODELING, ZULUF FIELD,
EASTERN SAUDI ARABIA.**

BY

Waleed Mohamed El Hassan

A Thesis Presented to the
DEANSHIP OF GRADUATE STUDIES

KING FAHD UNIVERSITY OF PETROLEUM & MINERALS

DHAHRAN, SAUDI ARABIA

In Partial Fulfillment of the
Requirements for the Degree of

MASTER OF SCIENCE

In

GEOLOGY

NOVEMBER 2002

UMI Number: 1411742

UMI[®]

UMI Microform 1411742

Copyright 2003 by ProQuest Information and Learning Company.
All rights reserved. This microform edition is protected against
unauthorized copying under Title 17, United States Code.

ProQuest Information and Learning Company
300 North Zeeb Road
P.O. Box 1346
Ann Arbor, MI 48106-1346


**KING FAHD UNIVERSITY OF PETROLEUM AND MINERALS
DHAHRAN 31261, SAUDI ARABIA**


DEANSHIP OF GRADUATE STUDIES

This thesis written by **Waleed Mohamed El Hassan** under the direction of his thesis advisor and approved by his thesis committee, has been presented to and accepted by the Dean of Graduate Studies, in partial fulfillment of the requirements for the degree of MASTER OF SCIENCE IN GEOLOGY.

Thesis Committee


Dr. Mahbub Hussain (Advisor)



Dr. Abdulazeez Abdulraheem
(Co-advisor)


Dr. Gabor Korvin (Member)


Dr. Osman Abdullatif (Member)

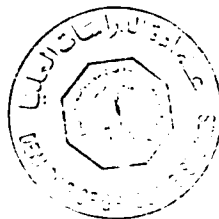

Dr. Mohammed Mohuiddin (Member)


Dr. Mustafa M. Hariri
Department Chairman


Prof. Osama A. Jannadi
Dean of Graduate Studies

31/12/2002

Date





ACKNOWLEDGEMENT

First and foremost I am most grateful to Alla, the almighty, for giving me the will, patience, and ability to complete this study. May his peace and blessing be upon His last noble prophet, Mohamed. Furthermore, the financial assistance and research facilities provided by King Fahd University of Petroleum and Minerals (KFUPM) are fully appreciated.

A word of gratitude is extended to my thesis committee chairman, Dr. Mahbub Hussain for his guidance and help. Special gratitude to Dr. Abdulazeez Abdulraheem, the co-chairman of this study, who first introduced me to the area of petroleum-related rock mechanics, for his continued support and help at all stages of this study. I would like to thank the thesis committee members Drs. Gabor Korvin, Osman Abdullatif, and Mohammed Mohiuddin for their constructive comments and valuable contribution. I wish to thank the Earth Sciences Department chairman Dr. Mustafa Hariri for his support and assistance during my study at KFUPM and for reviewing part of my thesis as well. Likewise, I would like to thank Earth Sciences Department faculty and staff. I am also grateful to my colleagues in the department for their support.

I am highly thankful to Petroleum Engineering Section of the Research Institute for providing rock material and technical support. Special thanks to the rock mechanics team, Research Institute, Dr. Mohammed Azeemuddin, Dr. M.R. Awal, Mr. Khaqan Khan, and Mr. Noman Khan for their cooperation and assistance. The help of Lameed Babalola, Yunis Umar, and Mushabab Asiri is well appreciated.

The patience, understanding, encouragement, and prayers of my big and small family are the cornerstone in completing this study in the present form.

TABLE OF CONTENTS

Title page.....	i
Certification.....	ii
Acknowledgement.....	iv
Table of contents.....	v
List of figures.....	x
List of tables.....	xiii
List of plates.....	xiii
Appendices.....	xiv
Abstract.....	xvi
الخلاصة.....	xvii

CHAPTER ONE INTRODUCTION

1.1 Introduction.....	1
1.2 Importance of rock mechanical properties.....	2
1.3 Study area.....	4
1.4 Tectonic and depositional environment.....	4
1.5 Description of the problem.....	9
1.6 Objectives.....	10
1.7 Methodology.....	11

CHAPTER TWO LITERATURE REVIEW

2.1. Introduction.....	14
2.2. Geology.....	15
2.3. Geological parameters.....	18
2.4. Calibration of rock mechanics	21

2.5. In-situ stress.....	25
---------------------------------	-----------

CHAPTER THREE
GEOLOGICAL PARAMETERS

3.1. Introduction.....	29
3.2. Grain size.....	30
3.2.1. Introduction.....	30
3.2.2. Grain size parameters.....	31
3.2.3. Correlation and discussion.....	33
3.3. Mineralogy and grains contact.....	45
3.3.1. Introduction.....	45
3.3.2. Mineralogical composition.....	45
3.3.2.1. Result.....	46
3.3.2.2. Correlation and discussion.....	55
3.3.3. Grains contact.....	55
3.3.3.1. Result.....	57
3.3.3.2. Correlation and discussion.....	57
3.4. Depositional environment.....	60
3.4.1. Introduction.....	60
3.4.2. Khafji reservoir depositional environment.....	61
3.4.3. Grain size and depositional environment.....	61
3.4.3.1. Textural parameters.....	62
3.4.3.2. Factor analysis.....	64
3.5. Sequence stratigraphic study.....	70
3.5.1. Introduction.....	70
3.5.2. Well log interpretation.....	71
3.5.3. Sequence stratigraphic model and discussion.....	73
3.6. Conclusion.....	73

CHAPTER FOUR

CALIBRATION OF MECHANICAL PROPERTIES

4.1 Elastic properties of rocks.....	79
4.2. Elastic theory.....	80
4.2.1. Introduction.....	80
4.2.2. Inelastic behavior in rocks.....	80
4.3. Acoustic log.....	82
4.3.1. Acoustic waves.....	82
4.3.2. Acoustic tools.....	83
4.3.2.1. Early tools.....	83
4.3.2.2. Dual receiver tools.....	83
4.3.2.3. Borehole compensated (BHC) tool.....	84
4.3.2.4. Long spacing sonic (LSS) tool.....	84
4.3.3. Vertical resolution.....	84
4.3.4. Depth of investigation.....	86
4.3.5. Logging problems.....	89
4.3.5.1. Noise.....	89
4.3.5.2. Cycle skipping.....	89
4.3.5.3. Mud arrivals.....	89
4.3.5.4. Altered zone arrivals.....	90
4.4. The difference between static and dynamic moduli in rocks.....	90
4.5. Biot's constant.....	92
4.5.1. Introduction.....	92
4.5.2. In-situ stress and Biot's constant.....	92
4.6. Rock mechanics test and calibration.....	93
4.6.1. Mechanical properties.....	93
4.6.1.1. Triaxial test.....	94
4.6.1.2. Biot's constant.....	94
4.6.2. Calibration of mechanical properties.....	94
4.6.2.1. Regression method.....	95
4.6.2.2 FORMEL method.....	95

4.6.2.3. AUTOSCAN method.....	97
4.6.3. Factors influencing calibration.....	98
4.7. Result and discussion.....	98
4.7.1. Rock mechanics.....	98
4.7.2. Biot’s constant.....	100
4.7.3. Calibration.....	100
4.7.4. Quantitative comparison.....	108
4.7.5. Lithology calibration factor.....	108
4.8. Conclusion.....	110

CHAPTER FIVE
IN-SITU STRESS MODELING

5.1. Introduction.....	111
5.2. Determination of in-situ stress.....	112
5.3. Applications of in-situ stress information	115
5.3.1. Wellbore stability	115
5.3.2. Hydraulic fracture orientation.....	115
5.3.3. Enhance oil recovery.....	115
5.4. In-situ stress regimes.....	116
5. 5. Regional geotectonics.....	116
5.6. In-situ stresses calculation.....	118
5.7. In-situ stresses determination for Khafji reservoir.....	120
5.7.1. In-situ stress orientation.....	121
5.7.2. Magnitude of vertical stress.....	121
5.7.3. Magnitude of horizontal stresses.....	121
5.8. Conclusion.....	124

CHAPTER SIX
CONCLUSIONS AND RECOMMENDATIONS

6.1. Conclusions.....	128
6.2. Recommendations.....	131
Nomenclature.....	156
References.....	158

LIST OF FIGURES

Figure 1.1. Location map of the study area.....	5
Figure 1.2. Generalized Cretaceous stratigraphic succession in eastern Saudi Arabia showing lithology and reservoir units	6
Figure 1.3. Khafji type log showing reservoir zonations for the northern offshore area.....	8
Figure 1.4. Methodology chart.....	13
Figure 3.1A. Grain size distribution for C1 samples.....	34
Figure 3.1B. Grain size distribution for C2 samples.....	34
Figure 3.1C. Grain size distribution for C3 samples.....	35
Figure 3.1D. Grain size distribution for C4 samples.....	35
Figure 3.1E. Grain size distribution for C5 and C6 samples.....	36
Figure 3.2. Correlation between median size and Young's modulus.....	39
Figure 3.3. Correlation between median size and Poisson's ratio.....	39
Figure 3.4. Correlation between mean size and Young's modulus.....	40
Figure 3.5. Correlation between mean size and Poisson's ratio.....	40
Figure 3.6. Correlation between sorting and Young's modulus.....	41
Figure 3.7. Correlation between sorting and Poisson's ratio.....	41
Figure 3.8. Correlation between skewness and Young's modulus.....	42
Figure 3.9. Correlation between skewness and Poisson's ratio.....	42
Figure 3.10. Correlation between kurtosis and Young's modulus.....	44
Figure 3.11. Correlation between kurtosis and Poisson's ratio.....	44
Figure 3.12. Classification of Khafji reservoir studied samples on the basis of QFL components.....	51
Figure 5.13. Typical x-ray diffractogram showing general clay mineralogy of sample C1 T13.....	52
Figure 3.14. Typical x-ray diffractogram showing general clay mineralogy of sample C4 T7.....	53

Figure 3.15. Photomicrographs showing (A) and (B) general view of samples (C) kaolinite (D) drilling additives (E) halite crystals. (F) pyrite crystal	54
Figure 3.16. Correlation between quartz percentage and Young's modulus.....	56
Figure 3.17. Correlation between quartz percentage and Poisson's ratio.....	56
Figure 3.18 Correlation between grain contact percentage and Young's modulus..	59
Figure 3.19. Correlation between grain contact percentage and Poisson's ratio.....	59
Figure 3.20. Plots of the mean grain size and standard deviation of the grain size distribution.....	63
Figure 3.21. Plot of normalized factor components.....	67
Figure 3.22. Grain size distribution curves for different end member samples	68
Figure 3.23. Sequence stratigraphic interpretation of the Khafji reservoir, well Zuluf-A.....	74
Figure 3.24. Sequence stratigraphic interpretation of the Khafji reservoir, well Zuluf-AA.....	75
Figure 3.25. Correlations among sequence stratigraphic interpretation and dynamic Young's modulus and Poisson's ratio.....	76
Figure 4.1. Conventional upper-transmitter two-receiver array at right gives horns at cave boundaries.....	85
Figure 4.2. Schematic drawing of a two-receiver sonde.....	87
Figure 4.3. Theoretical response of acoustic log to a thin bed of high velocity material for two receiver spans.....	87
Figure 4.4. Variation of Young's modulus with porosity for the Khafji reservoir rock samples.....	101
Figure 4.5. Variation of Poisson's ratio with porosity for the Khafji reservoir rock samples.....	101
Figure 4.6. Variation of static Biot's constant with porosity	103
Figure 4.7. Comparison of calibrated and dynamic mechanical properties of the Khafji reservoir, Zuluf-A well.....	105
Figure 4.8. Linear regression between static and dynamic Young's modulus.....	106
Figure 4.9. Linear regression between static and dynamic Poisson's ratio.....	106
Figure 4.9. Linear regression between static and dynamic Poisson's ratio.....	106

Figure 5.1. Relationships between principal stresses and type of faults.....	117
Figure 5.2. Tectonic features of Saudi Arabia and adjacent area.....	119
Figure 5.3. Zuluf-C FMI illustrating the breakout directions.....	122
Figure 5.4. (A) Minimum and (B) maximum horizontal stress directions for Zuluf field.....	123
Figure 5.5. Leak-off test data from Zuluf-D well.....	125
Figure 5.6. Minimum and maximum horizontal stress gradient for well Zuluf-A..	126

LIST OF TABLES

Table 1.1. Domain of rock mechanics in petroleum industry.....	3
Table 3.1. Descriptive measures of grain size distribution according to Folk (1974).....	32
Table 3.2. Descriptive statistics results for the studied samples	37
Table 3.3. Mineralogical composition of core samples from well Zuluf-A	47
Table 3.4. Textural attributes of core samples from well Zuluf-A	58
Table 3.5. Eigenvalues, total percentage, and cumulative percentage.....	65
Table 3.6. Varimax factor matrix with three related factors.....	66
Table 4.1 Summary of rock mechanics tests on rock samples obtained from Zuluf-A well	99
Table 4.2. Biot's constant values for Zuluf-A well samples	102
Table 4.3. Parameters used for calibration of mechanical properties	104
Table 4.4. Summary of error for different calibration methods.....	109
Table 4.5. Lithology calibration factor for different lithologies.....	109

LIST OF PLATES

Plate 3.1. Photomicrographs of typical composition of sample C6-T4 dominated by quartz (X10). A: Under plane light, B: Under cross-polarized light	48
Plate 3.2. Photomicrographs of typical composition of sample C2-T1 showing the highest amount of matrix (X10). A: Under plane light, B: Under cross-polarized light	50

APPENDICES

Appendix A. Thin section photomicrographs.....	133
Figure A.1. Thin section photomicrograph, X10 under plane and cross-polarized light, for sample C1-T20.....	134
Figure A.2. Thin section photomicrograph, X10 under plane and cross-polarized light, for sample C1-T13.....	135
Figure A.3. Thin section photomicrograph, X10 under plane and cross-polarized light, for sample C1-T6.....	136
Figure A.4. Thin section photomicrograph, X10 under plane and cross-polarized light, for sample C1-T3.....	137
Figure A.5. Thin section photomicrograph, X10 under plane and cross-polarized light, for sample C2-T21.....	138
Figure A.6. Thin section photomicrograph, X10 under plane and cross-polarized light, for sample C2-T11.....	139
Figure A.7. Thin section photomicrograph, X10 under plane and cross-polarized light, for sample C2-T8.....	140
Figure A.8. Thin section photomicrograph, X10 under plane and cross-polarized light, for sample C2-T1.....	141
Figure A.9. Thin section photomicrograph, X10 under cross-polarized light, for sample C3-T23.....	142
Figure A.10. Thin section photomicrograph, X10 under plane and cross-polarized light, for sample C3-T20.....	143
Figure A.11. Thin section photomicrograph, X10 under plane and cross-polarized light, for sample C3-T14.....	144
Figure A.12. Thin section photomicrograph, X10 under plane and cross-polarized light, for sample C4-T23.....	145
Figure A.13. Thin section photomicrograph, X10 under plane and cross-polarized light, for sample C4-T11.....	146
Figure A.14. Thin section photomicrograph, X10 under plane and cross-polarized light, for sample C4-T7.....	147
Figure A.15. Thin section photomicrograph, X10 under plane and cross-	

polarized light, for sample C4-T1.....	148
Figure A.16. Thin section photomicrograph, X10 under plane and cross-polarized light, for sample C5-T10.....	149
Figure A.17. Thin section photomicrograph, X10 under plane and cross-polarized light, for sample C5-T3.....	150
Figure A.18: Thin section photomicrograph, X10 under plane and cross-polarized light, for sample C6-T20.....	151
Figure A.19. Thin section photomicrograph, X10 under plane and cross-polarized light, for sample C6-T4.....	152
Appendix B. Lithological description of reservoir rock samples.....	153

ABSTRACT

NAME: Waleed Mohamed El Hassan

TITLE OF THESIS: Khafji Reservoir Mechanical Properties Calibration and In-Situ Stress Modeling, Zuluf Field, Eastern Saudi Arabia.

MAJOR FIELD: Geology

DATE OF DEGREE: November 2002.

The understanding of the mechanical properties of petroleum reservoir is important for drilling, wellbore completion, stimulation, and monitoring processes.

The objectives of the study are to investigate the relationships between the geological parameters and depositional environment and the mechanical properties of the Khafji reservoir, Zuluf field, offshore Saudi Arabia. The study also made an attempt to establish a relationship between static and dynamic elastic moduli and model the in-situ stress affecting the field.

The relationships between grain size parameters and mechanical properties (Young's modulus and Poisson's ratio) were not significant.

The XRD study revealed that kaolinite is the main clay mineral in the samples. The EDS emphasized quartz enrichment and the presence of kaolinite that appeared in XRD test. The relationship between quartz percentage and grain contact percentage Young's modulus was not significant whilst it was significant with Poisson's ratio.

To investigate the effect of depositional environment, Muiola and Weiser (1968) analysis was used. Beach sand samples characterized by lowest average Young's modulus and lowest average Poisson's ratio relative to river sand. Also, factor analysis was used and three factors were identified. Beach environment has lower values of Young's modulus and Poisson's ratio relative to gravitational settling environment. Sequence stratigraphic model was interpreted. The main sand and the upper stringer sand represent a (LST) and succeeding (TST). The (LST) has the highest Young's modulus and Poisson's ratio relative to the (TST).

Three methods were used to calibrate dynamic into static mechanical properties. They are linear regression, FORMEL, and AUTOSCAN methods. Only, AUTOSCAN method calibrated successfully both Young's modulus and Poisson's ratio.

The azimuths of the minimum and maximum horizontal stress are approximately northwest and northeast, respectively. Typical values of minimum and maximum horizontal stress gradients are 0.82 psi/ft and 0.9 psi/ft, respectively. While the vertical stress gradient is 1.1 psi/ft. The relationship among the magnitudes of the three principal stresses ($\sigma_v > \sigma_H > \sigma_h$) suggests a normal fault regime.

**MASTER OF SCIENCES DEGREE
KING FAHD UNIVERSITY OF PETROLEUM AND MINERALS
Dhahran, Saudi Arabia
November 2002**

الخلاصة

الإسم: وليد محمد الحسن

عنوان الرسالة: معايرة الخصائص الميكانيكية ونمذجة الإجهادات الأرضية لمكمن الخفجى البترولى بحقل الظلوف، شرق المملكة العربية السعودية.

التخصص الرئيسى: الجيولوجيا.

تاريخ نيل الدرجة: نوفمبر 2002 م.

تعتبر الخصائص الميكانيكية لصخور المكامن البترولية ذات أهمية لعمليات الحفر، إكمال البئر، زيادة نفاذية المكمن، مراقبة المكمن بعد الحفر وغيرها.

تهدف الدراسة لتحرى علاقة العوامل الجيولوجية والبيئة الترسيبية مع الخصائص الميكانيكية لمكمن الخفجى البترولى بحقل الظلوف، شرق المملكة العربية السعودية. إضافة إلى معايرة الخصائص الميكانيكية العملية والحقلية ونمذجة الإجهادات الأرضية المؤثرة فى الحقل.

أوضحت الدراسة ضعف العلاقة بين الخصائص الميكانيكية للمكمن وعوامل حجم الحبيبات وقوتها بين الخصائص الميكانيكية للمكمن وكل من نسبة معدن الكوارتز ونسبة ملامسه الحبيبات. بناءً على طريقة Moiola and Weiser (1968) تم تقسيم المكمن إلى رمل ذو بيئة نهريّة وأخر ذو بيئة شاطئية. ووجد أن الرمل ذو البيئة الشاطئية يتميز بخصائص ميكانيكية منخفضة من تلك التى للرمل ذو البيئة النهريّة. أيضاً تم استخدام طريقة تحليل المعامل لنفس الغرض. وبعد تحديد ثلاث معاملات وجد أن البيئة الشاطئية تتميز بخصائص ميكانيكية منخفضة مقارنة مع البيئة ذات الترسيب الجانبيّه. تم تفسير نموذج للتتابع الطبقي المميز للمكمن ووجد أن (LST) تتميز بخصائص ميكانيكية مرتفعه مقارنة مع (TST).

أستعملت ثلاث طرق لمعايرة الخصائص الميكانيكية العملية مع الحقلية وهى الطريقة الخطيه، فورمل (FORMEL)، و أوتوسكان (AUTOSCAN). ولقد وجد ان طريقة أوتوسكان هى الوحيدة التى عايرت بنجاح القيم العملية مع الحقلية.

أوضحت الدراسة أن إتجاها الإجهادين الأرضيين الأفقيان الأصغر والأكبر هما شمال غرب وشمال شرق على التوالي. كما أن قيم الإجهادات الأرضية الرأسية، الأفقية الصغرى، والأفقية العظمى هى 1.1، 0.82، و 0.9 psi/ft على التوالي. هذه العلاقة بين الإجهادات الأرضية تشير الى نظام صدع عادى.

درجة ماجستير العلوم
جامعة الملك فهد للبترول والمعادن
الظهران - المملكة العربية السعودية
نوفمبر 2002م

CHAPTER ONE

INTRODUCTION

1.1. INTRODUCTION

Rock is the host of oil and gas; therefore rock mechanical behavior is a central component of many oil industry problems. The correct rock mechanics characterization of formations in terms of behavior is thus of technical and economical importance (Santarelli, 1994). The mechanical properties of a rock normally refer to the constants in the constitutive equation, which the rock is assumed to obey. A rock would hence be described by four mechanical parameters: two elastic parameters (Young's modulus and Poisson's ratio) and two failure parameters (friction angle and uniaxial compressive strength). Young's modulus measures the resistance of a rock against being compressed by uniaxial stress, while Poisson's ratio measures the lateral expansion relative to longitudinal contraction (Fjaer et al., 1992).

Rock mechanical properties depend on the interaction between extrinsic and intrinsic factors. The most important extrinsic factors are confining pressure and strain rate. The important intrinsic geological factors include porosity, grain size, mineralogy, and types of cement (Donath and Fruth, 1971; Plumb et al., 1992; Sarda et al., 1993).

1.2. IMPORTANCE OF ROCK MECHANICAL PROPERTIES

An understanding of mechanical properties is important in drilling and better management of a reservoir. Concerns range from drilling, completion, production, and monitoring of reservoir processes. Table 1.1 presents different industrial aspects that have a rock mechanical content.

Rock layers encountered during drilling a wellbore have a variety of pore pressures, permeabilities, mechanical properties, and fluid contents. Wellbore pressure must be high enough to prevent excessive fluid influx into the wellbore and to maintain wellbore stability, and be low enough to prevent loss of drilling mud circulation. With insufficient mud gradient, stress in the wall can lead to rock failure and leading to wellbore instability (Meehan, 1994).

Production problems involving the rock mechanics include sand control, stimulation issues, and perforation design. Sand production is a particular problem caused due to failure of friable formations around a wellbore. Well stimulation is a mean of improving the reservoir flow properties to overcome damage or improve the flow capacity of low-permeability wells. The primary stimulation techniques for vertical wells are acidization and hydraulic fracturing (Meehan, 1994). Perforations may mitigate excess near-wellbore friction observed in many vertical and most highly deviated wells. Optimum perforation length and density strongly depend on rock mechanical properties (Warpinski, 1992).

Monitoring of reservoir processes involves rock mechanics for many specialized applications including (Meehan, 1994):

1. Subsidence monitoring: Reduced reservoir pressures lead to increase in effective stresses leading to reservoir compaction. Decreased reservoir thickness causing surface

TABLE 1.1. Domain of rock mechanics in petroleum industry
(after Santarelli, 1994).

Domain	Rock mechanical content
Drilling	Wellbore stability, coring, mud losses, casing collapse, and rock bit interaction.
Production	Sand production, perforation, and hydraulic fracturing
Surface activities	Site investigation, subsidence, and waste management.
Reservoir	Stress and compressibility vs depletion, water injection, and fracture identification.
Exploration	Hydrocarbon migration, fractures, seal efficiency, and basin modeling

subsidence, specifically for shallow reservoirs.

2. Monitoring enhanced recovery: Enhanced recovery requires injection of fluids to displace oil. Knowledge of where to inject fluids is essential to optimal economics.

1.3. STUDY AREA

Zuluf field, one of the giant oilfields located in the northern part of the Arabian Gulf offshore, Saudi Arabia, is located 240 km north of Dhahran (Figure 1.1). Zuluf field was discovered in 1965 and production started in 1973. Currently, the field is being produced primarily from the Cretaceous age Khafji reservoir, which generally consists of two productive zones, the Khafji main sand and the upper Khafji stringer (Al-Ghamdi et al., 2001).

Khafji reservoir is a part of the Khafji Member of the Middle Cretaceous Wasia Formation (Figure 1.2). The Khafji Member overlies the Lower Cretaceous Shu'aiba Formation and in turn is conformably overlain by Safaniya Member. The Khafji Member in the Zuluf field consists of a thick sequence of quartz sandstone, siltstone, shale, and various types of ironstone. It also has minor amounts of limestone, amber, and a few coal beds.

1.4. TECTONIC AND DEPOSITIONAL ENVIRONMENT

The Wasia Formation was deposited on the Arabian shelf during Mid-Cretaceous. The Wasia Formation and its equivalent are known to be the primary oil producing horizons in the Gulf region. The Formation is divided into seven members: Khafji, Safaniya, Mauddud, Wara, Ahmadi, Rumaila, and Mishrif (Sharief et al., 1989). The sedimentary cover dips gently eastward. The Eastern half of the Arabian Plate was a passive plate margin dominated by carbonate and evaporite deposition since the Middle Jurassic. During the Middle Cretaceous, the Arabian Plate was still

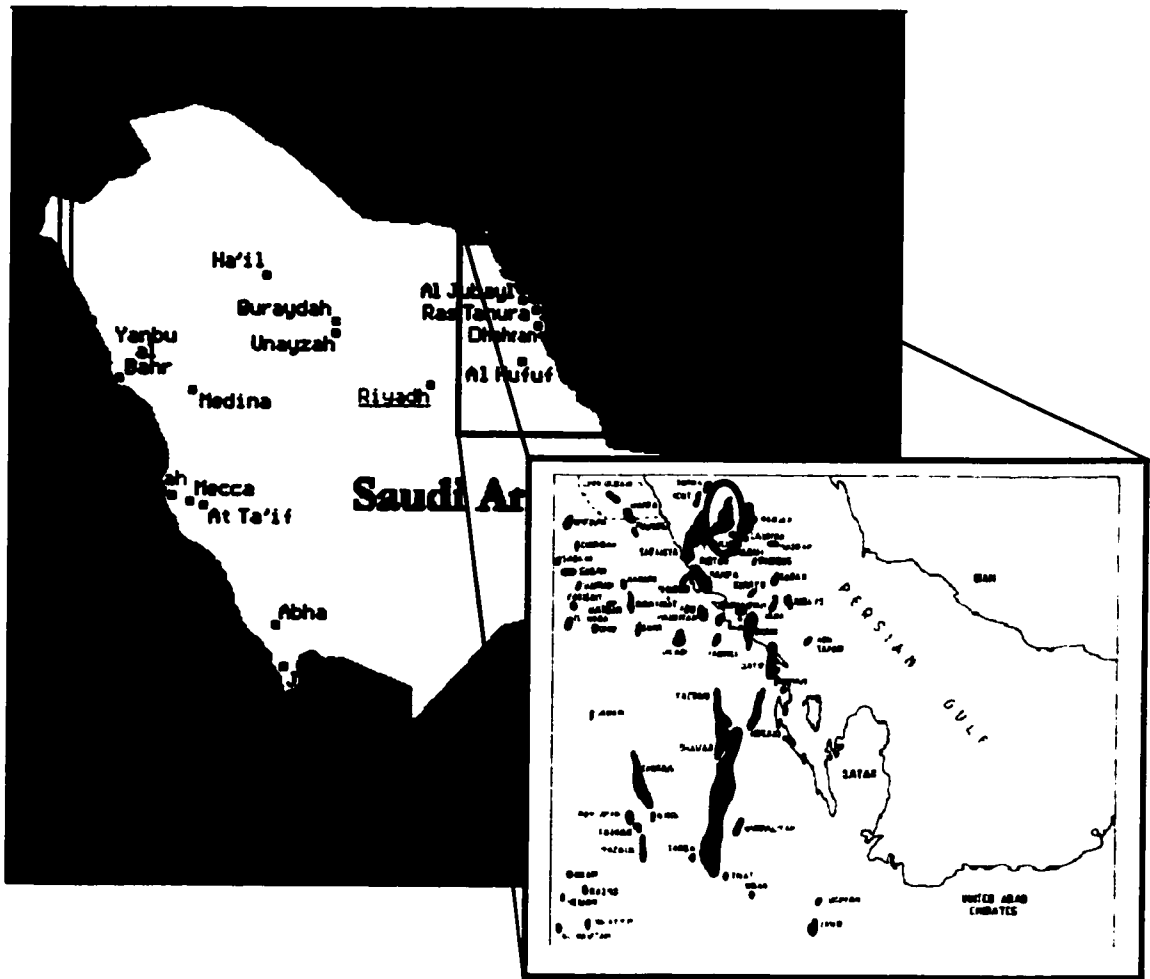


Figure 1.1. Location map of the study area (after Edgell, 1992).

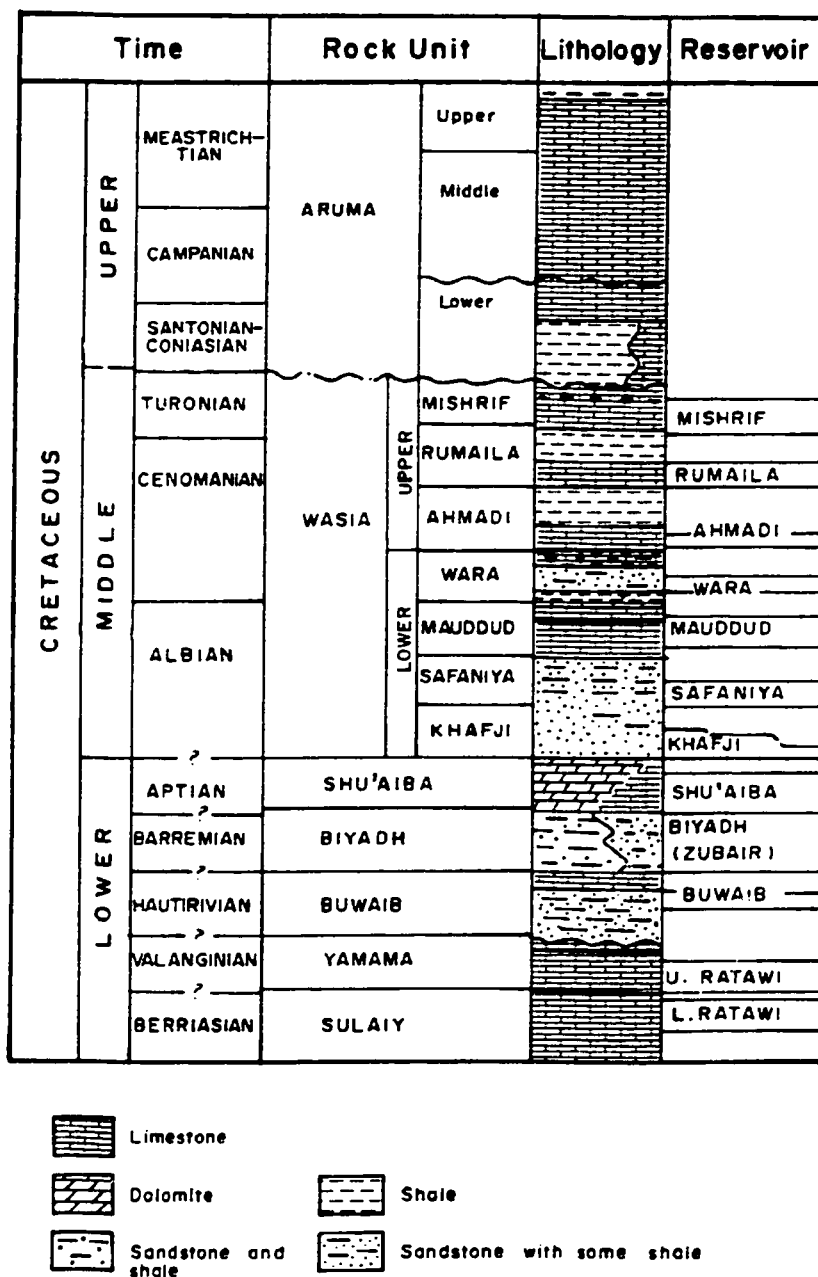


Figure 1.2. Generalized Cretaceous stratigraphic succession in eastern Saudi Arabia showing lithology and reservoir units (after Sharief et al., 1989).

attached to North Africa and separated from the Iranian plate by the Zagros arm of the Tethys seaway. Because of the Tethys seaway continued to close, the plate movement increased during Middle Cretaceous (Entsminger, 1981).

The change from carbonates to siliciclastics in the Wasia indicates that tectonic activity made a new source of sediments available in the Mid-Cretaceous. The most probable sources of Wasia sediments are the older formations and the Arabian shield that eroded when the Pre-Wasia Unconformity was active (Entsminger, 1981; Alsharhan and Nairn, 1986; Sharief et al., 1989).

As well as being a time of active plate tectonics, the Early to Mid-Cretaceous is also a period of widely recognized transgressions (Cooper, 1977). Transgression events in the region correlate well with the marine limestone units and regressive events to the siliciclastic units. After the Aptian transgression resulted in the extensive and uniform deposition of a shallow water carbonate of Shu'aiba Formation, a major regression in Early Albian represented by the deposition of the Khafji Member had occurred (Entsminger, 1981; Alsharhan and Nairn, 1986).

The overall depositional setting of the Khafji Member is one of fluvially dominated deltaic facies that prograded seaward in response to base level lowering. This resulted in the deposition of delta-front mouth bar and distributary channels sand (the main sand interval) over distal-delta front and prodelta deposits. Continued progradation of the delta system caused lower delta-plain and upper delta-plain facies (the upper stringer sand interval) to stack on the top of the amalgamated sand facies of the delta-front environment (Grant and Al-Humam, 1994) (Figure 1.3).

The upper stringer sand interval is interpreted to have been deposited in a delta-plain setting consisting of meandering channels and associated point-bar deposits,

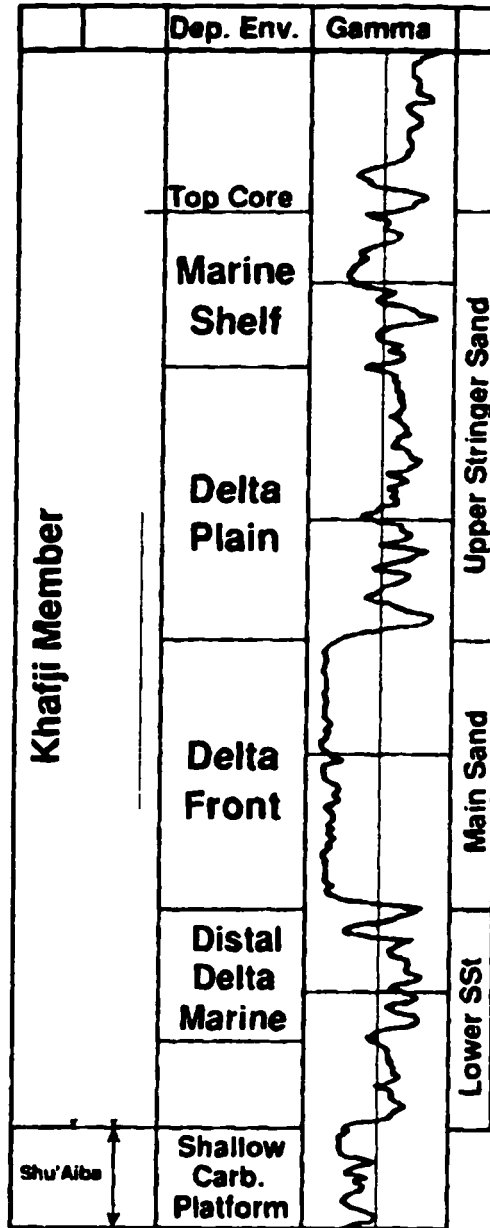


Figure 1.3. Khafji type log showing reservoir zonation for the northern offshore area (after Senalp et al., 1988).

distributary channels, crevasse splays, levees, and interdistributary bay environments. Facies associated with it are characterized by much more laterally extensive shales and laterally discontinuous sandstones than the main sand interval. While the main sand interval is interpreted to have been deposited in a delta-front setting consisting of delta-front mouth bar and distributary channel complexes. The main sand interval is dominated by laterally continuous, massive to cross-bedded sandstones that are locally broken up laterally by discontinuous shales. Shales in the main sand interval were deposited as marine flooding surfaces that were subsequently eroded by the multilateral-multistory distributary sands (Grant and Al-Humam, 1994).

1.5. DESCRIPTION OF THE PROBLEM

Today's economic conditions emphasize the need for better designs in drilling, well completion, and reservoir production and monitoring. Knowledge of rock mechanical behavior of reservoir rocks is of great value in connection with wellbore stability problems, fracturing operations, subsidence problems and sand production problems.

The mechanical properties of a formation may be divided into the following three groups (Fjaer et al., 1992):

- 1. Elastic parameters:** The important method for estimation of elastic parameters for the reservoir rock is acoustic logging, which measures the wave velocities.
- 2. Strength parameter:** Strength of a material is dependent on the level of confining stress. Failure criteria used to describe the actual behavior normally have at least two to three adjustable parameters.
- 3. In-situ stresses:** Technically, the in-situ stresses are not mechanical properties of the rock. However, in-situ stresses influence both the elastic parameters and the

strength parameters. The in-situ stress is a key parameter in a number of applications such as induced fracturing, sand production control, and borehole instability.

Cores are the only medium of obtaining direct measurement of rock mechanical properties. Cores are, however, available only from discrete levels and sometimes unavailable due to cost or technical constraints, while the mechanical behavior of the complete strata may be of vital importance the analysis of rock mechanics related problems. Therefore, wire-line logs are used to estimate the mechanical properties of the complete layers. Since the wire-line logs (dynamic values) and core measurements (static values) are measured under different conditions, the former is calibrated in order to have a continuous profile of the mechanical properties. Many techniques are used for the calibration purpose such as linear regression and FORMEL (formation mechanical log).

The numerical analysis of wellbore stability, sand production, and in-situ stress must deal with a wide variety of rocks ranging from sandstones through siltstones to mudstones and shales. Identification of the dominant composition and textural elements governing rock failure is necessary for understanding the mechanical properties of petroleum reservoirs.

1.6. OBJECTIVES

The study will attempt to establish a relationship between static and dynamic elastic moduli of the Khafji reservoir, Zuluf field, offshore Saudi Arabia. Furthermore, the study will investigate the effect of the geological parameters on the mechanical properties through the study of textural and compositional elements of the core samples. The reservoir to be investigated covers the producing intervals i.e., the upper stringer sand interval and the main sand interval.

More specifically, the objectives for this study are:

1. Investigate the effect of the geological parameters (texture and composition) on the mechanical properties.
2. Investigate the effect of depositional environment on the mechanical properties.
3. Develop an empirical correlation to calibrate dynamic mechanical properties using static mechanical properties of the reservoir.
4. Investigate the effect of lithology on calibration factor.
5. Characterize reservoir in-situ stresses.

1.7. METHODOLOGY

To study the effect of geological parameters on reservoir mechanical properties, sieve analysis and petrographic investigation were carried to determine the compositional and the textural elements for the samples. For that purpose, a total of forty end piece core samples were disaggregated and sieved. Sieve analysis was carried out by shaking a weighted sample through a series of sieves with decreasing mesh openings. Each sieve filtered out a certain percentage of the entire sample with the finest material collected at the bottom pan. The weight percentages were plotted against the size of mesh openings for the whole sample to provide an insight into the grain size distribution. For thin section investigation, samples were impregnated with epoxy under vacuum pump. The impregnation was allowed to cure overnight. The samples were smoothly polished with calcium carbide and mounted on glass slides. The glass-mounted samples were subsequently polished for thin section microscopy investigation. For the purpose of determining clay minerals x-ray diffraction x-ray diffraction (XRD) and scanning electron microscope (SEM) analysis were carried out.

To study the effect of the depositional environment, Muiola and Weiser (1968) analysis, factor analysis, and sequence stratigraphy were carried out.

Triaxial strength measurements were made on 1.5 inch diameter by 3 inch long vertical core plugs. The core plugs were drilled from preserved whole core. The cores were preserved in plastic tubes to keep them moist as they were. The ends of the core plugs were trimmed and ground. The triaxial measurements were made in a triaxial cell by recording axial and radial strain as the sample was loaded axially under constant confining stress. A confining stress of 2900 psi was used for all samples to simulate approximate reservoir stress condition. At 50% of the failure stress Young's modulus and Poisson's ratio were then calculated. For calculating dynamic mechanical properties, acoustic and density logs were used to calculate the Young's modulus and Poisson's ratio. Static and dynamic reservoir mechanical properties were then calibrated to generate a continuous record of the mechanical properties with respect to depth.

In-situ stress can be characterized after determination of Poisson's ratio, Biot's constant, vertical stress, and reservoir pore pressure. Figure 1.4 summarizes the methodology used in this study.

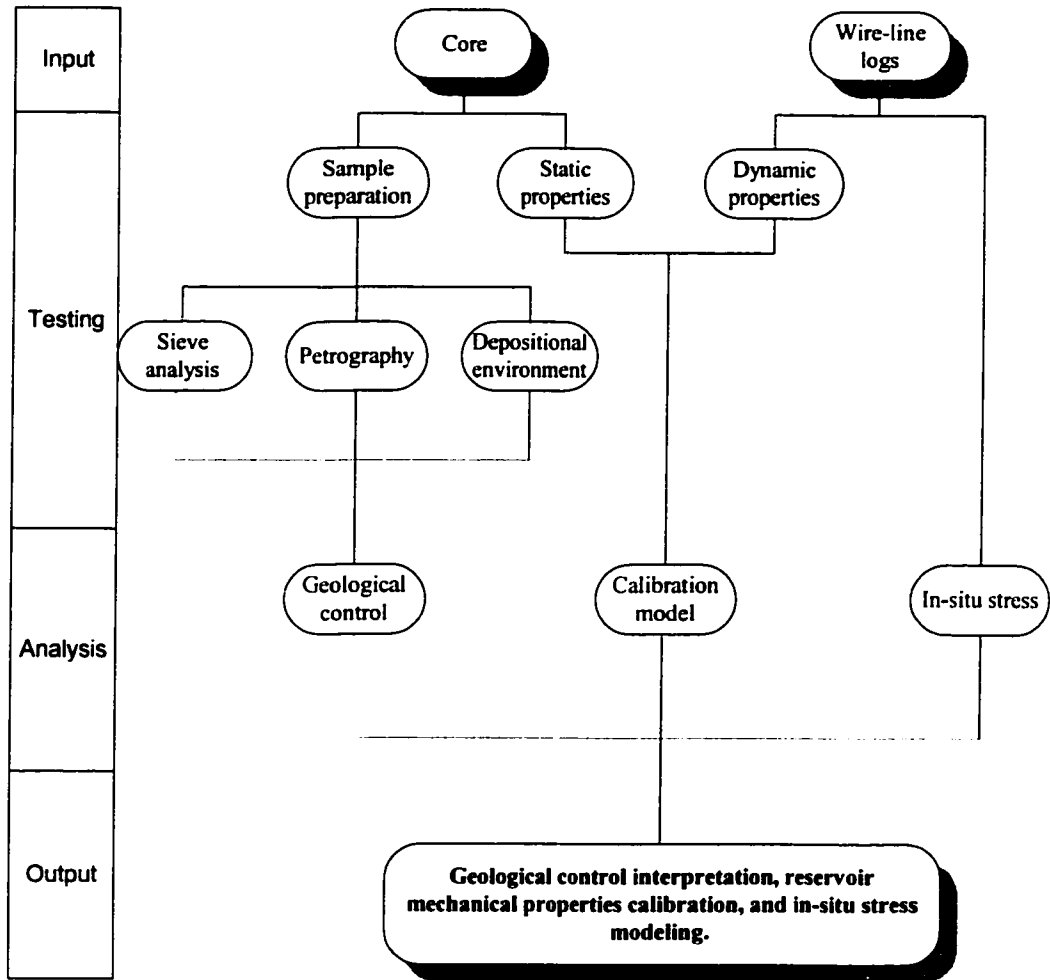


Figure 1.4. Methodology chart.

CHAPTER TWO

LITERATURE REVIEW

2.1. INTRODUCTION

The Wasia Formation and its equivalent are known to be one of the primary oil producing horizons in the Gulf region. The most striking example is the Safaniya field (world's largest offshore oil field) in Saudi Arabia where the Wasia Formation is the major oil producer. Because of the economic importance of the Middle Cretaceous sequence as hydrocarbon bearing rock in offshore Saudi Arabia, a lot of work has been documented in the literature. The Wasia Formation-Khafji reservoir has been studied in both subsurface and outcrops by many geologists.

Compared to the dynamic properties obtained from acoustic logs, the static rock properties better represent the actual rock behavior. This is because the rates of static stress loading are closer to that of the field and of orders of magnitude lower than rates of stress imposed by wave propagation. Determination of the static properties is routinely done in the laboratory, and most of the time the static and dynamic sets of properties do not agree (Motmayeur and Graves, 1985; Edlmann et al., 1998). The relationships between these properties vary depending upon the characteristics of the rocks. In the literature, several techniques are reported which are used to estimate static properties from dynamic properties.

2.2. GEOLOGY

The name Wasia, first proposed by Steneike et al. (1958) based on outcrop at Al-Armah escarpment in the central Arabia, was formally defined and described in details in both outcrops and subsurface by Powers et al. (1966) and Powers (1968). Powers (1968) subsequently subdivided the Wasia Formation in the subsurface to seven (7) members namely; the Khafji Sandstone, Safaniya Sandstone, Mauddud Limestone, Wara Sandstone, Ahmadi Shale, Rumaila and Mishrif Carbonate members.

Moshrif (1978, 1980) deduced a dominantly fluvial alluvial depositional environment for the Biyadh and Wasia Formations and ascribed the intervening Shu'aiba Formation to very shallow marine environment.

Murris (1980) studied the stratigraphy evolution and oil habitat of the Middle East. He concluded that the Aptian sea rise was of lesser magnitude and duration than the Late Jurassic one. The climate was also more humid than during the Late Jurassic, though evaporites were again deposited on the northern end of the platform. The temporary flooding during Aptian was followed by the most pronounced regression since the Late Triassic. By Mid of Albian time the clastic regime had spread across the whole platform except for a narrow belt in the northeast. The coastal and alluvial sandstones of this interval (Khafji Member) are very rich reservoirs in the northern Gulf area. They are sealed by interbedded shales, and have access to charge from the Early Cretaceous deposits.

According to Moshrif and Kelling (1984), the Wara, Ahmadi, and Mishrif members in the subsurface are equivalent to the exposed Wasia Formation in central Saudi Arabia. Van Eck (1985) considered the Sakaka Sandstone as Wasia Formation and subdivided it into Lower, Middle, and Upper members.

Alsharahan and Nairn (1986) reviewed the stratigraphy, depositional environments and status of the Biyadh and Wasia Formations. The authors ascribed the difficulties in correlating the outcrops of these formations to their being dominantly siliciclastic with poor to total lack of fossils compared to their better-defined and fossiliferous subcrop equivalents. They delineated two depositional cycles in the Middle Cretaceous. The lower cycles dominated by siliciclastic sediments is called the Nahr-Umr-Mauddud cycle while the carbonate dominated upper cycle was named as the Wara-Mishrif cycle.

Sharief et al. (1989) subdivided the Wasia Formation in the subsurface into Lower Wasia consisting of Khafji, Safaniya, Mauddud and Wara and Upper Wasia composed of Ahmadi, Rumaila, and Mishrif members. Wallace et al. (1997) upgraded the Wasia Formation to group status and subdivided the group into Lower Wasia Group and Upper Wasia Group.

Al-Sabti (1991) developed a program to determine lithology from well log measurements for the Mauddud, Safaniya, and Khafji members of Wasia Formation in Safaniya, Zuluf, Marjan, and Maharah fields. Analysis was based on 6700 feet of core description data obtained from twelve wells from which eight basic electrofacies were identified: shale, clean sandstone, argillaceous sandstone, iron-rich sandstone, iron-rich shale, ironstone, clean limestone, and argillaceous limestone. A suite of well log traces (gamma ray, density, sonic, neutron, and caliper) were loaded into the program with the intent of predicting the lithologies observed in the extracted core from the log-measured values. Comparison of the log-predicted lithologies to the core data yielded results between 95% and 99% accuracy with an average predicting accuracy of 97%.

Grant and Al-Humam (1994), constructed a geostatistical three-dimensional model for the reservoir in the northern offshore area of Saudi Arabia. They concluded that porosity and permeability cubes generated from the conditional indicator simulations are geologically realistic and capture the large-scale level of heterogeneity envisioned for the Khafji section in the study area.

Christian (1997) studied the Cretaceous subsurface geology of the Middle East region. He concluded that the regional structural and isopach/lithofacies maps provided an overview of the major tectonic and stratigraphic development in the leading petroleum basins of the world. The structural map showed that most of the tectonic elements of the region, including the main anticlinal trends with oil fields remained active during and after the Late Cretaceous. The isopach and lithofacies maps of the Lower, Middle, and Upper Cretaceous indicated the development of broad intra-shelf basins along the Cretaceous platform, which controlled the regional distribution of lithofacies.

Al-Fares et al. (1998) studied the Middle to Lower Cretaceous stratigraphy, offshore Kuwait. They collected 500 samples from eleven wells and conducted biostratigraphic analyses on them. They concluded that after the deposition of Shu'aiba Formation, The Middle Cretaceous commences with a newly recognized hiatus of approximately six million years duration. Uplift of the cratonic source areas to the west caused a renewed influx of sands over large parts of the basins in the Early Middle Albian. The Burgan Formation (equivalent to Khafji Member) is characterized by thick deltaic sands in the west, thinning to an average thickness of 1100 feet in the offshore.

Ziegler (2001) generated a series of paleofacies maps for given time intervals between the Late Permian and Holocene to reconstruct the depositional history of the

Arabian Plate. The succession of changing lithological sequences controlled by the interplay of eustasy and sediment supply with regional and local tectonic influences. The Late Early Cretaceous period spanned the deposition of Shu'aiba Formation and its regional equivalents. He marked a regional unconformity and sedimentary hiatus at Late Aptian. The gradually rising sea level that followed the pre-Albian unconformity caused the oscillating deposition of shale and carbonate.

Davies et al. (2002) incorporated the maximum flooding surfaces (MFS) in the Early to Mid-Cretaceous mixed carbonate-clastic shelfal systems of the Arabian Plate into a new sequence stratigraphic model that links Kuwait, Iran, Saudi Arabia, Qatar, and United Arab Emirates to Oman and Yemen. It is based on regional sequence stratigraphic concepts supported by biostratigraphical, sedimentological, and mineralogical data. The model has predicted that in many places (MFS) are located in the basal parts of clean carbonates even though these are not the deepest-water sediments. Examples are Shu'aiba and Mauddud sections of the northern Gulf. For Wasia Formation, they placed the intra-Aptian unconformity at the base of the main sand of the Khafji Member.

2.3. GEOLOGICAL PARAMETERS

The mechanical properties of a rock, together with its petrophysical properties, are important parameters when considering rock characteristics. The mechanical properties of a rock depend primarily on its compositional and textural features. A number of studies were conducted to investigate the relationships between rock mechanical properties and the composition and texture of the rocks.

Bell (1978) studied Fell Sandstone in England. First, he subjected the samples (3 meters depth) to petrographic examination to analyze the packing and grain size

distribution. Secondly, from the same depth interval, he determined their physical and mechanical properties (density, porosity, strength, hardness, and elastic moduli). This various measures were then correlated to investigate the influence of each property and to consider them as an index properties.

Fahy and Guccione (1979) tried to estimate strength of sandstone by using petrographic thin section data. They indicated that sandstone with smaller mean grain size had higher strength value. Also, they noted that the sphericity inversely correlated with compressive strength and showed the strongest correlation among all the petrographic properties. Significant correlations were reported between some types of grain contacts and strength and Young's modulus.

Shakoor and Bonelli (1991) studied the relationship between petrographic characteristics, engineering index properties, and mechanical properties of selected sandstones. Conversely to Fahy and Guccione (1979), they reported that mean grain size did not show any significant correlation with strength and elastic properties of sandstones. Also, they did not find any relationship between packing density and mechanical properties whilst the percentage of angular grains was weakly related to strength and elastic properties.

Plumb et al. (1992) investigated the influence of composition and texture on compressive strength variations in the Travis Peak Formation. They found a correlation between rock strength and parameters related to deformation mechanisms. They showed that grain size, grain contacts, and percent of fines are directly related to rock strength and mechanical behavior. Also, the most accurate strength models included information on both extrinsic and intrinsic rock properties. Their method suggested a new approach to quantify rock strength from well logs.

Plumb (1994) identified new relationships between the composition and texture of clastic rocks and their Coulomb failure parameters, unconfined compressive strength, and friction angle. Rocks examined in this study have varied in their porosities and clay content. He concluded that porosity and clay content both have a significant influence on the unconfined compressive strength. Young's modulus provided the best relative indicator of unconfined strength. Friction angle decreased with increasing effective confining pressure.

Ulusay et al. (1994) tested sandstone samples from a borehole drilled in Black Sea, Turkey. First, he determined uniaxial compressive strength, elastic parameters, unit weight, porosity, and quality index. Then, fifteen selected samples were subjected to petrographic examination. Based on the statistical analysis results, polynomial prediction equations were developed for estimating mechanical properties from petrographic characteristics. The study revealed that the influence of textural characteristics appear to be more important than mineralogy for predicting the mechanical properties. It is also noted that type of contacts, grain shape and size, and rock fragments are the petrographic characteristics, which have significant influence upon the mechanical properties.

Bell and Lindsay (1999) studied the petrographical and geomechanical properties of Newspaper Member, South Africa. They found that few of petrographical properties of this sandstone have a notable influence on the mechanical properties. However, increasing clay content lowered the unconfined compressive strength whilst increasing quartz content enhanced it.

Chatterjee and Mukhopadhyay (2001) studied the petrophysical and mechanical properties of reservoir rocks from two major basins on the east coast of

India using samples cored from 19 wells. The purpose of the study was to investigate the relationships between the properties of the rocks including dry density, effective porosity, uniaxial compressive strength, tensile strength, and Young's modulus. The relationships were further elucidated using regression analysis. The results indicated that the petrophysical and geomechanical properties vary widely for the different sedimentary rocks.

2.4. CALIBRATION OF ROCK MECHANICS

There is a growing awareness and recognition in petroleum industry of the value of rock mechanic-based analytical approaches to wellbore stability and sand production problems. Since mechanical testing is often expensive and limited, many scientists prefer to employ the wire-line logs for calculation of mechanical properties.

As mentioned, static and dynamic mechanical properties differ because of different test conditions. The mechanical properties, specifically the Young's modulus and Poisson's ratio of the rock play a crucial role in the design and simulation of drilling, well completion, and stimulation processes. For hydraulic fracturing and other important completion jobs, a vertical profile of mechanical properties with depth is needed. It is highly impractical to develop this vertical profile by static tests on cores. Therefore, the industry standard method is to calibrate the dynamic properties calculated using acoustic and density logs with the static measurements on cores.

The industry has relied on the simple regression technique to calibrate acoustic log derived mechanical properties with static measurements. In this method, as discussed by Gattens et al. (1990) and Ahmed et al. (1991), a transfer function is obtained between the static and dynamic mechanical properties with cross plotting and curve fitting procedures.

Coon (1968), van Heerden (1987), Jizba and Nur (1990), and Morales (1993) developed correlations by comparing elastic properties obtained from laboratory tests on core samples to elastic properties calculated from acoustic logs run in the cored wells. From the plot of dynamic versus static data for several wells in a specific formation, a cloud of points was obtained and a curve fitted to it. Most of the correlations are a variant of the following equation:

$$\text{static} = (A \times \text{dynamic}^c) + B \quad (2.1)$$

where static is the static elastic property and dynamic is the corresponding dynamic elastic property. The constants A, B, and c are determined from the static and dynamic properties data; c is commonly assigned a value of 1. These correlations can be used to obtain first estimates of the static Young's modulus and Poisson's ratio of a formation from dynamic measurements.

Tokle et al. (1986) presented a method to generate a continuous plot of uniaxial compressive strength with respect to depth. The method was based on correlation between standard log parameters with laboratory measured rock data. The developed correlation is applicable to new wells in the same field. The method has been applied to two wells in a North Sea field.

Eissa and Kazi (1988) studied different statistical relations between static and dynamic Young's modulus of the rock. They observed that the linear relationship gives a low coefficient of correlation. They presented a better estimate of the static Young's modulus obtained from an empirical relation between the logarithm of static Young's modulus and the logarithm of the product of dynamic Young's modulus and density.

Tutuncu and Sharma (1992) showed that Young's modulus obtained from ultrasonic > Young's modulus obtained from logs > Young's modulus obtained from

static measurements for tight gas sands. They noted that the dynamic Young's modulus is controlled by factors like stress, clay content, saturation and frequency. These parameters also control the P- and S-wave velocities. In addition to these parameters the static elastic modulus is influenced predominantly by microcracks. They attributed the difference between static and dynamic moduli for both dry and saturated samples to the presence of intergranular contacts and the resulting viscoelastic behavior of the rock.

Farquhar et al. (1994) demonstrated how porosity could be employed as a mechanical index to enable rock mechanical properties to be estimated using general and field specific correlation. General correlations existed between porosity and the uniaxial compressive strength and Young's modulus of sandstones and carbonates. They concluded that the utility of porosity as a mechanical index enabled existing cores and log data to be utilized to extend the use of limited core material.

Yale and Jamieson (1994) carried out a comparison between static and dynamic mechanical properties from two wells in the Chase and Council Grove carbonate sequences of the Hugoton and Panoma fields, Kansas. The purpose of the study was to characterize the mechanical properties of different facies and calibrate the dynamic mechanical properties. Consequently, acoustic logs from other wells can be utilized effectively in determining areal and lithological variation in mechanical properties of the field. Results showed that Young's modulus correlated strongly with lithofacies and porosity. The carbonate sequences could be separated to six "mechanical facies".

Raaen et al. (1996) tested a new method for estimating in-situ mechanical properties from logs. The method –FORMEL (FORmation MEchanical Logging)- was

based on a new constitutive model, describing processes, which occur in rock during mechanical loading. The method has been compared with results from over 200 rock mechanical tests made on cores. It compared favorably with direct correlations based on porosity or sonic compressional transit time; for estimating strength at non-zero confining stress and for porosities below 35%.

Edlmann et al. (1998) proposed a technique of predicting the profile of rock mechanical parameters like Young's modulus, Poisson's ratio, UCS, internal friction angle, cohesion and triaxial stress factor by correlating these with wireline porosity. They calibrated the calculated parameters with laboratory-measured parameters. The correlation of the rock mechanical parameters with the porosity was based on a linear fit. In most of the cases there was considerable scatter. Moreover, this technique was applied only to sandstone and may not be applicable to more inhomogeneous rocks like limestones.

Larsen et al. (2000) showed that static and dynamic Poisson's ratio behave differently with increasing shear stress. Relation between static and dynamic Poisson's ratio was established for the entire stress range of a standard rock mechanics test from initiation up to failure. It gave good prediction of how Poisson's ratio develops during the test. However, occasionally over predicts the Poisson's ratio compared to observations.

Wang (2000) illustrated that the large difference between dynamic and static elastic moduli is mostly caused by the difference in strain amplitudes deployed in measurements and the porous nature of rocks. The difference is large in soft rocks with loose grain boundaries, fractured rocks, and rocks with pores. While in hard and non-fractured rocks the difference is small.

Al-Qahtani and Rahim (2001) presented a mathematical algorithm for modeling geomechanical rock properties of the Khuff and Pre-Khuff reservoirs in Ghawar field. The algorithm consists of calibrating the dynamic Young's modulus and Poisson's ratio with static values, evaluating the minimum horizontal stress using the calibrated parameter and then calibrating the evaluated minimum horizontal stress with measured stress or history matched results. They came up with an estimate of tectonic strain in the minimum and maximum horizontal stress directions.

Rahim and Al-Qahtani (2001) presented sensitivity study on geomechanical properties to determine their impact on fracture dimensions and gas production in the Khuff and Pre-Khuff formations, Ghawar field. Several examples with actual field data have been presented for the reservoirs with multiple producing zones in which fracture is initiated in one or many intervals simultaneously so that the impact of perforations, mechanical properties, and flow characteristics could be identified and calculated. They concluded that increased height and length are obtained in rocks with high Young's modulus. Variation in fracture height and length due to variation in Young's modulus is more pronounced in formations with large in-situ stresses. While Poisson's ratio influences in-situ stress profile, its effect on fracture geometry is minimal.

2.5. IN-SITU STRESS

A representative in-situ minimum horizontal stress profile with depth is a key to the success of any hydraulic fracture design. The stress profile cannot be constructed from the field measurements of in-situ stress. Hence, the stress profile is estimated using calibrated mechanical properties and then calibrated with field measurements of in-situ stress.

Gatens et al. (1990) have presented a scheme to calculate the in-situ stress of low permeability Devonian shales from acoustic logs. It requires calibration of dynamic and static moduli in the first step and then calibration of evaluated in-situ stress using the measured in-situ stress values.

Ahmed et al. (1991) have presented a procedure to evaluate continuous in-situ stress values using log-measured P and S wave travel times. The procedure can be summarized in the following points:

- Calibrate the log derived Poisson's ratio with the static Poisson's ratio using a correlation or regression technique.
- Calculate (σ_h) using the equation

$$\sigma_h = \nu (\sigma_v - \alpha p) / (1 - \nu) + \alpha p \quad (2.2)$$

where ν is the calibrated Poisson's ratio, σ_v is the overburden stress, p is the pore pressure and α is the poroelastic constant.

- Compare the calculated σ_h with the measured σ_h . Minimum horizontal stress is usually measured using microfrac tests.
- If calculated σ_h does not match with measured σ_h , then calibrate the calculated σ_h with respect to the measured σ_h .

Cipolla et al. (1994) presented a case study of the Moxa Arch area, in which measured stress data on three wells were used to calibrate open hole logs to provide an estimate of stress profiles throughout the area. Acoustic log-derived stress profiles were correlated to measured stress data (minifrac tests). Calibrated stress profiles from Acoustic log and the measured data were then used to develop a correlation between gamma ray log and in-situ stress. The log-based stress data was further improved with

the addition of number of minifrac tests. The calibrated stress profile was used to predict the hydraulic fracture geometry.

Blanton and Olson (1997) proposed a model to calculate in-situ stress from acoustic log by incorporating additional terms pertaining to thermal and tectonic strains to fit the calibration standard. This strain corrected method can also provide the estimate of both maximum and minimum horizontal stresses.

Warpinski et al. (1998) compared in-situ stress and moduli derived from different techniques. The in-situ stresses were measured at several points by conducting microfrac tests and then compared to those calculated from the acoustic log. They concluded that the stresses calculated from the log cannot adequately reproduce the actual stress profile and most likely underestimate the magnitude of the in-situ stress contrast that exists around a reservoir zone. They found that the calculated stress using the logs were always lower than the measured stress. They attributed the difference between calculated and measured values to tectonic stress.

Temeng et al. (1999) described the nature of the in-situ stresses in the Permian Khuff reservoir of the Ghawar field. The goal of the study was to obtain the information necessary for designing hydraulic fracturing jobs and for modeling the stability of horizontal wells. Laboratory core data, field tests, and logs comprised the basic data set used in the study. The available data indicated abnormal stress behavior across the field. High anisotropy was observed with respect to the horizontal stresses. The principal stress directions showed general consistency across the field. Analysis of the available information suggested that the vertical overburden stress was not the maximum stress, but rather of intermediate value.

Avasthi et al. (2000) presented a procedure similar to Ahmed et al. (1991) to evaluate the continuous in-situ stress values. They have presented an algorithm to predict the shear velocity, V_s , in case only P wave velocity, V_p , is available. The calibrated continuous in-situ stress values were used in a 3-D fracture simulator to design fracture jobs for maximum pay. They presented two case studies; one dealing with fracture design and another case dealing with wellbore instability.

Salamy and Finkbeiner (2000) addressed the impact of depletion rate on wellbore stability in openhole horizontal completion, Shaybah field, Saudi Arabia. The results of their study indicated that the in-situ stress state could be characterized as a normal faulting environment in which the maximum horizontal stress is oriented N-S.

Onaisi et al. (2000) reported severe wellbore instabilities while drilling horizontal drains at depth of about 2,600 m in offshore Abu Dhabi. The rock mechanics study indicated that the in-situ stress regime is at frontier between thrust and strike-slip, with a major horizontal stress acting NE-SW.

From the previous review, it is clear that the Khafji reservoir was studied extensively in outcrop as well as subsurface. However, no study was carried out to investigate the effect of texture, composition, and depositional environment on the mechanical properties. Also, its dynamic mechanical properties were not calibrated to static mechanical properties.

CHAPTER THREE

GEOLOGICAL PARAMETERS

3.1. INTRODUCTION

From the point of view of rock mechanics, it is the present state of a sedimentary rock and its present mechanical properties, which are of interest. However, one may recognize the fact that the rock has undergone long and complicated processes from its initial state of loose sediment to its present state as a rock (Fjaer et al., 1992).

In addition to erosion, changes in sedimentation environment, changes in sedimentation rate, solution and precipitation of cementing material, a sedimentary basin may be exposed to tectonic forces creating repeated cycles of elevation and depression. These geological activities thus should affect the mechanical properties of a reservoir. Therefore, some knowledge of geological processes is often valuable (Fjaer et al., 1992).

Evaluating rock mechanical behavior is fundamental to the analysis of rock deformation problems encountered in the petroleum industry. Numerical analysis of wellbore stability, sand production, and in-situ stress must deal with a wide variety of rocks ranging from clay-free reservoir sandstones through siltstones to mudstones and shales. Identification of the dominant compositional and textural elements governing rock failure is necessary for improving the knowledge of rock's mechanical behavior.

Rock mechanical properties depend on the interaction between extrinsic and intrinsic factors. Till 1992, quantitative relationships between intrinsic properties and the failure properties of rocks are poorly established because previous studies have not considered the effects of both clay content and porosity. For example, in rocks with nearly constant porosity but varying clay content, strength decreases with increasing clay content, decreasing the average number of grain to grain contacts, decreasing grain size, and decreasing Young's modulus (Plumb et al., 1992; Plumb, 1994).

This chapter describes the geological parameters of the Khafji reservoir (Zuluf field) in well Zuluf-A and its effect on the mechanical properties. It provides a detailed lithologic description of the reservoir as well as compositional and textural analysis based on grain size analysis, petrographic investigation, XRD, and SEM. The main objective is to determine the relationship between compositional, textural elements, and the mechanical properties of the reservoir. Also, the effect of confining pressure. The samples for this study (end pieces of the core samples used for rock mechanical testing) were selected from the same depth intervals, where mechanical tests were carried out.

3.2. GRAIN SIZE

3.2.1. INTRODUCTION

Grain size is a fundamental attribute and thus one of the important descriptive properties of sedimentary rocks. Because of the wide range of particle sizes that occur in rocks, logarithmic or/and geometric scales are more useful for expressing size than linear scales. Udden-Wentworth scale is a geometric scale divided into four major categories (clay, silt, sand, and gravel). A useful modification of the Udden-Wentworth scale is the logarithmic phi scale, which allows grain size data to be expressed in units

of equal value for the purpose of graphic plotting and statistical calculations. This scale, proposed by Krumbein (1934), is based on the following relationship

$$\phi = - \log_2 S$$

where ϕ is phi size and S is the grain size in millimeters (Boggs, 1995).

To investigate the relationship between grain size and rock mechanical properties for the Khafji reservoir, sieve analysis was carried out. Grain size analysis and statistical analysis were performed on twenty one core samples obtained from Zuluf-A. In order to conduct the test, disaggregation was performed to separate the grains without crushing them and to remove all chemically precipitated substances. Folk's (1974) disaggregation method was used.

3.2.2. GRAIN SIZE PARAMETERS

The size frequency distribution of a sediment may be summarized in a table or presented graphically. A grain size cumulative frequency curve is generated by plotting grain size against cumulative weight percent frequency. Statistical parameters provide valuable information about the sample. They can be calculated from certain critical points on the cumulative curve (equations in Table 3.1). These parameters are (Folk, 1974):

1. **Median:** Half of the particles by weight are coarser than the median, and half are finer. It is the diameter corresponding to the 50% mark on the cumulative curve.
2. **Mean:** It is the average of the grain sizes.
3. **Sorting:** Folk's formula includes 90% of the distribution and is the best overall measure of sorting. According to his classification, 0.35ϕ and less is very well sorted, $0.71-1.0\phi$ is moderately sorted, and over 4.0ϕ is extremely poorly sorted.
4. **Skewness:** Measures the degree of asymmetry of the grain size frequency curve, and

TABLE 3.1. Descriptive measures of grain size distribution according to Folk (1974).

Parameters	Equation
Median	$M_d = \phi_{50}$
Mean	$M_z = (\phi_{16} + \phi_{50} + \phi_{84})/3$
Sorting	$\sigma_1 = [(\phi_{84} - \phi_{16})/4] + [(\phi_{95} - \phi_5) / 6.6]$
Skewness	$Sk_1 = [(\phi_{16} + \phi_{84} - \phi_{50}) / 2(\phi_{84} - \phi_{16})] + [(\phi_5 + \phi_{95} - 2\phi_{50}) / 2(\phi_{95} - \phi_5)]$
Kurtosis	$K_G = [(\phi_{95} - \phi_5) / 2.44(\phi_{75} - \phi_{25})]$

whether the curve has a negative or positive skewness. According to Folk's classification, over 0.3ϕ is strongly fine skewed, 0.1 to -0.1ϕ is near symmetrical, and less than -0.3ϕ is strongly coarse skewed. Symmetrical curves have skewness = 0, those with excess fine material have positive skewness and those with excess coarse material have negative skewness.

5. Kurtosis: Measures the degree of peakedness of grain size frequency curve. For normal curves kurtosis = 1.0; leptokurtic curves have skewness over 1.0; platykurtic curves have skewness less than 1.0.

3.2.3. CORRELATION AND DISCUSSION

Figures 3.1A through 3.1E summarize the grain size distribution for the studied samples. Generally, the samples are well sorted to moderately well sorted. Table 3.2 summarizes the descriptive statistics result. As shown in the table, the samples have a wide range of median (between 3.65 and 0.75) and mean (between 3.57 and 0.8), and different degree of sorting, skewness, and kurtosis.

Young's modulus (E) and Poisson's ratio (ν) related to different confining pressure were correlated with the grain size parameters of the Khafji reservoir. These rock mechanical properties were measured from core samples collected at different depth intervals of the well. Simple linear regression was applied to explore the existence of a relationship between the grain size parameters and rock mechanical properties. The following observations were found:

1. Median: The linear regression between median grain size and the mechanical properties Young's modulus and Poisson's ratio does not show any significant correlation. The values of correlation coefficient (r) are 0.07 for Young's modulus (1000 psi) and 0.16 for Young's modulus (2900 psi). While it is 0.37 for Poisson's ratio

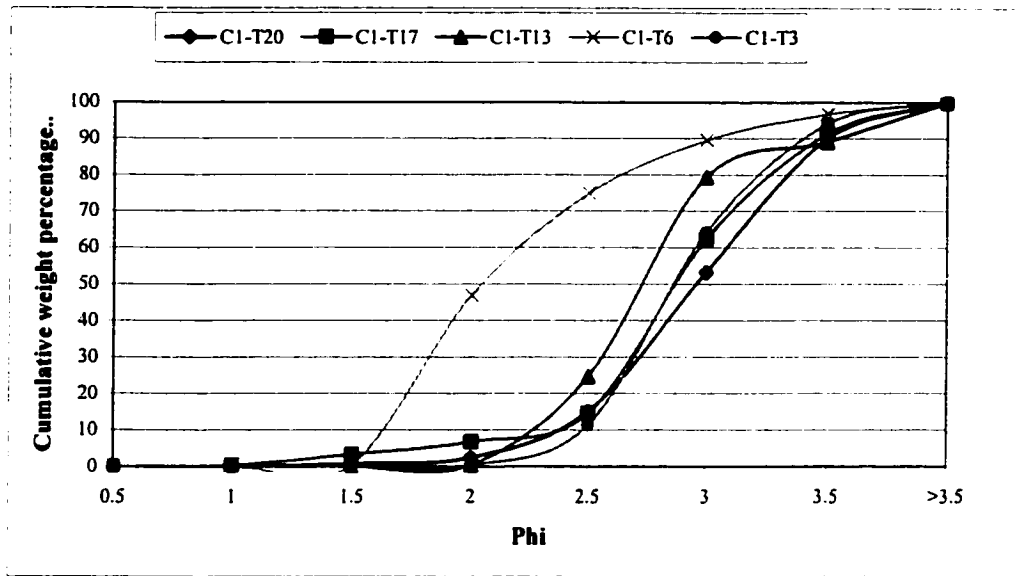


Figure 3.1A. Grain size distribution for C1 samples.

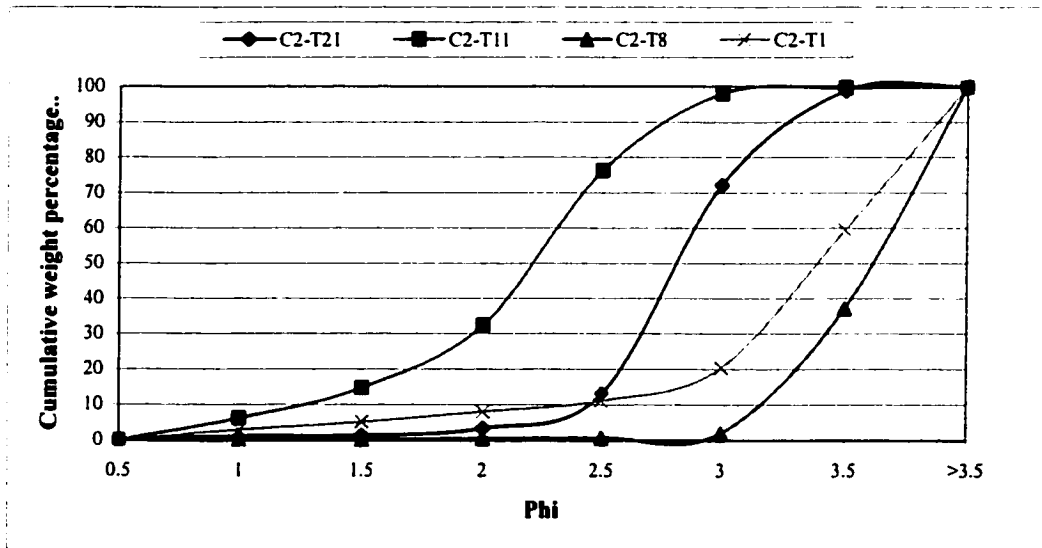


Figure 3.1B. Grain size distribution for C2 samples.

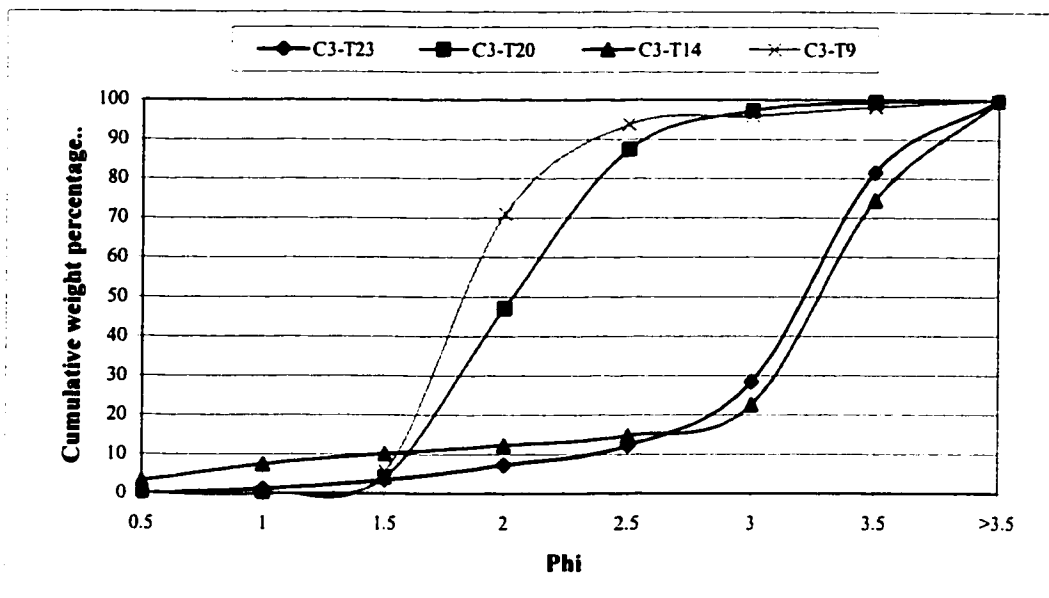


Figure 3.1C. Grain size distribution for C3 samples.

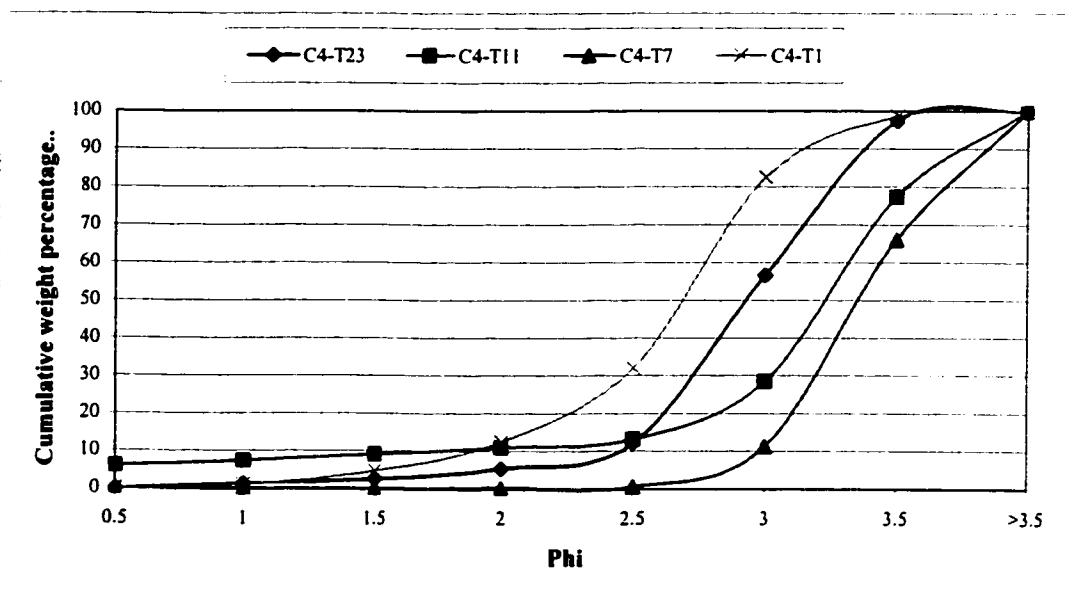


Figure 3.1D. Grain size distribution for C4 samples.

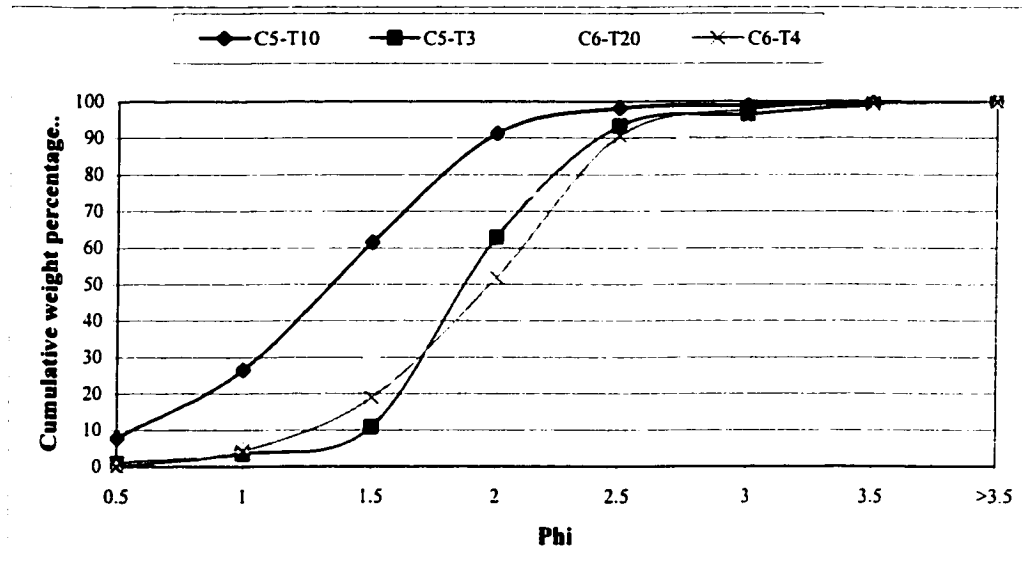


Figure 3.1E. Grain size distribution for C5 and C6 samples.

TABLE 3.2. Descriptive statistics results for the studied samples.

Sample #	Median	Mean	Sorting	Skewness	Kurtosis	Conf. Pressure (psi)	E _{static}	v _{static}
C1-T20	2.95	2.97	0.49	1.38	0.45	2900	1.71E+06	0.184
C1-T17	2.83	2.90	0.52	1.14	0.51	2900	1.84E+06	0.255
C1-T13	2.73	2.78	0.48	1.67	0.31	2900	1.57E+06	0.228
C1-T6	2.05	2.17	0.57	2.17	0.57	2900	1.66E+06	0.170
C1-T3	2.85	2.9	0.39	1.16	0.33	2900	1.41E+06	0.210
C3-T23	3.2	3.15	0.55	0.68	0.46	2900	1.13E+06	0.150
C3-T20	2.05	2.04	0.42	1.04	0.34	2900	1.38E+06	0.161
C3-T14	3.25	3.18	0.73	-1.68	0.66	2900	1.54E+06	0.246
C3-T4	1.8	1.85	0.37	1.07	0.22	2900	1.91E+06	0.238
C2 -T21	2.8	2.85	0.35	0.87	0.20	1000	8.64E+05	0.214
C2 -T11	2.2	2.12	0.58	0.49	0.6	1000	1.07E+06	0.242
C2-T8	3.6	3.57	0.32	1.15	0.21	1000	8.57E+05	0.227
C2-T1	3.35	3.28	0.61	-0.11	0.59	1000	5.83E+05	0.299
C4 -T23	2.9	2.92	0.41	0.85	0.33	1000	1.06E+06	0.200
C4 -T11	3.2	3.13	0.78	-1.78	0.82	1000	1.10E+06	0.305
C4-T7	3.35	3.38	0.35	1.12	0.26	1000	1.24E+06	0.243
C4-T1	3.65	2.92	0.52	-1.53	0.44	1000	1.02E+06	0.144
C5-T10	0.75	0.8	0.5	0.82	0.51	1000	1.08E+06	0.119
C5-T3	1.85	1.9	0.43	0.83	0.36	1000	9.98E+05	0.147
C6-T20	1.75	1.8	0.64	1.78	0.79	1000	1.27E+06	0.167
C6-T4	1.95	1.9	0.53	0.81	0.54	1000	8.43E+05	0.140

(1000 psi) and 0.01 for Poisson's ratio (2900 psi). (Figures 3.2 and 3.3). For Young's modulus case, increasing confining pressure lead to increase Young's modulus value. However, this not clear for Poisson's ratio.

2. Mean: The linear regression between mean grain size and the mechanical properties Young's modulus and Poisson's ratio does not show any significant correlation. The values of correlation coefficient (r) are 0.07 for Young's modulus (1000 psi) and 0.13 for Young's modulus (2900 psi). While it is 0.49 for Poisson's ratio (1000 psi) and 0.01 for Poisson's ratio (2900 psi). (Figures 3.4 and 3.5). For Young's modulus case, increasing confining pressure lead to increase Young's modulus value. However, this not clear for Poisson's ratio.

3. Sorting: The linear regression between sorting and the mechanical properties Young's modulus and Poisson's ratio does not show any significant correlation. The values of correlation coefficient (r) are 0.01 for Young's modulus (1000 psi) and 0.01 for Young's modulus (2900 psi). While it is 0.07 for Poisson's ratio (1000 psi) and 0.01 for Poisson's ratio (2900 psi). (Figures 3.6 and 3.7). For Young's modulus case, increasing confining pressure lead to increase Young's modulus value. However, this not clear for Poisson's ratio.

4. Skewness: The linear regression between sorting and the mechanical properties Young's modulus and Poisson's ratio does not show any significant correlation. The values of correlation coefficient (r) are 0.02 for Young's modulus (1000 psi) and 0.03 for Young's modulus (2900 psi). While it is 0.1 for Poisson's ratio (1000 psi) and 0.11 for Poisson's ratio (2900 psi). (Figures 3.8 and 3.9). For Young's modulus case, increasing confining pressure lead to increase Young's modulus value. However, this not clear for Poisson's ratio.

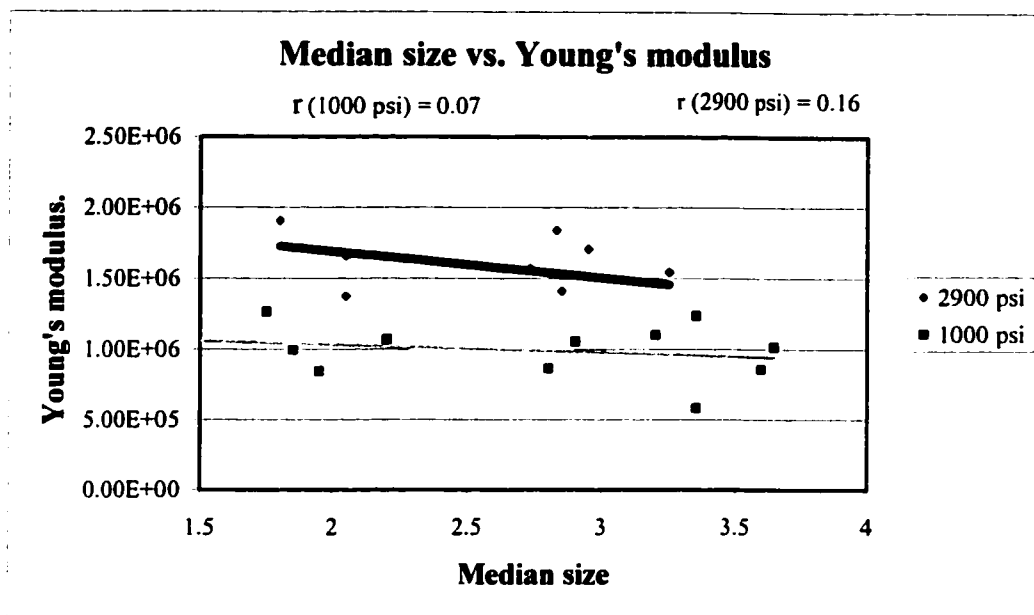


Figure 3.2. Correlation between median size and Young's modulus.

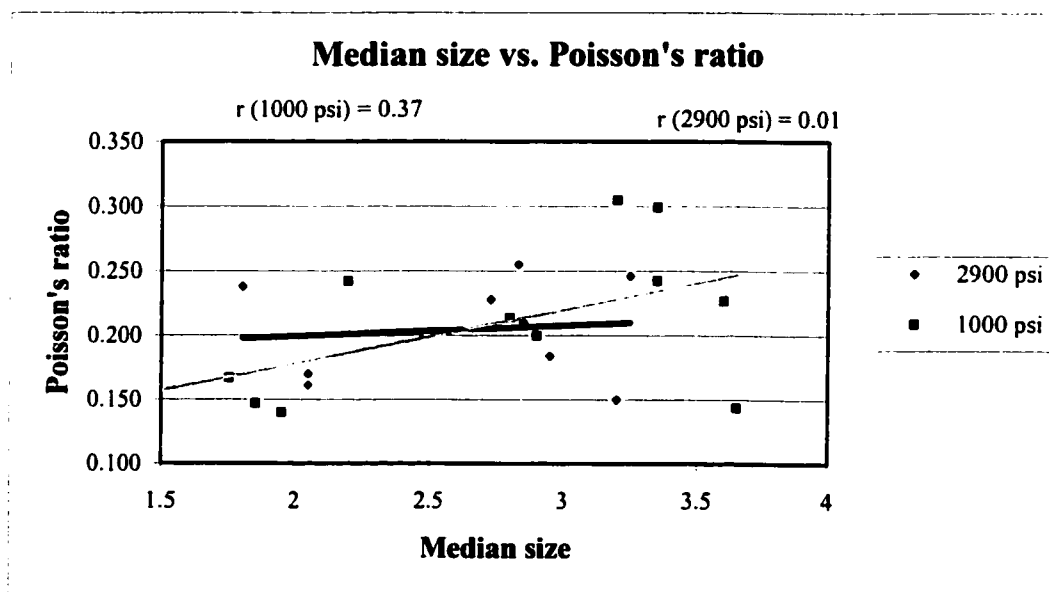


Figure 3.3. Correlation between median size and Poisson's ratio.

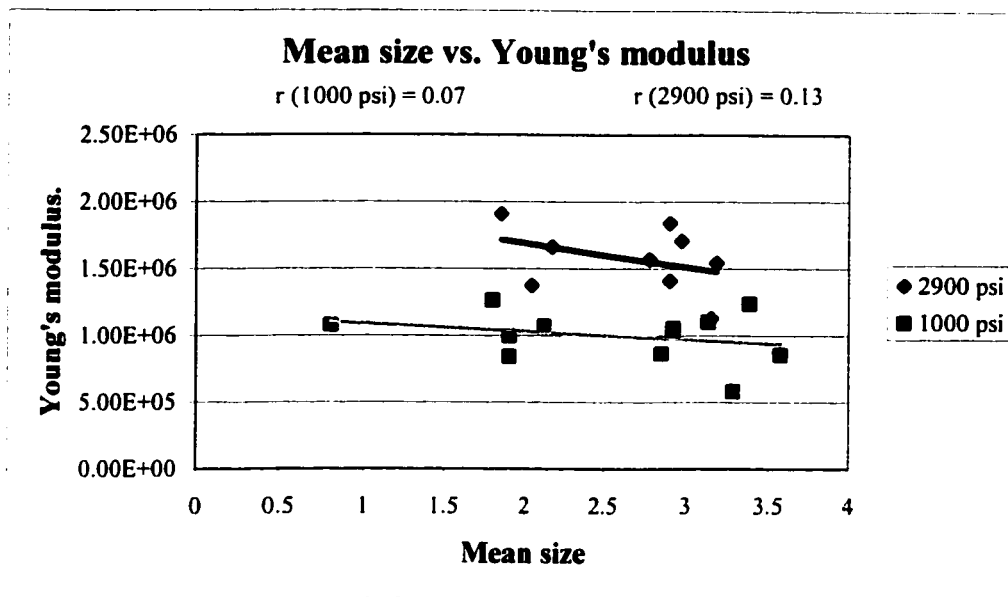


Figure 3.4. Correlation between mean size and Young's modulus.

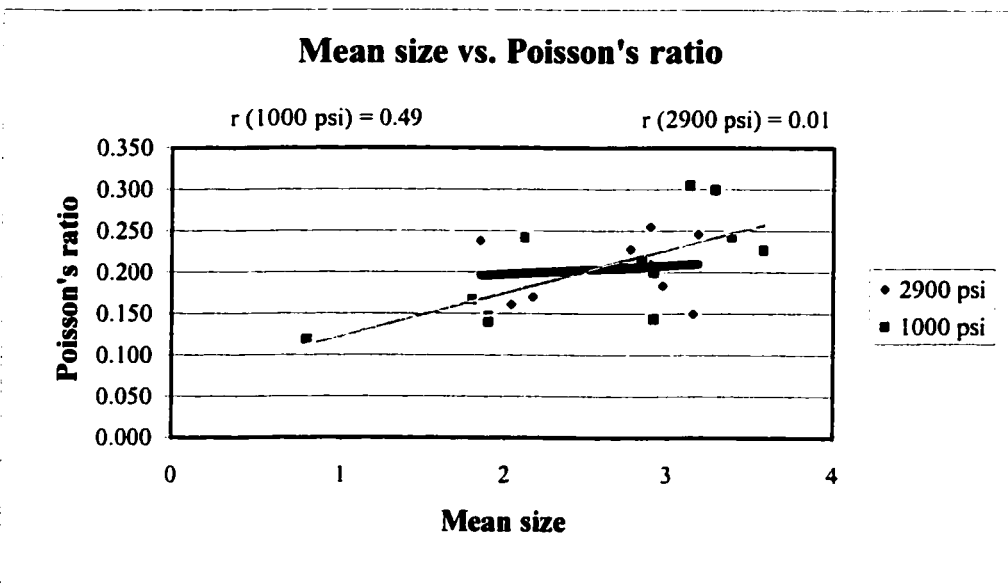


Figure 3.5. Correlation between mean size and Poisson's ratio.

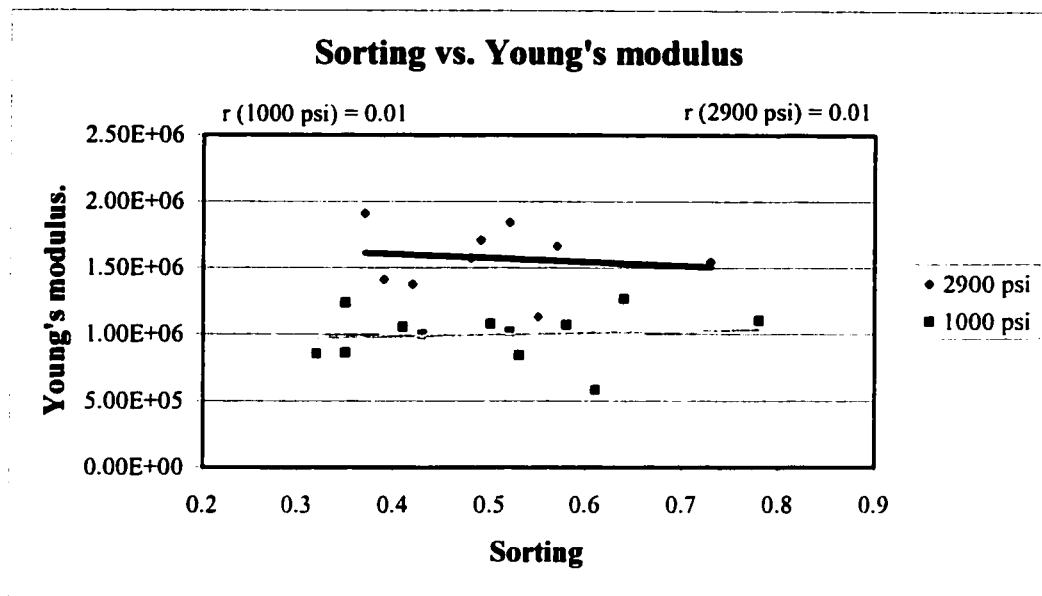


Figure 3.6. Correlation between sorting and Young's modulus.

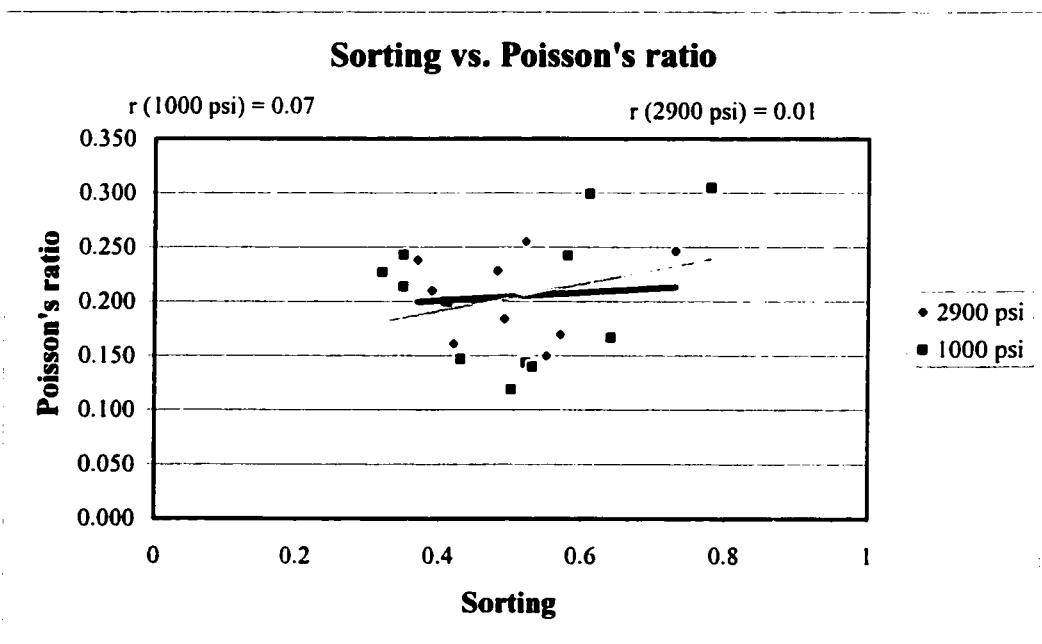


Figure 3.7. Correlation between sorting and Poisson's ratio.

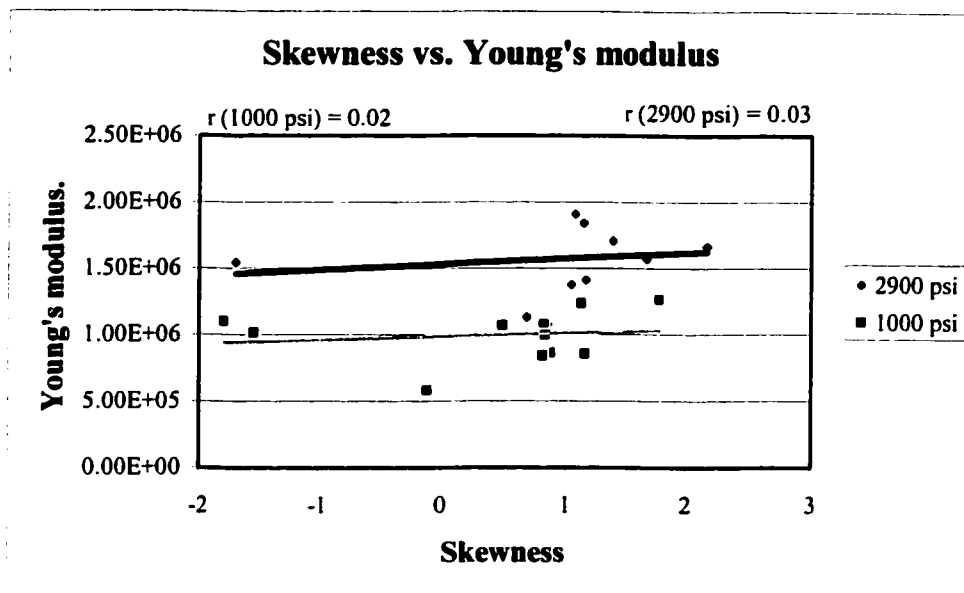


Figure 3.8. Correlation between skewness and Young's modulus.

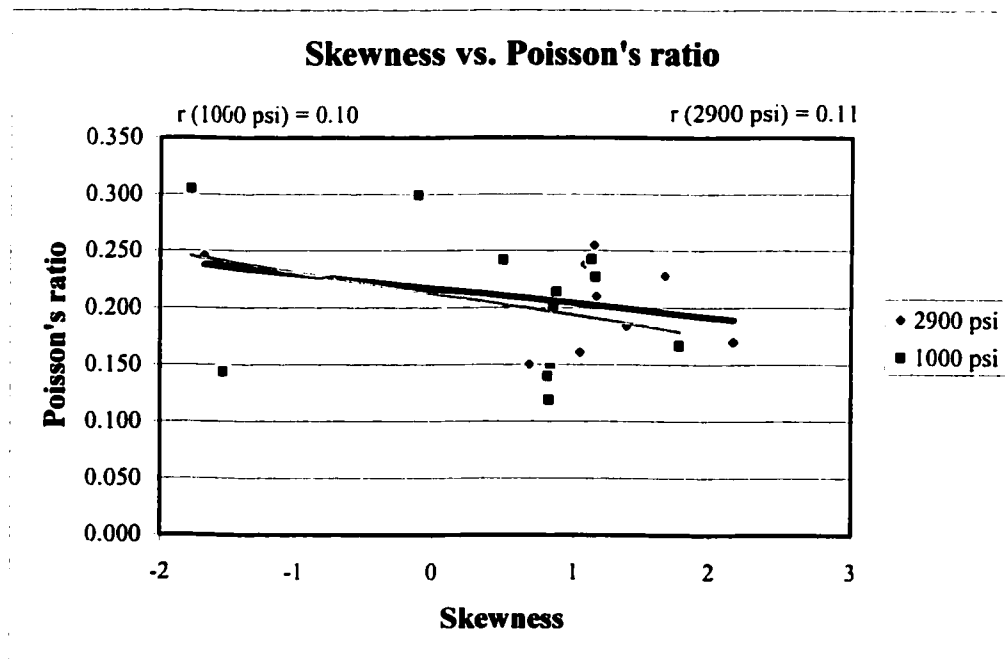


Figure 3.9. Correlation between skewness and Poisson's ratio.

5. Kurtosis: The linear regression between kurtosis and the mechanical properties Young's modulus and Poisson's ratio does not show any significant correlation. The values of correlation coefficient (r) are 0.04 for Young's modulus (1000 psi) and 0.01 for Young's modulus (2900 psi). While it is 0.02 for Poisson's ratio (1000 psi) and 0.01 for Poisson's ratio (2900 psi). (Figures 3.10 and 3.11). For Young's modulus case, increasing confining pressure lead to increase Young's modulus value. However, this not clear for Poisson's ratio.

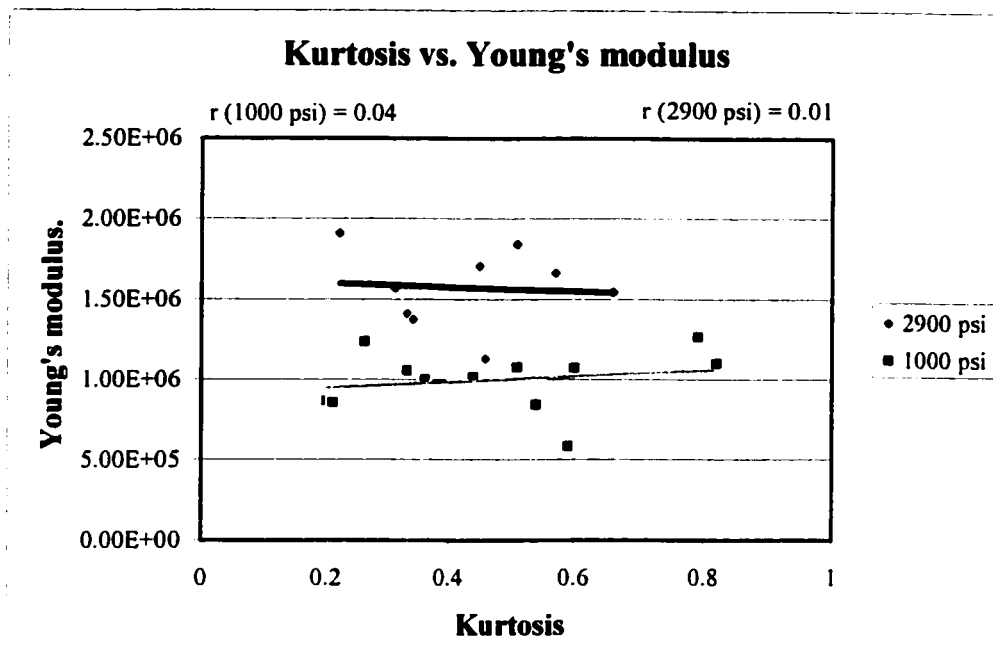


Figure 3.10. Correlation between kurtosis and Young's modulus.

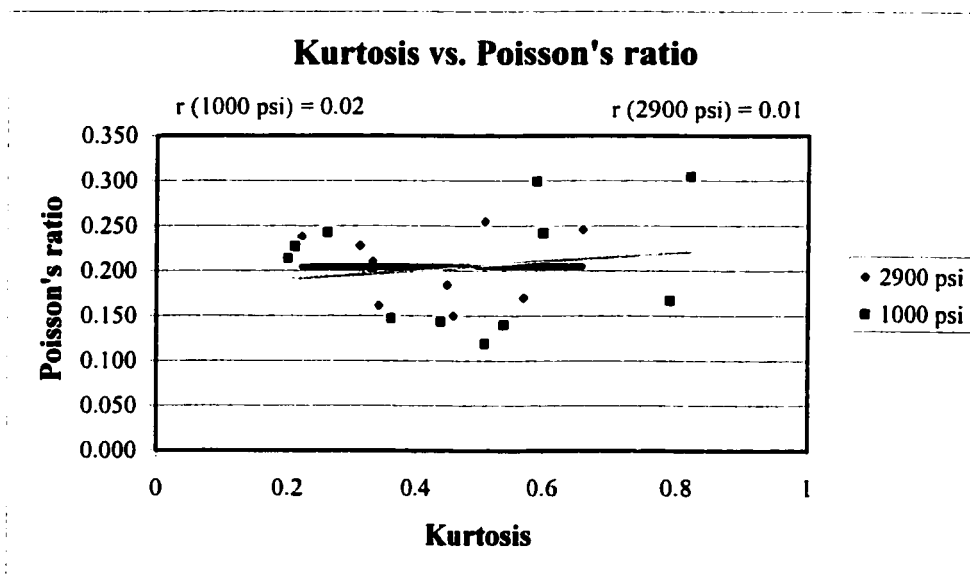


Figure 3.11. Correlation between kurtosis and Poisson's ratio.

3.3. MINERALOGY AND GRAINS CONTACT

3.3.1. INTRODUCTION

Intrinsic rock properties of the Khafji reservoir were qualified by petrographic analysis. The long dimension of the thin section was cut parallel to the bedding.

In Zuluf field, Khafji reservoir consists of a thick sequence of quartz sandstone, siltstone, shale, and various types of ironstone. The following information was recorded for each sample:

1. Mineralogical composition: Constituent minerals such as quartz, feldspar, chert, clay, and opaque.
2. Grain to grain contact: The total number of grain to grain contact was recorded.

3.3.2. MINERALOGICAL COMPOSITION

Composition is a fundamental property of sedimentary rocks. Furthermore, it is the most useful sediment property for the purpose of rock classification. Siliciclastic sedimentary rocks are composed predominantly of terrigenous constituents derived by subaerial weathering processes and terrestrial volcanism. Although hundreds of silicate minerals are known, a very small number of mineral varieties, together with rock fragments, make up all siliciclastic sedimentary rocks. The most common siliciclastic minerals and rock fragments are (Boggs, 1987):

1. **Quartz:** Is the dominant mineral in most siliciclastic sedimentary rocks. Quartz makes up about 65% of the average sandstone and 30% of the average mudrock (Blatt et al., 1980).
2. **Feldspars:** These are less abundant than quartz in most siliciclastic sedimentary rocks, they are the second most abundant mineral in siltstones and sandstones.

Feldspars make up about 10-15% of the constituents of average sandstone and about 5% of average mudrock (Blatt et al., 1980).

3. Clay minerals: These minerals make up about 25-35% of the constituents of siliciclastic sedimentary rocks as a whole, but they may compose more than 60% of the minerals in mudrocks. They must be identified by X-ray diffraction techniques, electron microscopy, or other nonoptical methods. The most common clay mineral groups are illite, smectite, kaolinite, and chlorite.

4. Accessory minerals: They have an average abundance in sedimentary rocks of less than about 1%. These minerals include the common micas, biotite and muscovite, and the heavy minerals.

5. Rock fragments: These make up about 10-15% of the grains in average sandstones.

3.3.2.1. RESULT

Percentage of minerals was determined for each sample. Table 3.3 summarizes the result of the mineralogical composition investigation for samples from well Zuluf-A. Quartz dominates the composition of the studied samples with its values varied between 49% and 98% (Plate 3.1). The monocrystalline type is the dominant variety. Under normal light quartz grains are colourless. When examined under cross polarizing light, quartz grains exhibits sweeping pattern of extinction (Plate 3.1B).

Feldspar is very rare in the studied samples. Depending on the optical properties, most of the feldspar grains are plagioclase. While muscovite is not observed in the studied samples.

Opaque minerals are occurs as minor (up to 8%). It is present in almost all the samples. Also, rock fragments occur as minor (up to 2%). A few grains of cherts are identified.

TABLE 3.3. Mineralogical composition of core samples from well Zuluf-A.

Sample*	Q %	F %	Ch %	Ma %	Op %	Ot %
C1-T20	94	0	1	1	2	2
C1-T13	77	2	5	10	3	3
C1-T6	97	0	0	1	1	1
C1-T3	95	1	1	1	1	1
C3-T23	96	0	0	2	1	1
C3-T20	98	0	0	0	1	1
C3-T14	76	1	1	20	1	1
C3-T4	59	0	5	30	4	2
C2-T21	73	0	0	25	1	1
C2-T11	83	0	0	15	1	1
C2-T8	83	0	2	10	4	1
C2-T1	49	0	2	40	8	1
C4-T23	97	0	1	0	1	1
C4-T11	60	1	2	27	6	4
C4-T7	88	0	0	11	0	1
C4-T1	96	0	0	2	1	1
C5-T10	99	0	0	0	0	1
C5-T3	97	0	0	1	1	1
C6-T20	89	0	0	5	5	1
C6-T4	98	0	1	0	0	1

* Detailed lithology in Appendix B

Q - quartz, F- feldspar, Ch - chert, Ma - matrix, Op - opaque, Ot – others.

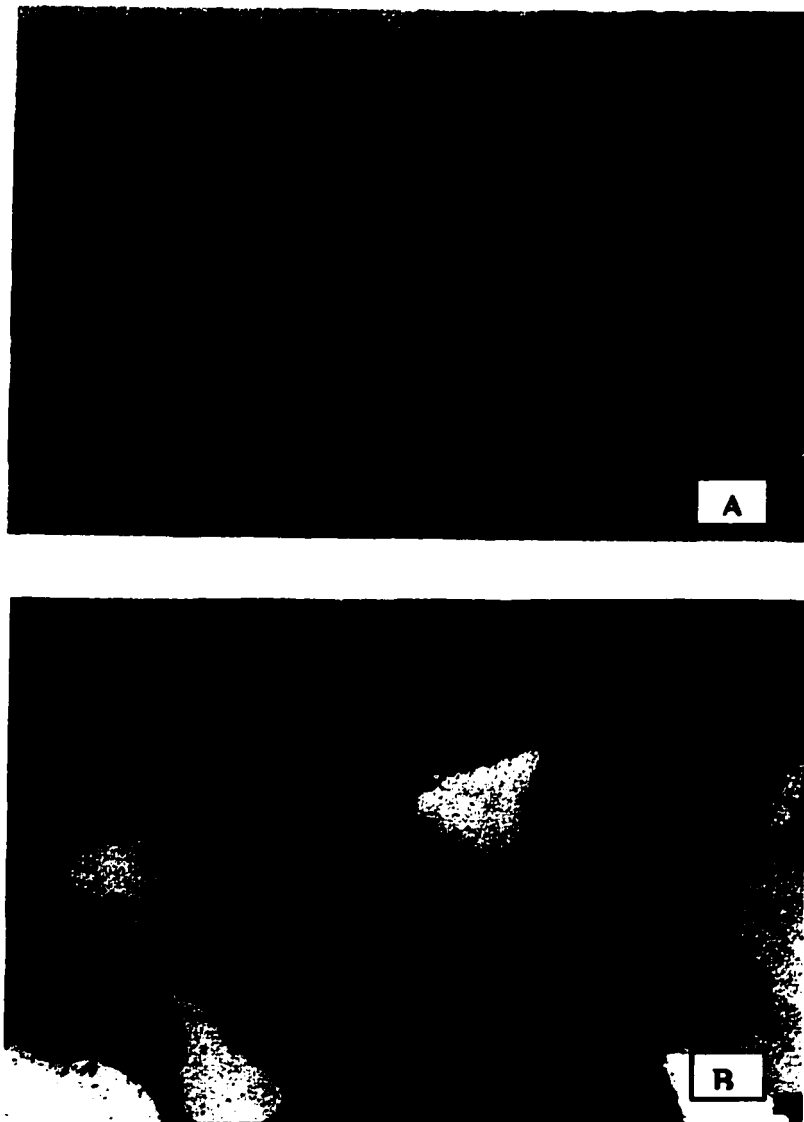


Plate 3.1. Photomicrographs of typical composition of sample C6-T4 dominated by quartz (X10). A: Under plane light, B: Under cross-polarized light.

The amount of matrix in the investigated samples is ranging from 0% to 40% (Plate 2). However, values greater than 10% recorded in 9 samples.

On the basis of the quartz, feldspar, and lithic (QFL) classification, the main sand reservoir studied samples are classified as quartz arenite. While the stringer sand reservoir samples are dominated by quartz wacke (Figure 3.12).

The clay fractions of two samples were separated using the standard technique of Folk (1974). This technique helps to perform a complete separation of the clay portion out of the clay rich silt and fine sand sediments. The clay fractions were analyzed for their mineralogical phases using a XRD device.

The XRD study, which is mainly used to complement the microscopic results, proved to be of limited success. The huge percentage of quarts in the studied samples dominated the result. Making it difficult to identify the clay minerals. However, the XRD data revealed that kaolinite is the main clay mineral in the samples (Figures 3.13 and 3.14).

Representative samples were investigated by using scanning electron microscope (SEM) and the energy dispersive x-ray (EDS). The EDS of samples shows that most of the samples are rich in silica, which indicates quartz enrichment. The relatively high content of Al may indicate the presence of kaolinite that appeared in XRD test (Figures 3.15 A and 3.15B).

SEM study shows quartz growth in pore fills. Also, shows clay minerals mainly kaolinite coating quartz grains and some drilling additives, halite, and pyrite crystals (Figures 3.15D, 3.15E, and 3.15F). Granular morphology of kaolinite is revealed by SEM as well (Figures 3.15C).

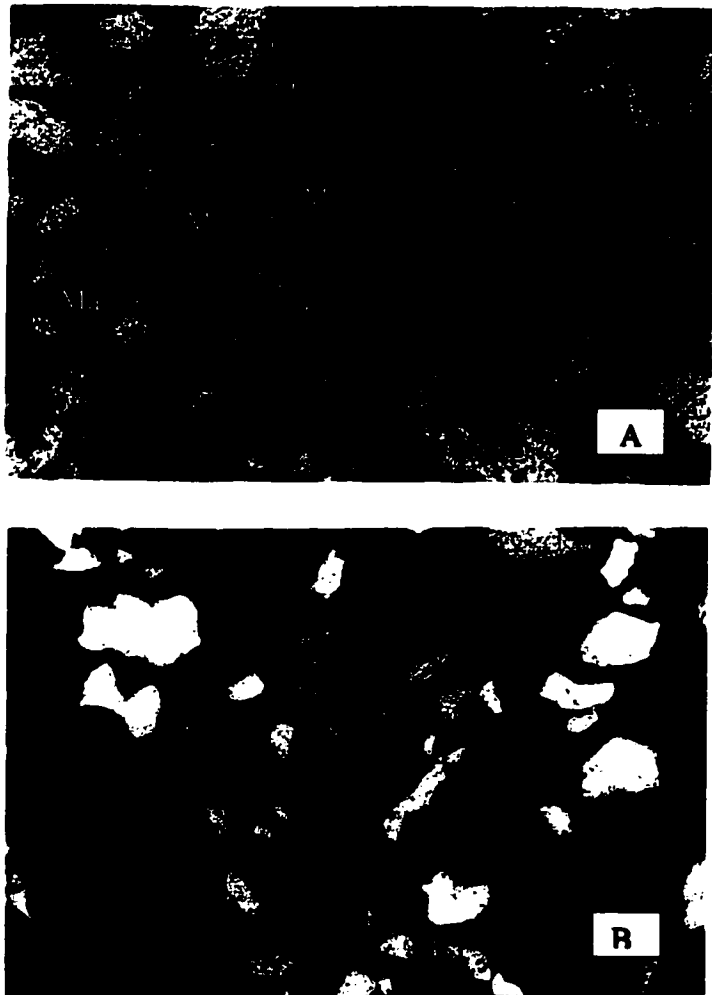


Plate 3.2. Photomicrographs of typical composition of sample C2-T1 showing the highest amount of matrix (X10). A: Under plane light, B: Under cross-polarized light.

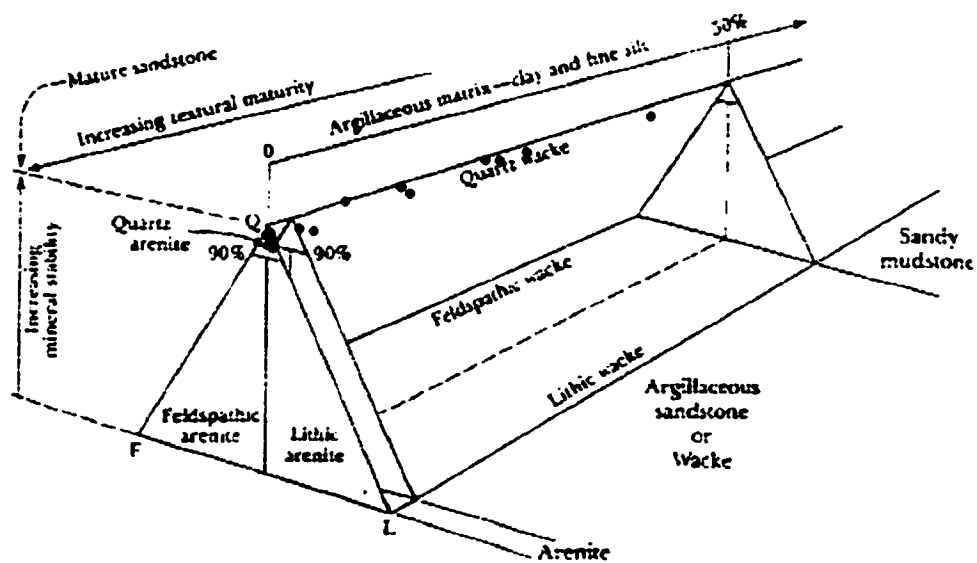


Figure 3.12. Classification of Khafji reservoir studied samples on the basis of QFL components (Dot, 1964).

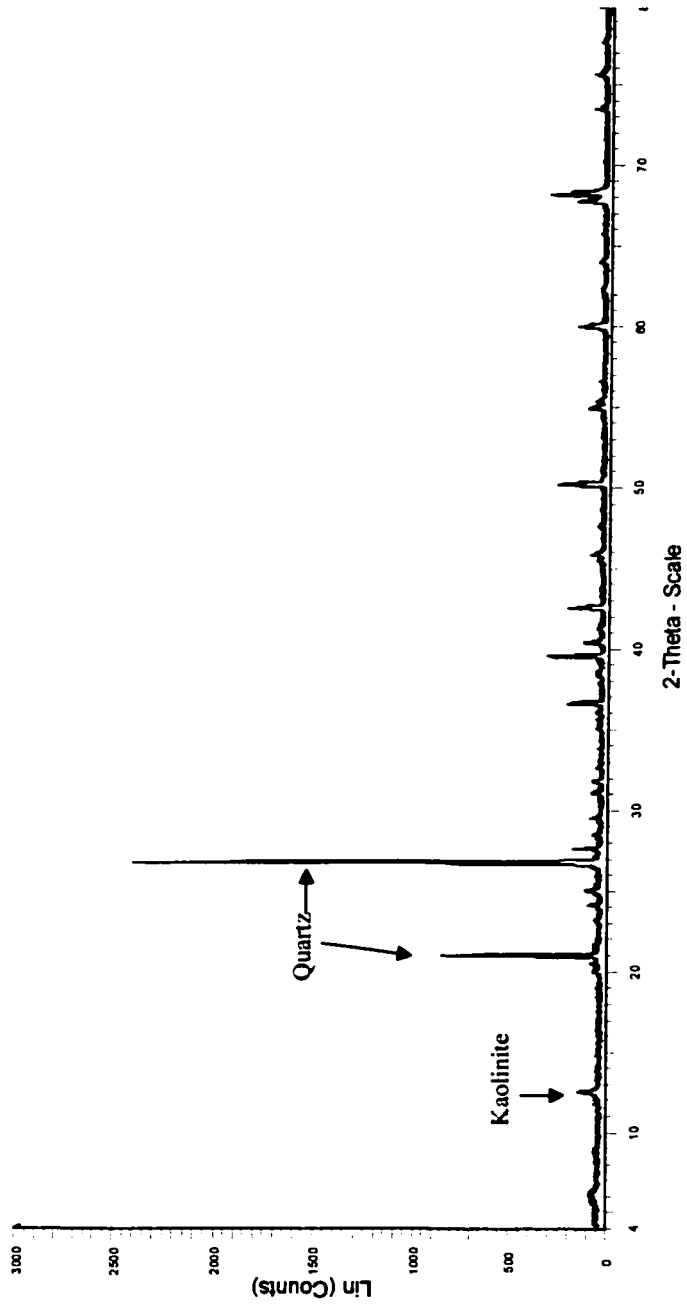


Figure 3.13. Typical x-ray diffractogram showing general clay mineralogy of sample C1-T13.

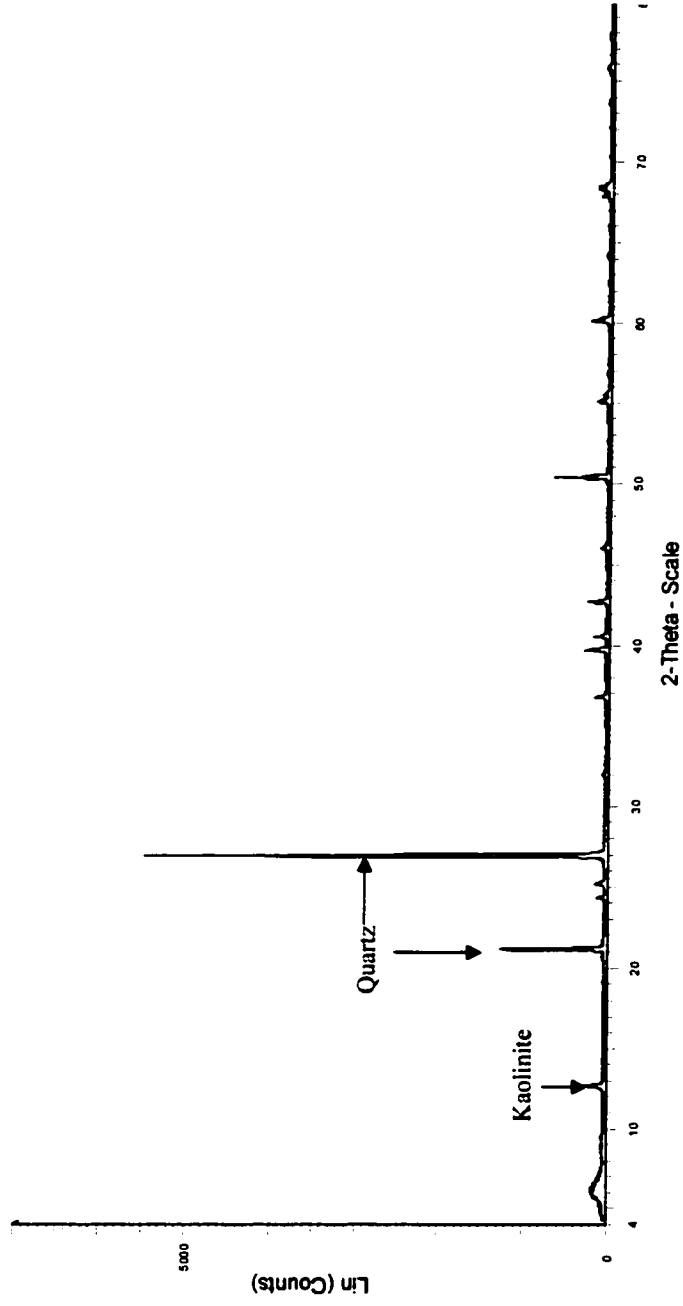


Figure 3.14. Typical x-ray diffractogram showing general clay mineralogy of sample C4-T7.

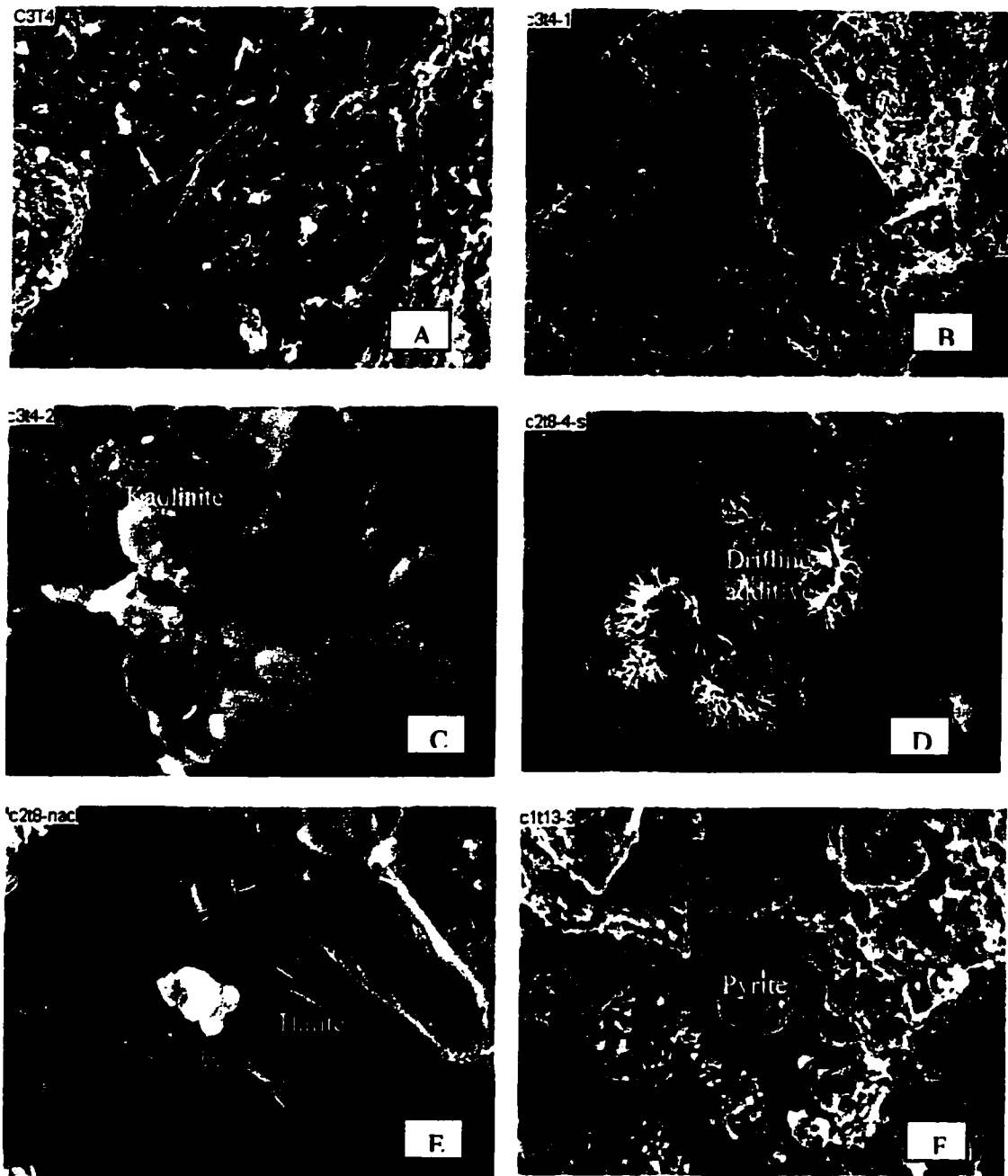


Figure 3.15. Photomicrographs showing (A) and (B) general view of samples (C) kaolinite (D) drilling additives (E) halite crystals. (F) pyrite crystal.

3.3.2.2. CORRELATION AND DISCUSSION

Simple linear regression was applied to explore the existence of a relationship between calculated percentages of quartz and rock mechanical properties, i.e, Young's modulus and Poisson's ratio.

The linear regression between quartz percentage and Young's modulus and Poisson's ratio does not show any significant correlation for the former and a significant correlation for the later. The values of correlation coefficient (r) are 0.24 for Young's modulus (1000 psi) and 0.42 for Young's modulus (2900 psi). While it is 0.73 for Poisson's ratio (1000 psi) and 0.71 for Poisson's ratio (2900 psi). (Figures 3.16 and 3.17). For Young's modulus case, increasing confining pressure lead to increase Young's modulus value. However, this not clear for Poisson's ratio.

3.3.3. GRAINS CONTACT

The properties of sedimentary rocks change continuously during burial. Sediment compaction is driven by mechanical stress from the overburden and by the chemical reactions controlled by thermodynamics and kinetics (Bjorlykke, 2001).

Compaction forces grains into closer contact and causes changes in the types of grain to grain contacts. Taylor (1950) identified four types of grain contacts that can be observed in thin sections: tangential contact, or point contact; long contact, appearing as straight line in the plane of a thin section; concavoconvex contact, appearing as a curved line in the plane of a thin section; and sutured contact, caused by mutual stylolitic interpretation of two or more grains.

In very loosely packed fabric, some grains may not make contact with other grains in the plane of the thin section and are referred to as floating grains. Contact types are related to both the particle shape and the packing. Tangential contacts occur

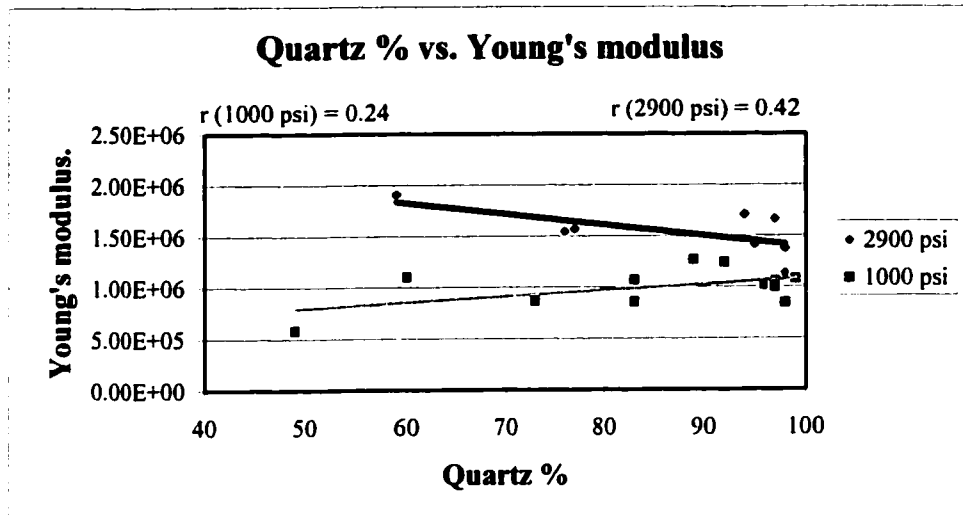


Figure 3.16. Correlation between quartz percentage and Young's modulus.

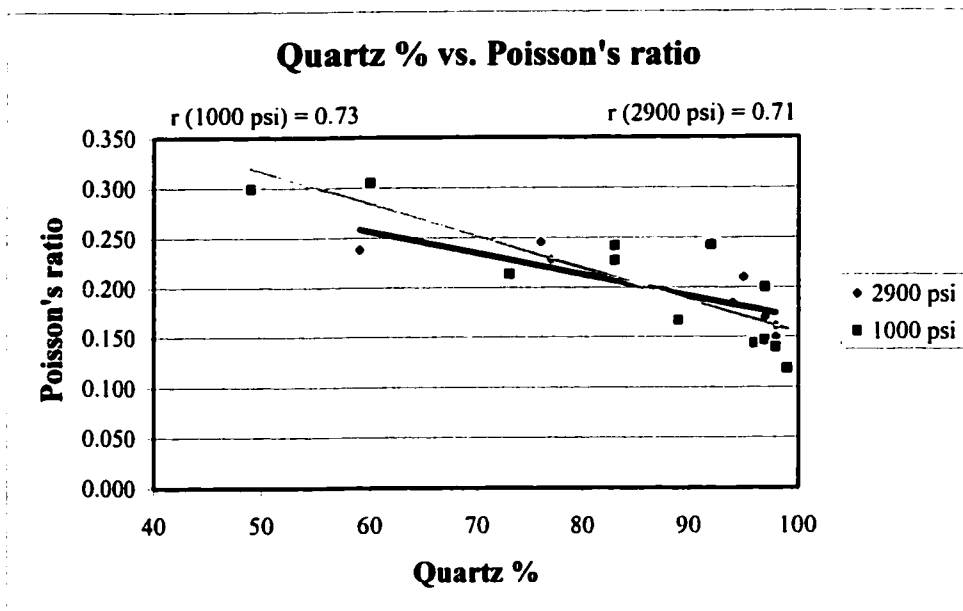


Figure 3.17. Correlation between quartz percentage and Poisson's ratio.

only in loosely packed sediments or sedimentary rocks, whereas concavoconvex contacts and sutured contacts occur in rocks that have undergone considerable compaction during burial. The relative abundance of these various types of contacts can be used as a measure of degree of compaction and thus depth of burial of sandstones (Boggs, 1987).

3.3.3.1. RESULT

The relative grain contacts abundance of samples from well Zuluf-A was estimated during the thin-section petrographic study. Table 3.4. shows different types and percentages of grain contacts observed in thin section. A total of twenty one-thin sections were studied.

The upper stringer sands unit characterized by very fine to fine grain size and subangular to subrounded grains. On the other hand, the main sand unit is characterized by medium to coarse grain and subangular to subrounded grains.

3.3.3.2. CORRELATION AND DISCUSSION

Simple linear regression was applied to explore the relationship between calculated percentage grain contact and rock mechanical properties.

The linear regression between percentage of grain contact and Young's modulus and Poisson's ratio does not show any significant correlation for the former and a significant correlation for the later. The values of correlation coefficient (r) are 0.02 for Young's modulus (1000 psi) and 0.39 for Young's modulus (2900 psi). While it is 0.77 for Poisson's ratio (1000 psi) and 0.73 for Poisson's ratio (2900 psi) (Figures 3.18 and 3.19). For Young's modulus case, increasing confining pressure lead to increase Young's modulus value. However, this not clear for Poisson's ratio.

TABLE 3.4. Textural attributes of core samples from well Zuluf-A.

Sample	Grain size	Contact %
C1-T20	Fine	98
C1-T17	Fine	70
C1-T13	Fine	85
C1-T6	Medium	95
C1-T3	Fine	87
C3-T23	Fine	95
C3-T20	V. fine to fine	95
C3-T14	V. fine to fine	84
C3-T4	V. fine to fine	71
C2-T21	Fine	70
C2-T11	Fine to medium	57
C2-T8	V. fine	54
C2-T1	V. fine to fine	20
C4-T23	Fine	95
C4-T11	V. fine to fine	7
C4-T7	V. fine to fine	40
C4-T1	Fine to medium	89
C5-T10	Coarse	99
C5-T3	Coarse	82
C6-T20	Medium to coarse	61
C6-T4	Medium to coarse	72

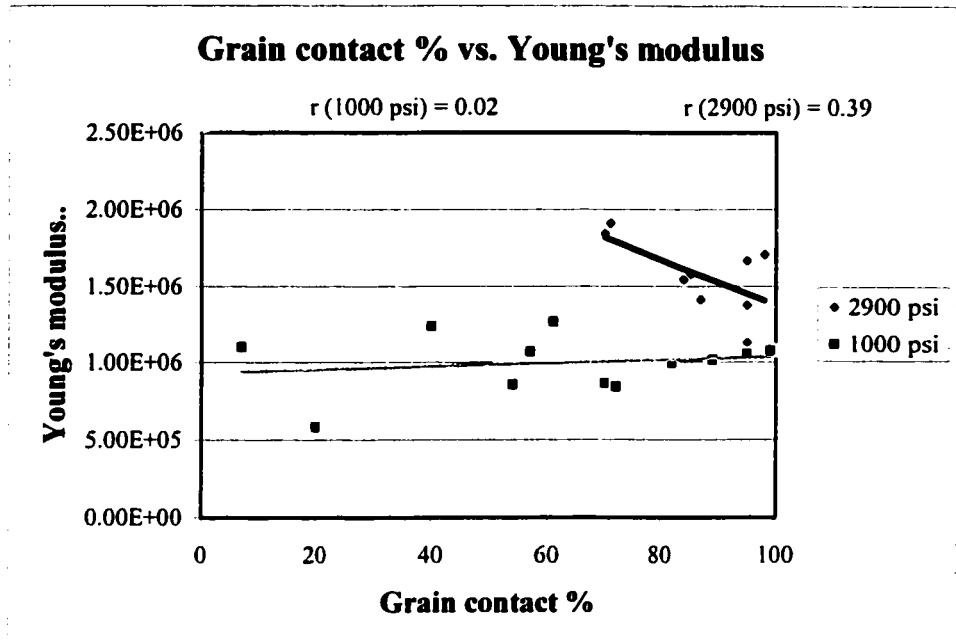


Figure 3.18. Correlation between grain contact percentage and Young's modulus.

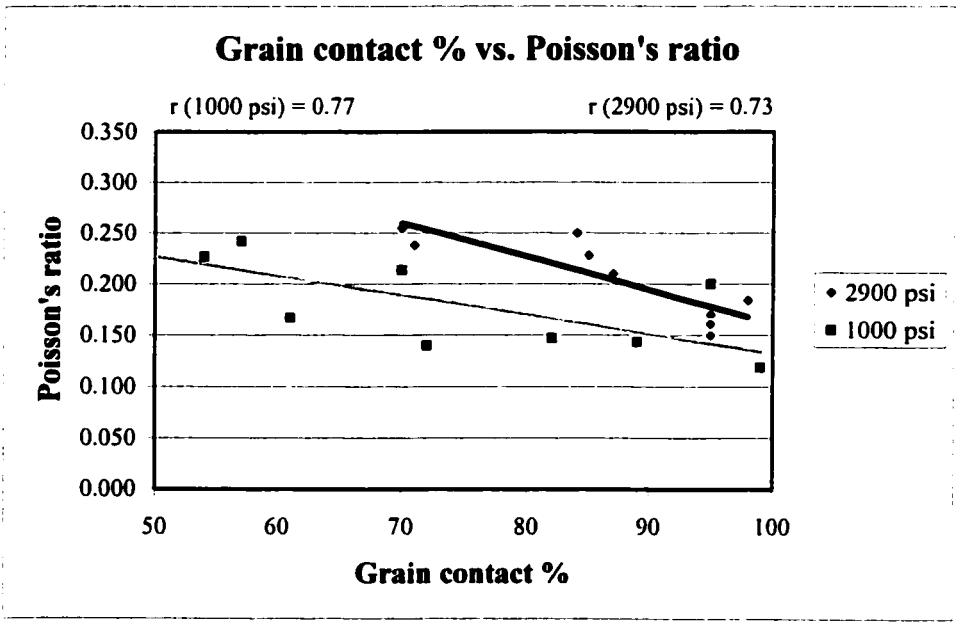


Figure 3.19. Correlation between grain contact percentage and Poisson's ratio.

3.4. DEPOSITIONAL ENVIRONMENT

3.4.1. INTRODUCTION

Rivers are the main agents that transport sediments from land to the coastal regions of seas and lakes, where these sediments are deposited in thick sequences or transported further to continental shelves and deep sea basins and produce deep water sediments. Deltas and deltaic deposits are formed from the interaction of fluvial and coastal processes. Thus, in a deltaic environment fluvial processes generally play a very important role. For practical purposes fluvial deposits can be grouped into three major groups (Reineck and Singh, 1980):

1. **Channel deposits.** They are sediment deposits formed mainly from the activity of river channels. They include channel lag deposits, point bar deposit, channel bar deposit, and channel fill deposit.
2. **Bank deposits.** They are sediment deposits formed on the river banks and are produced during flood periods. They include levee deposits and crevasse splay deposits.
3. **Flood basin deposits.** They are essentially fine-grained sediment deposits formed during heavy floods when river water flows over the levees into the flood plain. They include flood plain deposits and marsh deposits.

According to Reineck and Singh (1980), a delta is made up of:

1. **Topset deposits.** Mainly made of marsh deposits and deltafront. Also present are river channel deposits and natural levee deposits, together with crevasse splay deposits.
2. **Foreset deposits.** Made up of pro-delta and deltaic distributaries.
3. **Bottomset.** Made up of offshore clays under the influence of active deltas.

3.4.2. KHAFJI RESERVOIR DEPOSITIONAL ENVIRONMENT

According to Grant and Al-Humam (1994), the upper stringer sand interval of the Khafji reservoir was deposited in a delta-plain setting consisting of meandering channels and associated point-bar deposits, distributary channels, crevasse splays, levees, and interdistributary bay environments. Facies associated with it are characterized by much more laterally extensive shales and laterally discontinuous sandstones than the main sand interval. The main sand interval is interpreted to have been deposited in a delta-front setting consisting of delta-front mouth bar and distributary channel complexes. The main sand interval is dominated by laterally continuous, massive to cross-bedded sandstones that are locally broken up by laterally discontinuous shales.

3.4.3. GRAIN SIZE AND DEPOSITIONAL ENVIRONMENT

There have been numerous attempts to relate statistical parameters calculated from grain size distributions to deposition environments. Visher (1965) showed that various subenvironments of a fluvial sequence could be characterized by detailed grain size studies. Muiola and Weiser (1968) concluded that the combination of mean diameter and skewness is most effective in differentiating between beach and inland dune sands and inland dune and coastal dune sands. Also, they mentioned that the combination of mean diameter and standard deviation is the most effective in differentiating between beach and river sands and river and coastal dune sands. McLaren (1981) interpreted the trends of grain size. He mentioned that the use of sediment trend analyses should have many applications for the rapid determination of the probable relationships among depositional environments, important processes

operating in a system of subenvironments, sediment transportation directions, and identification of depositional environment.

In grain size analysis, each class interval is a discrete portion of a continuous range of grain sizes. The amount of sediments in each class is a unique attribute of the particular sediment sample. Then, every sediment sample can be considered to consist of as many components as there are class intervals and this makes the use of multivariate methods possible. Sample can be defined as a vector in 8-dimensional space whose position is uniquely determined by the amount of sediment in each of the eight classes. A table of similarity coefficients can be formed to show the degree of similarity between all the sample vectors. Factor analysis attempts to determine the minimum number of independent dimensions needed to account for the most of the information in the table of similarity coefficients (Klovan, 1966).

The following investigation is an attempt to interpret the depositional environment of the Khafji reservoir depending on grain size distribution data, and to relate those depositional environments to the mechanical properties. Also, factor analysis is used to make use of the entire spectrum of the grain size distribution.

3.4.3.1. TEXTURAL PARAMETERS

Moiola and Weiser (1968) analysis was used to classify Khafji reservoir samples. The classification gives a good cluster. Furthermore, it illustrates that most of the sample plots corresponds to the river domain (Figure 3.20). With respect to the rock mechanical properties, samples representing beach sand show lowest average Young's modulus and lowest average Poisson's ratio compared to the river sand. This may be due to the effect of sorting.

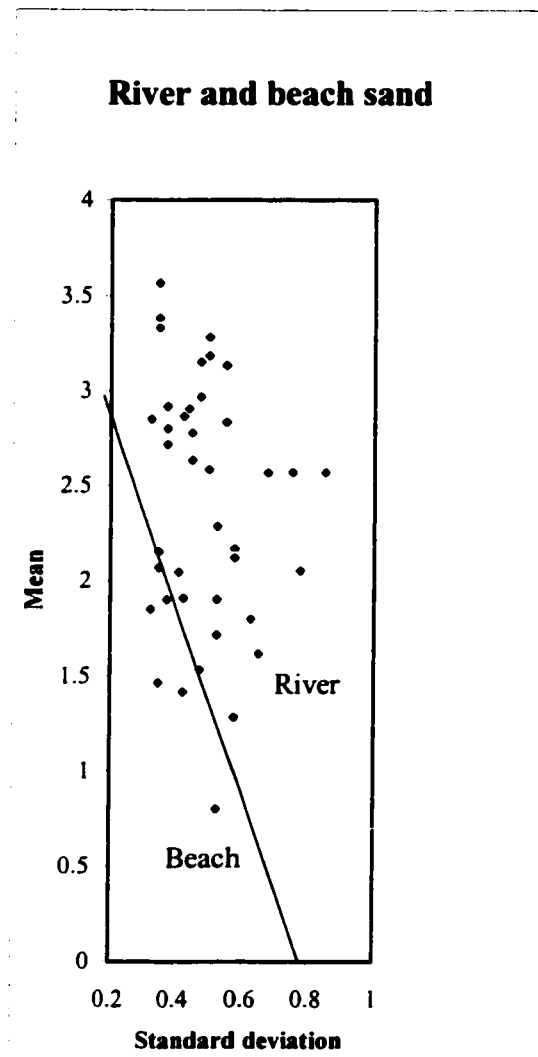


Figure 3.20. Plots of the mean grain size and standard deviation of the grain size distribution (according to Moiola and Weiser, 1968).

3.4.3.2. FACTOR ANALYSIS

Factor analysis of sediment grain size data yields useful information on the depositional environment. Klovan (1966) used factor analysis to determine the depositional environment from their grain size distribution. He applied the technique to sixty nine recent sediment samples collected from Barataria Bay, Louisiana. He concluded that, factor analysis offered a quick, simple, and effective means of illustrating significant grouping and trends among environmentally distinct sediment samples.

The grain size distribution was subjected to Q-mode analysis (principal component varimax) to determine the possible association of the analyzed samples. Table 3.5 shows the eigenvalues, their percentages, and their cumulative percentages. Three factors account for 84 percent of the variance. Most of the samples have a high communality. This means that only these factors were sufficient to describe them. The normalized factors (Table 3.6) were plotted on a ternary diagram to portray the relationship between them (Figure 3.21).

The ternary diagram shows that the samples were concentrated on the apex with less number of samples in the central part. The samples occurring nearest the apexes of the ternary diagram, namely C4-T23, C5-T3, and C4-T7 are end member samples. Sample C5-T3 (Factor 2) is sandstone with a highly truncated distribution; in fact it has the lowest median size diameter and high degree of sorting (9.98 E+05 psi, 0.147). Sample C4-T7 (Factor 3) is shaly sandstone with highly truncated distribution; it has the highest median diameter and high degree of sorting (1.24E+06 psi, 0.243). Sample C4-T23 (Factor 1) is very close approximation of the sandstone population with small amount of shale without truncation (1.06E+06 psi, 0.200) (Figure 3.22).

TABLE 3.5. Eigenvalues, total percentages, and cumulative percentages.

Factor	Eigenvalue	Total %	Cumulative eigenvalue %
1	16.75	41.87	41.87
2	12.33	30.83	72.70
3	4.34	10.85	83.55
4	3.28	8.19	91.74

TABLE 3.6. Varimax factor matrix with three related factors.

Sample #	Summ sqr cumm per cmm*	F1	F2	F3
C3-T23	0.88	0.16	0.03	0.81
C3-T14	0.88	0.03	0.06	0.91
C3-T9	0.56	0.04	0.95	0.01
C3-T20	0.87	0.01	0.98	0.01
C4-T7	0.88	0.04	0.05	0.91
C4-23	0.91	0.82	0.02	0.16
C4-T1	0.91	0.96	0.03	0.01
C4-T11	0.87	0.11	0.07	0.82
C5-T3	0.70	0.02	0.97	0.01
C5-T11	0.24	0.55	0.01	0.44
C6-T4	0.80	0.01	0.94	0.05
C6-T12	0.88	0.31	0.60	0.09
C6-T20	0.28	0.01	0.94	0.05
C2-T1	0.77	0.01	0.03	0.96
C2-T8	0.60	0.05	0.05	0.90
C2-T11	0.86	0.15	0.71	0.14
C2-T20	0.91	0.99	0.01	0.01
C5-T10	0.78	0.29	0.32	0.39
C1-T3	0.90	0.95	0.01	0.04
C1-T6	0.75	0.01	0.98	0.01
C1-T20	0.89	0.77	0.01	0.22
C1-T17	0.91	0.92	0.01	0.07
C1-T13	0.78	0.94	0.04	0.02
C1-T20-2	0.90	0.91	0.01	0.08
C1-T17-1	0.86	0.75	0.04	0.21
C1-T6-2	0.88	0.01	0.98	0.01
C1-T3-1	0.90	0.95	0.03	0.02
C2-T20-2	0.90	0.99	0.01	0.01
C2-T11-2	0.91	0.01	0.96	0.03
C2-T8-1	0.88	0.49	0.08	0.43
C3-T20-2	0.17	0.03	0.32	0.65
C3-T14-2	0.89	0.54	0.02	0.44
C4-T7-2	0.91	0.68	0.02	0.31
C4-T2-3	0.58	0.44	0.47	0.03
C4-T1-1	0.83	0.97	0.02	0.01
C5-T11-1	0.14	0.57	0.10	0.33
C5-T3-2	0.10	0.53	0.41	0.07
C6-T20-1	0.37	0.05	0.90	0.05
C6-T12-1	0.72	0.01	0.97	0.02
C6-T4-2	0.09	0.18	0.23	0.59

* Sums of squares cumulative percent communality

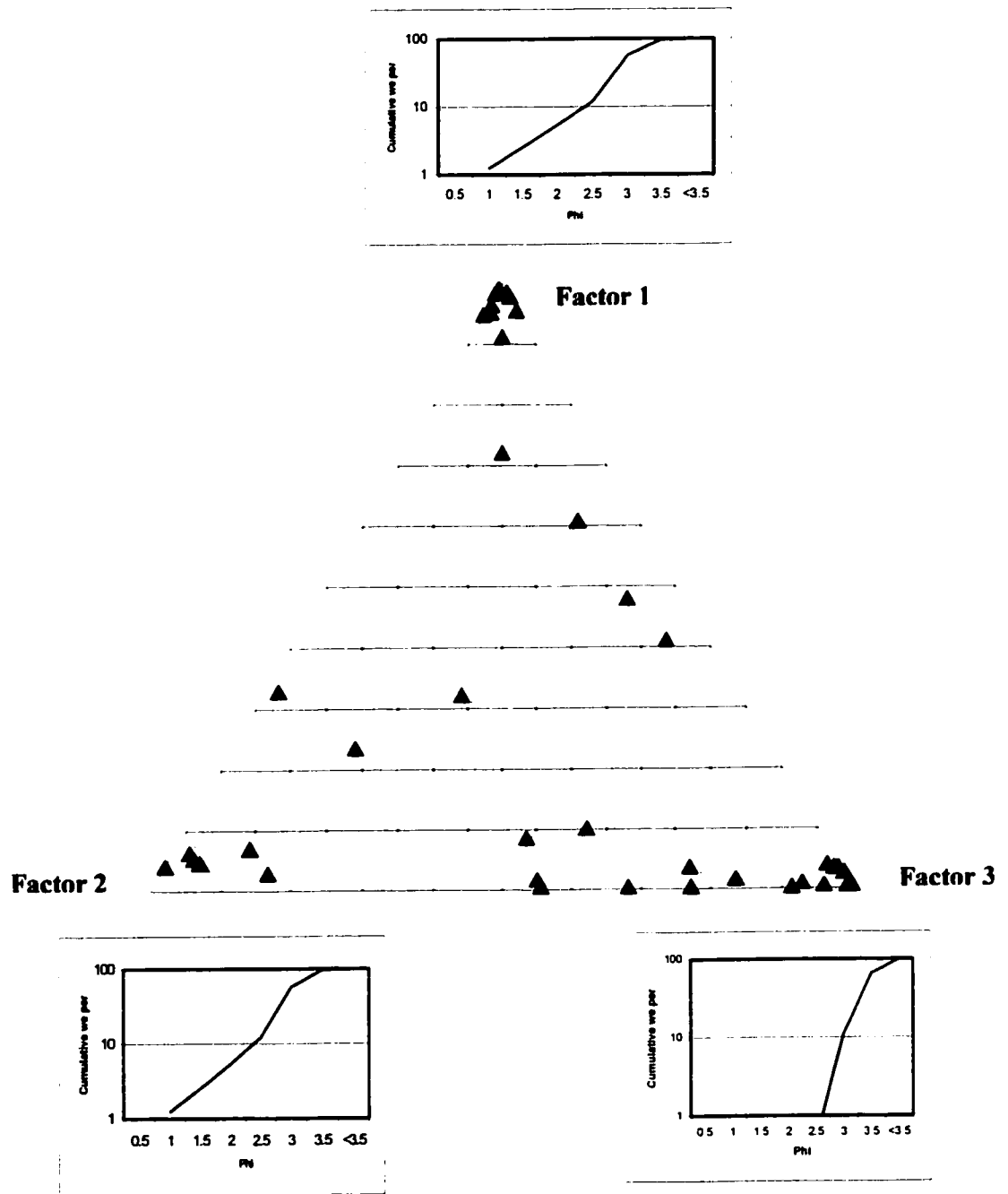


Figure 3.21. Plot of normalized factor components.

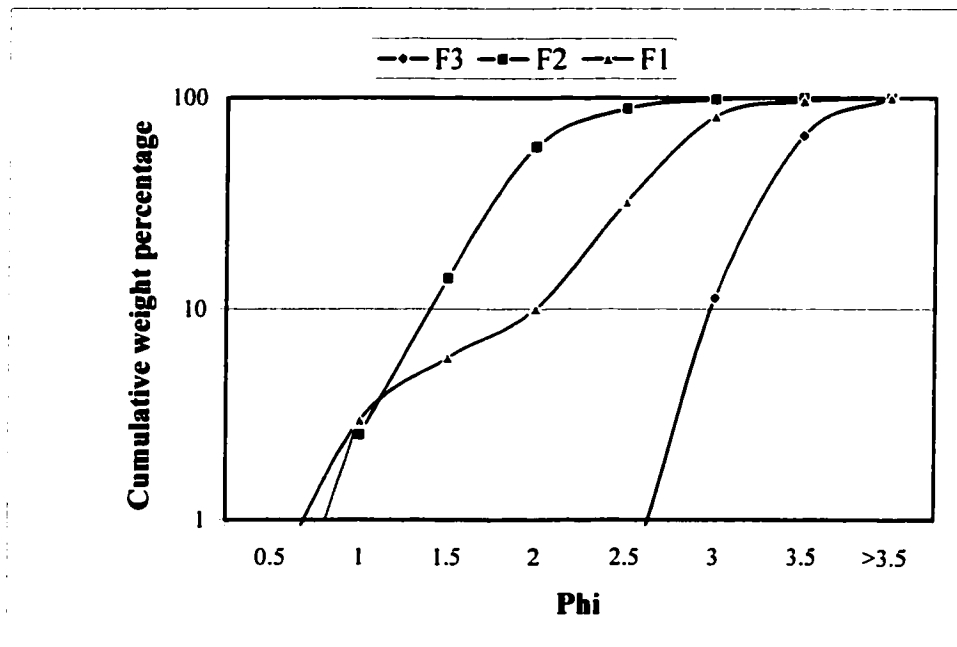


Figure 3.22. Grain size distribution curves for different end member samples.

To give the factors geological significance, the correspondence depositional environment should be deduced. Sample C5-T3 (Factor 2) with its truncated frequency curve probably represents deposition in a high-energy environment where there is reworking and winnowing of the fines. Beach environment would produce such a distribution. Factor 2, then, might tentatively be identified with surf energy with low Young's modulus and Poisson's ratio. Sample C4-T7 (Factor 3) is fine, well sorted sediment. It probably represents deposition in a very quiet environment. In this setting, the only source of energy available for deposition is that of gravity. Factor 3 may thus be identified with gravitational settling with high Young's modulus and Poisson's ratio. Finally, sample C4-T23 (Factor 1) shows bimodality and is a mixture of populations. Hence, Factor 1 might be interpreted to represent current energy with intermediate Young's modulus and Poisson's ratio.

The relationship between Factor 2, with the lowest Young's modulus and Poisson's ratio, and Factor 3 with the highest Young's modulus and Poisson's ratio, explains the relationship between depositional environments and rock mechanical properties. It was observed that beach environment has lower values of Young's modulus and Poisson's ratio relative to gravitational settling environment.

3.5. SEQUENCE STRATIGRAPHIC STUDY

3.5.1. INTRODUCTION

As the search for oil and gas becomes more sophisticated and producing basins and fields become more intensely developed, geoscientists need more accurate techniques for stratigraphic analysis. In basins or fields with a sufficient density of wells, the coupling of conventional well logs and cores with the techniques of sequence stratigraphy results in an ultra high-resolution chronostratigraphic framework for subsurface correlation (Wagoner et al., 1990)

Sequence stratigraphy is the study of the genetically related facies within a framework of chronostratigraphically significant surfaces. The sequence is the fundamental stratal unit for sequence stratigraphic analysis. The sequence is defined as a relatively conformable, genetically related succession of the strata bounded by unconformities or their correlative conformities (Mitchum, 1977). Sequence boundaries form in response to relative falls in the sea level. Parasequence and parasequence sets are the building blocks of sequences. A parasequence is defined as a relatively conformable, genetically related succession of beds or bedsets bounded by marine flooding surfaces or their correlative surfaces. A parasequence set is defined as a genetically related succession that form a distinctive stacking pattern, bounded in many cases by major marine flooding surfaces and their correlative surfaces (Van Wagoner, 1985; Van Wagoner et al., 1988).

Using well logs, cores, or outcrops, each sequence can be subdivided into stratal units called system tracts, based on their positions within the sequence, the distribution of parasequence sets, and facies association. System tracts are defined as a linkage of contemporaneous depositional system (Brown and Fisher, 1977). System

tracts provide a high degree of facies predictability within the chronostratigraphic framework of sequence boundaries. This predictability is important for the analysis of the reservoir, source, and seal facies within a basin and or a field (Wagoner et al., 1990).

System tracts are genetically associated stratigraphic units that are deposited during specific phases of the relative sea-level cycle. They are represented in the rock record as three-dimensional facies assemblages. They are defined on the basis of bounding surfaces, position within a sequence, and parasequence stacking pattern. Four kinds of system tracts are recognized. They are (Van Wagoner et al., 1988)

1. Lowstand system tracts (LST): This includes all the deposits that accumulated after the onset of relative sea-level fall, and as long as shoreline regression continues. Lies directly on Type 1 sequence boundary.

2. Highstand system tracts (HST): They are the regressive deposits that form when sediment accumulation rates exceed the rate of relative sea-level rise and increase in accommodation. Constitutes the upper system tract in either Type 1 or Type 2 sequence boundary.

3. Shelf margin system tracts (SMST): They are the lowermost system tracts, and are associated with Type 2 sequence boundary.

4. Transgressive system tracts (TST): They comprise the deposits that accumulated from the onset of coastal transgression until the time of maximum transgression of the coast, just prior to renewed regression.

3.5.2. WELL LOG INTERPRETATION

At the start of an interpretation of sequence stratigraphy using well logs the predominant sequence stratigraphic surfaces must be identified. The important

surfaces are maximum flooding surfaces (MFS) and transgressive surfaces (TS). These are coincided and are correlated with radioactive shales that are interpreted to have been deposited across relatively flat surfaces. Once the (MFS) and (TS) are established, then the sequence boundaries (SB) should be identified. These will tend to lie directly beneath the sand sized sediment fill of depressions on eroded and incised surfaces and over the prograding clinoforms of high stand system tracts (HST) (USC sequence stratigraphy web, 2002).

The second and often co-incident step in the interpretation of well logs and cores is the use of parasequence stacking patterns (the vertical occurrence of repeated cycles of coarsening or fining upwards sediment) to identify the lowstand system tracts (LST), transgressive system tracts (TST) and highstand system tracts (HST) that are enveloped by the (MFS), (TS) and (SB). These parasequence cyclic stacking patterns are commonly identified on the basis of variations in grain size and when these fine upwards are indicated by triangles whose apex is up while those that coarsen upwards are indicated by inverted triangles whose apex is down (USC sequence stratigraphy web, 2002).

The repeated stacking patterns for LST cycles are:

1. Cyclic fill of incised depressions that tend to fine upward.
2. Cyclic sand to shale bodies of basin floor fans that tend to fine and thin upward.
3. Cyclic sand to shale bodies of shelf margin clinoforms that tend to coarsen and thicken upward.

The repeated stacking patterns for TST cycles are:

1. Regressive cyclic shale to sand bodies that tend to coarsen and thin upward.

3.5.3. SEQUENCE STRATIGRAPHIC MODEL AND DISCUSSION

The model was interpreted based on gamma ray (GR) and other available logs for well Zuluf-A and well Zuluf-AA (Figures 3.23 and 3.24). The main sand and the upper stringer sand represent a (LST) and succeeding (TST).

A marked late-Aptian regional unconformity and sedimentary hiatus separates the Shu'aiba Formation from the Khafji Member. This break probably coincides with a worldwide lowstand in sea level (Haq et al., 1988) and was followed by a gradually rising sea level that culminated in maximum flooding surface (MFS) by the end of the Albian time. In general, by late Albian time, the Arabian Platform was widely inundated by shallow seas in which were deposited shallow to progressively deep marine carbonates in various subbasin around the plate margin (Ziegler, 2001).

By analog with Kuwait, Davies et al. (2002) placed the intra-Aptian unconformity at the base of the main sand of the Khafji Member. Entsminger (1981) identified the limestone within the upper Khafji shale as a major flooding event separating regressive episodes in the Khafji Member.

A comparison was carried out between the dynamic Young's modulus and Poisson's ratio with sequence stratigraphy model. Generally, it was observed that the (LST) has the highest Young's modulus and Poisson's ratio relative to the (TST) (Figure 3.25).

3.6. CONCLUSION

Principal goal of this part was to identify the composition and textural components that have the greatest influence on the rock mechanical properties. This was accomplished by performing a linear correlation analysis. The result of the correlation analysis was a correlation matrix, which gave the interdependence among

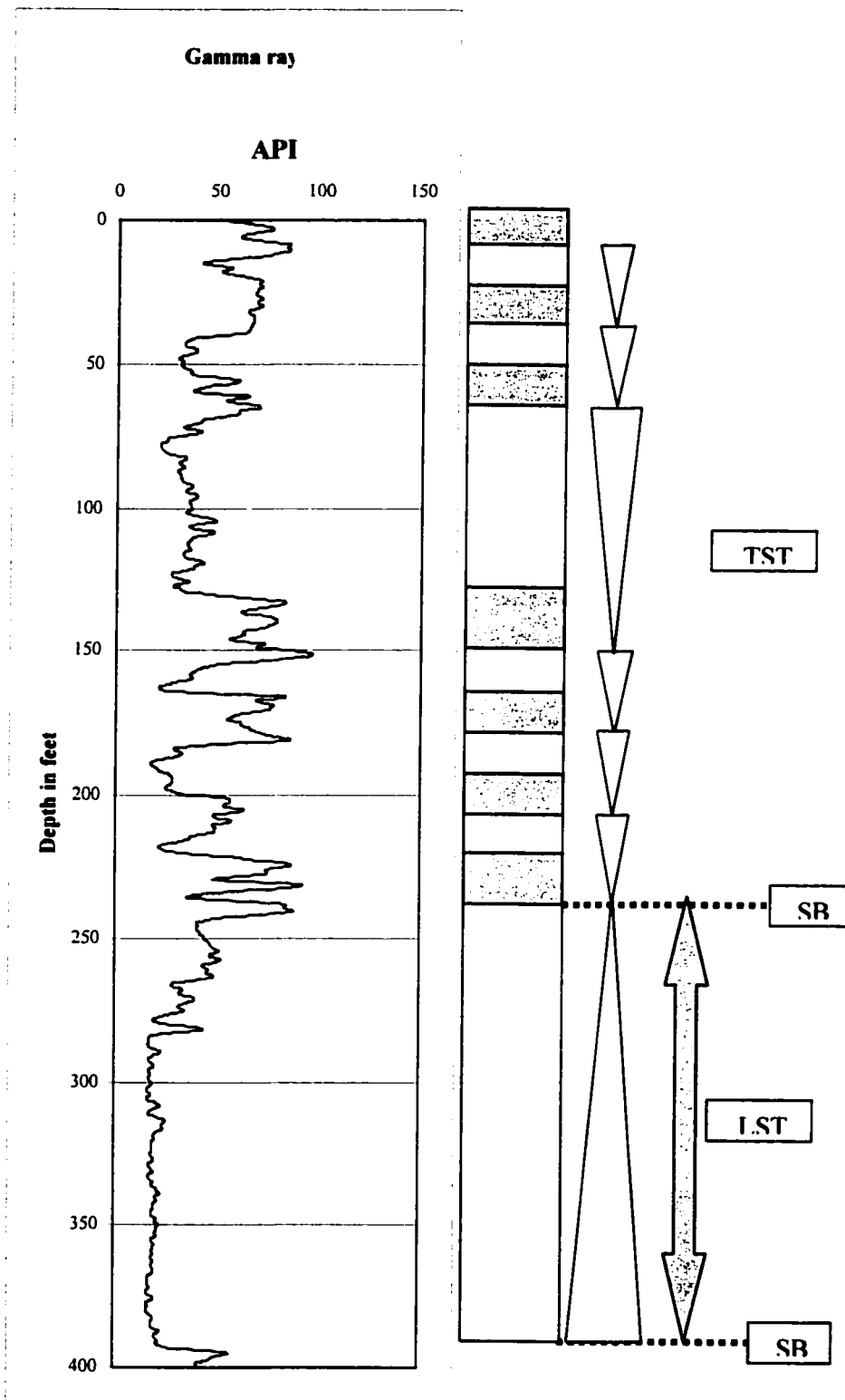


Figure 3.23. Sequence stratigraphic interpretation of the Khafji reservoir, well Zuluf-A.

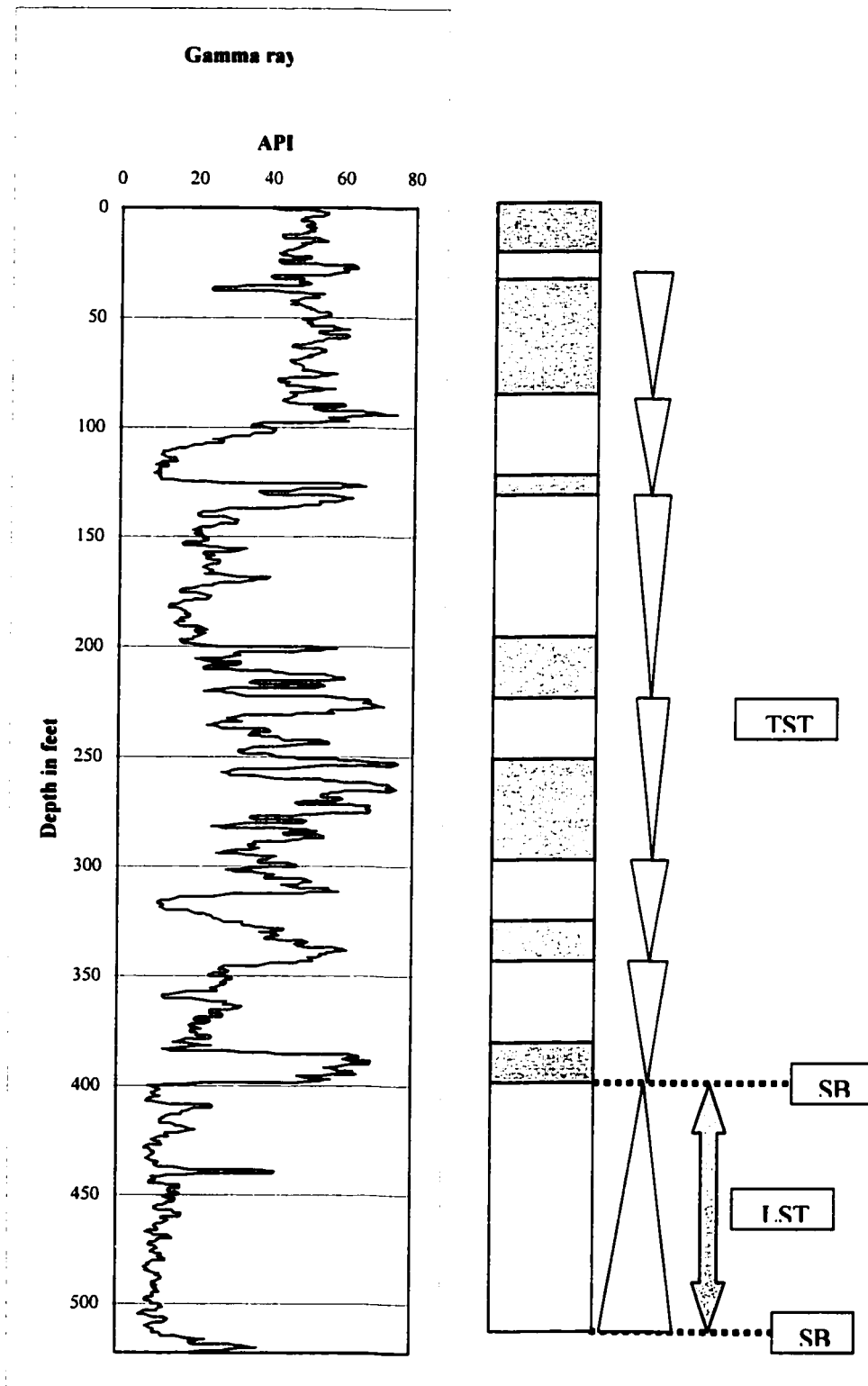


Figure 3.24. Sequence stratigraphic interpretation of the Khafji reservoir, well Zuluf-AA.

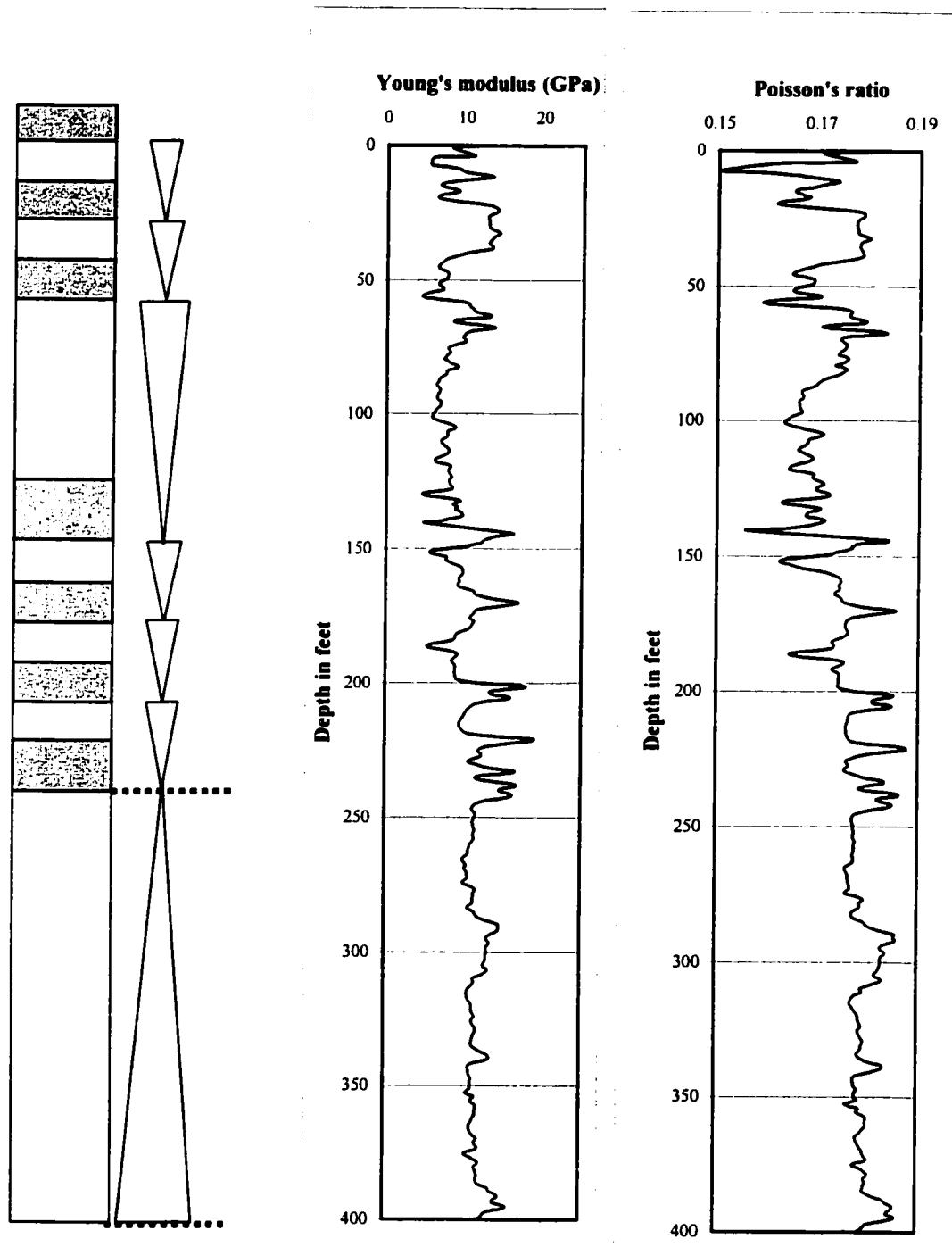


Figure 3.25. Correlations among sequence stratigraphic interpretation and dynamic Young's modulus and Poisson's ratio.

all pairs of variables. The elements of the correlation matrix are the correlation coefficients, r . A value of $r = 1$ represents a perfect correlation.

Previous works have shown that the strength of rocks generally decreases as grain size increases (Brace, 1961; Hoshino et al., 1972; Fahy and Guccione, 1979). For the Khafji reservoir, the direct (one to one) relationships between Young's modulus and Poisson's ratio and the grain size parameters (median, mean, sorting, skewness, and kurtosis) were not significant.

A good correlation was found between Poisson's ratio and quartz, and Poisson's ratio and grain contacts. On the other hand, a poor correlation was found between Young's modulus and quartz, and Young's modulus and grain contacts. It should be noted that Poisson's ratio is a property, which takes into account strains in two perpendicular directions. In this study, thin sections are nearly parallel to the bedding planes, or parallel to the lateral strain direction. Therefore, it is possible that petrographic characteristics parallel to the direction of lateral strain show a better correlation with Poisson's ratio.

The effect of confining pressure on the mechanical properties was investigated. It was observed that the value of Young's modulus increases with the increases of confining pressure. This may be due the resistance of the sample against axial loading. However, this relationship does not exist with Poisson's ratio.

The combination of grain mean diameter and the standard deviation analysis (Moiola and Weiser, 1968) was used to investigate the effect depositional environment of the Khafji reservoir on its mechanical properties. The samples were categorized into beach sand and river sand. Samples representing beach sand environment are characterized by the lowest average Young's modulus and Poisson's ratio.

By using factor analysis, three factors were determined. Each factor represents specific type of depositional environment. Factor 2 represents beach environment, Factor 3 represents gravitational settling environment, and Factor 1 represents current energy environment. It was observed that beach environment has lower values of Young's modulus and Poisson's ratio relative to gravitational settling environment.

A sequence stratigraphic model was interpreted for the Khafji reservoir. The main sand and the upper stringer sand represent a (LST) and succeeding (TST). It was observed that the (LST) has the highest Young's modulus and Poisson's ratio relative to the (TST).

CHAPTER FOUR

CALIBRATION OF MECHANICAL PROPERTIES

4.1. ELASTIC PROPERTIES OF ROCKS

Elastic properties define the ability of a rock to resist permanent deformation when deformed slightly. They include (Fjaer et al., 1992):

1. Young's modulus (E): It measures the sample resistance against compression by a uniaxial stress.

$$E = \sigma / \varepsilon \quad (4.1)$$

where σ is stress and ε is strain.

2. Poisson's ratio (ν): It measures the lateral expansion to longitudinal contraction.

$$\nu = - \varepsilon_y / \varepsilon_x \quad (4.2)$$

3. Bulk modulus (K): It is the ratio of hydrostatic stress σ_p relative to the volumetric strain ε_v .

$$K = \sigma_p / \varepsilon_v \quad (4.3)$$

4. Shear modulus (G): It measures the sample's resistance against shear deformation.

$$G = \sigma_{xy} / (\varepsilon_{xy} + \varepsilon_{yx}) \quad (4.4)$$

where σ_{xy} is the stress, ε_{xy} is xy strain, and ε_{yx} is yx strain.

4.2. ELASTIC THEORY

4.2.1. INTRODUCTION

Acoustic logging is the tool that responds to the elastic properties of formation. When the pressure of a pulse is created in a wellbore filled with fluid, the complex phenomena that occur at the boundary between the wellbore and the formation result in the propagation of several types of waves into the formation. The two type of waves of interest for estimating the elastic constants of a medium are compressional waves (P-waves) and shear waves (S-waves). The acoustic tool measures the characteristic propagation speed of the P- and S-waves (Serra, 1984).

In an isotropic medium, only two elastic constants, shear modulus (G) and Poisson's ratio (ν), are independent. They are related to the velocity of propagation of a P-wave (V_p), and that of S-wave (V_s), by (Fjaer et al., 1992):

$$G = \rho_b V_s^2, \text{ and} \quad (4.5)$$

$$\nu = (2 V_s^2 - V_p^2)/(2 V_s^2 + 2 V_p^2). \quad (4.6)$$

The propagation velocity can be replaced with the time Δt it takes for a wave to travel a fixed distance d (between the source and the receiver):

$$G = \rho_b d^2 / \Delta t_s^2, \text{ and} \quad (4.7)$$

$$\nu = (\Delta t_s^2 - 2 \Delta t_c^2)/(2 \Delta t_s^2 + 2 \Delta t_c^2). \quad (4.8)$$

where Δt_s and Δt_c are the S-wave and P-wave travel times, respectively.

Young's modulus (E) is related to the two constants by:

$$E = 2G(1 + \nu). \quad (4.9)$$

4.2.2. INELASTIC BEHAVIOR IN ROCKS

For linear elastic continuous materials such as most metals, the elastic properties are independent of stress and frequency. That is, whether the measurements

are performed under unconfined conditions or with varying confining stress, the values of the elastic constants are unchanged. Furthermore, whether these properties are determined statically, during compressional testing, or dynamically, using wave transmission or resonance techniques, the values of the elastic constants are the same. The elastic constants in metal are thus material properties characterizing their mechanical behavior independent of the stress applied on the material or the frequency (TerraTek, 2001).

Rocks do not behave in a similar manner. As a material, rock is discontinuous at all scales. Its stress-strain relationships are non-linear, inelastic and are rate-dependent. Furthermore, rocks undergo permanent deformation when subjected to sufficiently high stresses. These deformations change their mechanical properties drastically. When a metal is subjected to non-isotropic compressive stresses, the resulting volumetric strain is always compressive, thus the overall volume of the specimen continuously decreases as the compressive stresses increase. Eventually, during plastic deformation, the volume remains constant. In rocks, however, as the compressive stresses increase, the volume of the sample first decreases, then increases to its original volume and continues beyond this value, undergoing volumetric dilatation. This characteristic mechanical behavior of rock comes about due to its discontinuous nature, the brittleness of its constituent solids, and its ability to undergo microcracking to redistribute stresses from regions of high stress concentration. The generation and increase in population of stress induced microcracking causes rock to dilate under stress (TerraTek, 2001).

Despite these difficulties an effort is often made to characterize the load deformation behavior of rocks in terms of two linear elastic constants (Young's

modulus and Poisson's ratio). These two constants change with the variation in confining stress. Several tests are thus required to evaluate the dependence of the elastic moduli on the confining stress. The induced anisotropy is neglected and the material behavior at each particular confining stress is treated as isotropic.

4.3. ACOUSTIC LOG

The acoustic tool simply measures the time it takes for a sound pulse to travel from the emitter at one end of the logging tool to the receivers at the other end of the tool. The sound emissions from the tool generally have a frequency between 20-40 kHz. Acoustic log values are given in microseconds (μs) per foot (Rider, 1986). The acoustic velocities depend on elastic moduli and material density, but these parameters are obviously related also to different factors. These may be intrinsic characteristics; like rock type lithology, porosity, and degree of fluid saturation. The velocity may also depend on extrinsic factors such as the state of stress and temperature (Fjaer et al., 1992).

Traditionally, the acoustic log is used as a porosity log, but in recent years, development of logging tools and interpretation procedures have been directed more towards evaluation of mechanical properties (Fjaer et al., 1992).

4.3.1. ACOUSTIC WAVES

There are several types of sound waves, each one characterized by a particular kind of particle movement. They are (Serra, 1984):

1. Compressional wave (P): The particles move in a direction parallel to the direction of propagation. The speed of propagation is largest for this kind of wave compared to others and so it arrives first at the receiver. It is the only wave propagated in liquid.

2. Shear wave (S): Particle movement is in a direction perpendicular to the wave direction. The energy transmitted by shear wave is much higher than that of compressional wave and this feature therefore can identify the S-wave.

3. Surface wave: These waves are transmitted on the surface within a layer whose thickness is about equal to the wavelength. They are Rayleigh, Love, and coupled waves.

4.3.2. ACOUSTIC TOOLS

4.3.2.1. EARLY TOOLS

Early tools had one transmitter and one receiver. The body of the tool was made from rubber (low velocity and high attenuation material) to stop waves traveling preferentially down the tool to the receiver. There were two main problems with this tool. (i) The measured travel time was always too long because the time taken for the elastic waves to pass through the mud was included in the measurement. (ii) The length of the formation through which the elastic wave traveled was not constant because changes to the velocity of the wave depending upon the formation altered the critical refraction angle (Glover, 2002).

4.3.2.2. DUAL RECEIVER TOOLS

These tools were designed to overcome the problems in the early tools. They use two receivers a few feet apart, and measure the difference in times of arrival of waves at each receiver from a given pulse from the transmitter. This time is called the sonic interval transit time. The problem with this arrangement is that if the tool is tilted in the hole, or the hole size changes (Glover, 2002).

4.3.2.3. BOREHOLE COMPENSATED (BHC) TOOL

This tool compensates automatically for problems with tool misalignment and the varying size of the hole that were encountered with the dual receiver tools. It has two transmitters and four receivers, arranged in two dual receiver sets, but with one set inverted. Each of the transmitters is pulsed alternately, and t values are measured from alternate pairs of receivers. These two values are then averaged to compensate for tool misalignment, and changes in the borehole size (Glover, 2002).

A brief study of the left portion of Figure. 4.1 shows that, when the transmitter is below the receivers, the horns at the lower and upper cave boundaries are opposite in direction to those from the upper transmitter. The horns tend to cancel each other, when the interval of transit time measurements from the upper and lower transmitter are combined and averaged (Kokesh et al., 1965).

4.3.2.4. LONG SPACING SONIC (LSS) TOOL

It was recognized that in some logging conditions a longer transmitter- receiver distance could help. Hence Schlumberger developed the long spacing sonic (LSS), which has two transmitters two feet apart, and two receivers also two feet apart but separated from the transmitter by 8 feet. This tool gives two readings; a near reading with a 8-10 ft. spacing, and a far reading with a 10-12 ft. spacing (Glover, 2002).

4.3.3. VERTICAL RESOLUTION

Sedimentary series consists of a sequence of beds of various thicknesses, with differing lithological and petrophysical properties. In theory, each bed should be distinguished from the neighbors by its own characteristics. This is indeed seen in practice when the beds are thick. Thin beds present a different picture. Two factors must be taken into account, one related to the logging tool design, the other to the fact

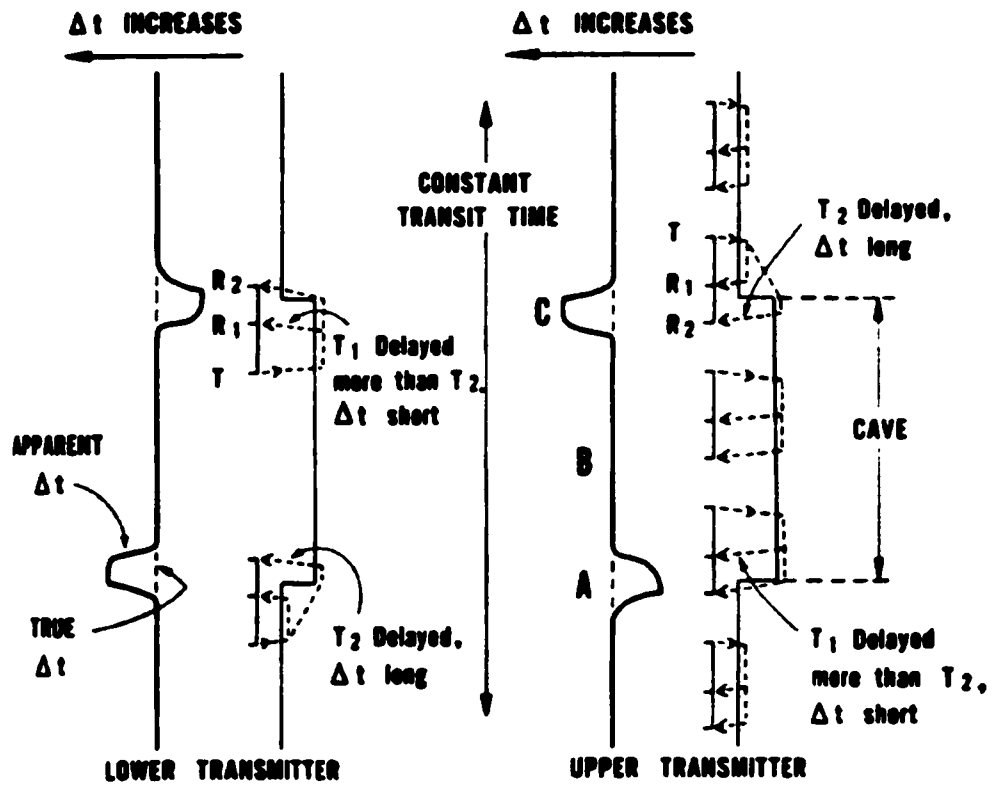


Figure 4.1. Conventional upper-transmitter two-receiver array at right gives horns at cave boundaries (after Kokesh et al., 1965).

that the measurement is made while the tool is moving (Serra, 1984).

In the two-receiver system the separation between receivers (span) determines the resolution (Figure. 4.2). The smaller the span, the greater the detail in logging thin bed. A single isolated bed, which is thinner than the receiver span, can be observed but will not have the signal fully developed. Figure 4.3 shows the result for a hard streak logged with spans both greater and smaller than its thickness (Kokesh and Blizard, 1959).

It appears, then, that this phenomenon will highly affect the reservoir mechanical properties, which are acoustic transit time dependant.

4.3.4. DEPTH OF INVESTIGATION

The path of the acoustic waves measured by borehole tools is essentially along the borehole wall with little penetration. The penetration in fact depends on wavelength (λ) ($\lambda = V/f$) of the waves. Laboratory experiments show that a thickness of at least 3λ is needed to propagate a pressure wave through several feet of formation. The depth of investigation varies between 12 cm and 1 m. For any given frequency, the higher the velocity the formation has, the larger the wavelength and the deeper the penetration (Serra, 1984; Rider, 1986).

The distance between the transmitter and the first receiver should be chosen large enough so that the first signal to reach this receiver travels through at least a small part of the formation which is to be measured. When formation velocity exceeds mud velocity, the minimum required spacing between transmitter and the first receiver is proportional to the stand-off and is a function of the ratio of mud velocity to formation velocity. The relationship may be delivered by straightforward computation of the total time for an acoustic pulse to travel from transmitter to receiver. The result

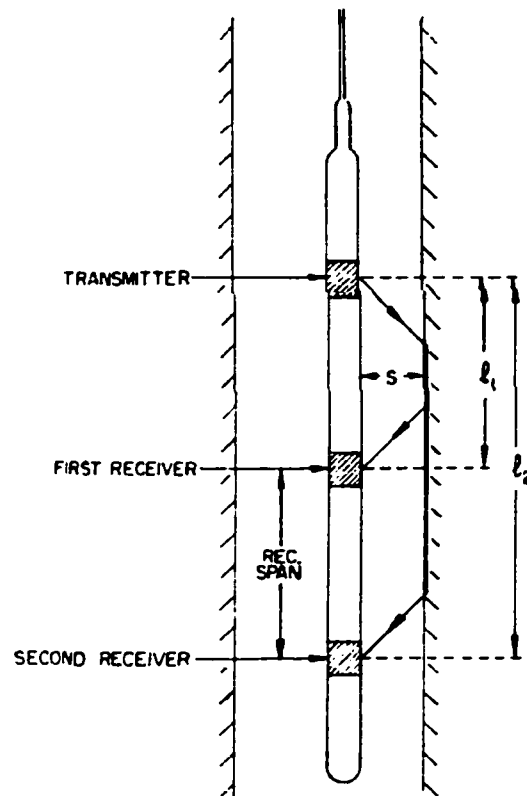


Figure 4.2. Schematic drawing of a two-receiver sonde (after Kokesh and Blizard, 1959).

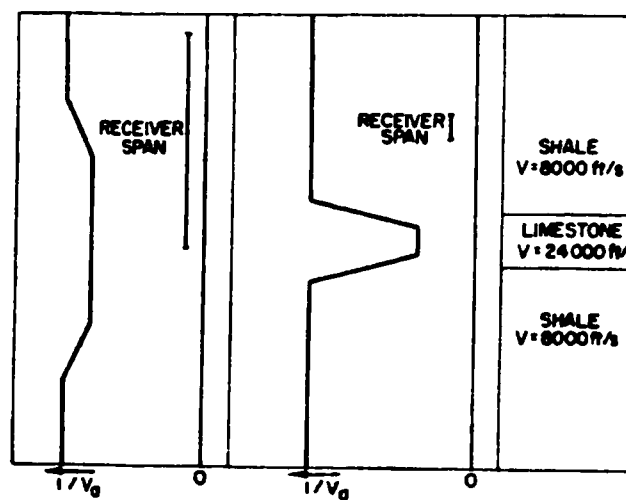


Figure 4.3. Theoretical response of acoustic log to a thin bed of high velocity material for two receiver spans (after Kokesh and Blizard, 1959).

is (Kokesh and Blizard, 1959):

$$l_{\min} / S = 2 [(1+\beta) / (1-\beta)]^{1/2} \quad (4.10)$$

where

l_{\min} = Minimum required distance between transmitter and receiver.

S = Stand-off.

β = Ratio of mud velocity to formation velocity.

If the formation adjacent to the well is changed by drilling stress, the ratio of velocity in altered zone to that in the virgin formation is designated by n . It is assumed that there is no stand-off, there is a sharp boundary between altered and virgin formations, the distance to the second receiver is twice that to the first receiver. For small depths of alteration the error is zero because the ray paths of least time to both receivers pass through the altered zone and include a portion of virgin formation. The transit times in the altered zone cancel, and the true velocity is measured. For the large depths of alteration the rays of least time to both receiver pass only through altered zone, and it is evident that it is the velocity of the altered zone, which is being measured (Kokesh and Blizard, 1959).

When the first arrival at the first receiver passes only through the altered zone, but that to the second receiver traverses virgin formation, the error increases linearly with the depth of alteration. The relation is (Kokesh and Blizard, 1959):

$$\text{Percent error in reciprocal velocity} = 2D (1-n^2)^{1/2} - [l_1(1-n)] / [n(l_2-l_1)] \quad (4.11)$$

where

D = Depth of alteration,

n = Ratio of velocity of altered zone to velocity of virgin formation.

4.3.5. LOGGING PROBLEMS

4.3.5.1. NOISE

Noise from stray electrical fields, the electronics package or derived from mechanically generated noise in rough holes can trigger the detection before the first arrival, causing a false apparent first arrival. To limit this effect, all receiver circuits are disabled for 120 microseconds after the pulse. As the remaining time for the possibility of a noise spike occurring is greater for the far detector than the near one, most noise spikes occur for the far detector, which leads to values of Δt that are too small (Glover, 2002).

4.3.5.2. CYCLE SKIPPING

This is the occurrence of a failure in the thresholding to detect the first cycle of the wave's first arrival. Triggering may then occur at the second or even third cycle. This causes a marked and sudden shift to higher Δt values, followed by a shift back again to the correct value (Glover, 2002).

4.3.5.3. MUD ARRIVALS

Clearly the first arrival should be from a P-wave that has traveled through the formation. In some circumstances the P-wave that has traveled directly through the mud arrives first. This occurs if the transmitter-receiver distance is smaller than a critical distance that depends upon the velocities of the P-wave through the formation and the mud, the diameter of the borehole and the diameter of the tool. Tools are designed to avoid this by making the transmitter-receiver distance large enough for most applications. However, in some large diameter holes, the mud arrivals may come first. This leads to there being no structure in the sonic log response because the travel time through the mud is all that is being recorded. In these circumstances the tool may

be run eccentric, but at the risk of picking up more noise spikes from the noise associated with the rough borehole surface (Glover, 2002).

4.3.5.4. ALTERED ZONE ARRIVALS

The formation next to the borehole may not be typical of the rock. For example, it may be filled with solid mud and have a higher velocity than the virgin formation, or it may be fractured or altered and have a lower velocity. This is an analogous problem to the mud arrival problem. If a low velocity altered zone exists, the transmitter-receiver spacing must be large to ensure that the P-wave from the virgin formation arrives before that from the altered zone. In this case an LSS should provide better data than a BHC type log (Glover, 2002).

4.4. THE DIFFERENCE BETWEEN STATIC AND DYNAMIC MODULI IN ROCKS

There is often considerable disagreement between the static modulus obtained from conventional static tests and the dynamic modulus obtained from wave velocities and density of the rock. Dynamic moduli are invariably higher than static moduli. The ratio of dynamic to static moduli ranges from approximately 1.5 to 3.0. The main reasons for the difference are (Siggins, 1993):

1. The thermodynamics of the two testing processes are distinctly different. Static tests can be considered to be carried out at constant temperature (isothermal). Dynamic tests are adiabatic, they generate local temperature changes, which effectively reduce the total strain for a given applied stress and consequently yield higher compressional modulus values.

2. The strain levels involved in these two experiments are different. Peak strains in dynamic tests are of the order of 10^{-7} compared with static values of 10^{-2} , a difference of five orders of magnitude.
3. Dynamic strain rates are generally many orders of magnitude higher than the corresponding static values.

An analytical relation between the isothermal modulus (static) and the adiabatic modulus (dynamic) is given by

$$K_T = K_s (1 + r^2 Q T K_s / C_p). \quad (4.12)$$

where K_T is the isothermal bulk modulus, K_s is the adiabatic bulk modulus (Pa), r is the coefficient of thermal expansion (K^{-1}), Q is the specific volume ($m^3 kg^{-1}$), T is the temperature (K) and C_p is the specific heat at constant pressure ($J kg^{-1} K^{-1}$).

For a typical rock, still the formula does not explain a discrepancy of more than 0.5%. Therefore, other reasons for the difference are cited as:

1. Localized crushing at the specimen ends during loading, effectively lowering the static modulus.
2. The role of porosity and cracks. Elastic waves tend to propagate through the matrix of the rock, thereby providing an overestimate of bulk moduli.

The more competent the rock, the lesser the discrepancy.

The dynamic elastic properties of a rock are a function of velocity and density. Log-based velocities are also used to map the lithology and saturation in a reservoir. A study by Marion and Jizba (1992) showed that the acoustic (20-50 Hz) and ultraacoustic (300-700 kHz) velocities of sandstone are controlled primarily by porosity, saturation, and the clay content.

4.5. BIOT'S CONSTANT

4.5.1. INTRODUCTION

Biot's constant is an important poroelastic parameter that finds use in many petroleum-related rock mechanics applications. Effective stresses are typically calculated from the total stresses using Biot's constant, α (Biot and Willis, 1957; Geertsma, 1957):

$$\sigma' = \sigma - \delta \alpha p \quad (4.13)$$

where σ' is the effective stress, σ is the total stress, δ is the Kronecker delta, and p is the internal pore pressure. Biot's constant thus determines the amount of stress borne by the rock grains in the presence of pore fluids. When $\alpha = 0$, the total (maximum) stress is felt by the rock grains, and when $\alpha = 1$, the stress felt by the grains is least. In soils, α is usually equal to unity, while in rocks it follows the inequality:

$$\Phi < \alpha < 1 \quad (4.14)$$

It has been shown that (Biot and Willis, 1957; Banthia et al., 1965; Nur and Byerlee, 1971):

$$\alpha = 1 - K_{ma} / K_b \quad (4.15)$$

where K_{ma} is the matrix or grain compressibility and K_b is the bulk (grains and pores) compressibility. The bulk compressibility of porous rocks is found to decrease with differential pressure, resulting in a decrease in the value of Biot's constant with pressure. Walsh (1965) found that the ratio K_{ma} / K_b depends on both porosity and pore shape.

4.5.2. IN-SITU STRESS AND BIOT'S CONSTANT

Minimum horizontal in-situ stress obtained from acoustic log commonly uses the following equation (Blanton et al., 1997; Temeng et al., 1999; Avasthi et al., 2000):

$$\sigma_h = \nu (\sigma_v - \alpha p) / (1 - \nu) \quad (4.16)$$

where ν is the Poisson's ratio, σ_v is the vertical overburden stress, and p is the pore pressure.

The poroelastic parameter, α , used in equation 4.16 for in-situ stress determination is obtained mainly from empirical correlations (Geertsma, 1961; Krief et al., 1990). A limited amount of experimental work is reported in the literature that deals with the various methods to determine, α , in the laboratory (Klimentos et al., 1998; Franquet and Abass, 1999; Azeemuddin et al., 2001). In most cases, it is limited to obtaining one static value to be used under all confining and differential pressures. In only a few cases, the effect of confining pressure and differential pressure has been considered (Fabre and Gustkiewicz, 1997; Klimentos et al., 1998; Azeemuddin et al., 2001), its transverse anisotropy has been ignored.

4.6. ROCK MECHANICS TEST AND CALIBRATION

4.6.1. MECHANICAL PROPERTIES

The mechanical properties of reservoir samples can be measured in the laboratory from triaxial tests (static) or they can be estimated from wire-line measurements (dynamic). Static measurements on cores are much more indicative of the mechanical properties of the reservoir than the dynamic measurement, however, information from wire line logs covers much more of the reservoir than core measurements and is less expensive.

Rock mechanical triaxial tests were conducted on samples obtained from well Zuluf-A. A total of 21 different depth intervals were tested. Static elastic moduli (Young's modulus, E , and Poisson's ratio, ν) and static Biot's constant were

determined from the results of the triaxial tests. The data was obtained from Research Institute, King Fahd University of Petroleum and Minerals.

4.6.1.1. TRIAXIAL TEST

A triaxial test is conducted by loading the sample axially while applying a constant confining pressure equivalent to the effective reservoir pressure (2900 psi). The stress-strain response was plotted for all tested samples and the elastic constants (Young's modulus and Poisson's ratio) were computed at 50% of the peak stress.

4.6.1.2. BIOT'S CONSTANT

Using test data from the triaxial compression test, the static values of the Biot's constant was then found using the following equations (Biot and Willis, 1957; Nur and Byerlee, 1971):

$$\alpha = 1 - K_{ma} / K_b \quad (4.17)$$

$$K_{ma} = E / 3(1-2\nu). \quad (4.18)$$

$$\nu = -\varepsilon_y / \varepsilon_x \quad (4.19)$$

$$E = \sigma / \varepsilon \quad (4.20)$$

4.6.2. CALIBRATION OF MECHANICAL PROPERTIES

The preferred method for obtaining a continuous log of elastic properties is to calibrate the acoustic log processing output with good quality results of core tests. The tests should be conducted on properly oriented cores (vertical) at a confining pressure similar to that in the formation downhole. The next step is to determine the depth shift between core and logs accurately so as to place the laboratory tests at the corresponding log measurements. The resulting calibration is usually applicable within the field (Edlmann et al., 1998).

In this work, the depth shift for the well was determined using log bulk density and the laboratory measured density. The depth shift is probably accurate to within 1 ft. Three methods are used to calibrate the mechanical properties. They are linear regression, FORMEL, and AUTOSCAN methods. A quantitative comparison between the three methods has been calculated. Also, lithology and saturation calibration factors are discussed in details.

4.6.2.1. REGRESSION METHOD

The regression method is the widely used technique in industry today. By knowing Δt_c and Δt_s and density from acoustic and density logs respectively, the following mathematical relationships are used for calculating dynamic Young's modulus and Poisson's ratio (Ahmed et al., 1991):

$$\nu = (2 - (\Delta t_s / \Delta t_c)^2) / (2 - 2(\Delta t_s / \Delta t_c)^2) \quad (4.21)$$

$$E = 2(1 + \nu) \rho (\Delta t_s)^2 \quad (4.22)$$

In regression method, a transfer function is obtained between the static and the dynamic elastic properties with cross plotting and curve fitting procedures. The transfer function is then used to rescale the dynamic Young's modulus and the dynamic Poisson's ratio.

4.6.2.2 FORMEL METHOD

FORMEL (Formation MEchanical Log) is a technique developed by Raaen et al. (1996) and is used here to calibrate the Young's modulus and the Poisson's ratio. The idea behind FORMEL was to provide a description of the main processes occurring in a sedimentary rock during loading. Of special importance were mechanisms, which give rise to differences between static and dynamic elastic moduli,

since an understanding of these would facilitate the optimum use of acoustic data (Fjear, 1999).

The aim was to come up with a model which could be described by two sets of parameters: one set which can be estimated from the well logs and other data available in a field; the other set being determined from a series of carefully designed and analyzed laboratory experiments. The latter set is expected to be the same for any given lithology (field independent), and may thus be determined once and for all. This does not mean that calibration cannot be improved, but that the parameter set is not expected to change significantly as one goes from well to well or field to field.

The following mechanisms are included in the model (Raaen et al., 1996):

1. Grain contact plastification or crushing. During loading, stresses are intensified at grain contacts. This means that irreversible deformation may take place at relatively low stress levels. This mechanism is valid even during hydrostatic loading, and gives the following relationship between static bulk modulus K and the dynamic bulk modulus K_d :

$$K = K_d / (1 + 3PK_d) \quad (4.23)$$

where P is a parameter quantifying the process of grain contact crushing and has a characteristic dependence on stress. The parameters controlling this dependence are determined from calibration experiments.

2. Closed sliding cracks. For shear loading, additional mechanisms may give rise to a difference between the static and dynamic moduli. Such mechanism is due to closed cracks or weak contacts, which may undergo shear sliding as a result of a static disturbance (large amplitude stress) but will not be activated by the acoustic waves

(low amplitude stress). This mechanism gives the following relationship for the Young's modulus:

$$E = E_d(1 - F)/(1 + PE_d), \quad (4.24)$$

where F is proportional to the density of sliding cracks. The parameter F further depends on the friction coefficient for sliding of the cracks. Note that $F = 1$ corresponds to zero static stiffness.

From equations (4.23) and (4.24), P and F were calculated using available static data and corresponding dynamic data. Using the average value of calculated P and F , Young's modulus was calculated along the depth. Poisson's ratio was calculated using the following relationship:

$$\nu = 0.5 (1 - E/(3K)) \quad (4.24A)$$

4.6.2.3. AUTOSCAN METHOD

A new technique, named the AUTOSCAN method, was developed at KFUPM, RI in 2000. This method freezes the shape of the log-based parameter as a function of depth, and seeks the optimal shift, which causes the minimization of the sum of squared errors between the core points and the corresponding log values of the parameter. The technique was developed using a computerized algorithm. Using thousands of synthetic core and log data sets, it has been established that the AUTOSCAN method ensures a unique minimum sum of squared errors. Thus, the calibration obtained by this method is also unique, meaning that there is no other possible translational shift of the log data that will generate another calibration curve with the same amount of least squared errors between the static and dynamic values.

The available static data for Young's modulus and Poisson's ratio were subtracted from the corresponding dynamic data and the differences were averaged.

The average value was subtracted from the dynamic data in case of Young's modulus and was added in case of Poisson's ratio.

4.6.3. FACTORS INFLUENCING CALIBRATION

Serra (1984) mentioned that many factors influence the acoustic log measurements and accordingly the calibration process. The matrix affects the speed of sound depending on the kind of minerals making up the rock. In the case of complex lithologies the individual mineral effect is determined by their volume fraction and their individual speed of sound.

Elastic properties of sedimentary rocks are known to be controlled by the properties of the solid frame, the pore fluid, and the frame/fluid interactions (Manificat and Gueguen, 1998). Wang (2000) differentiated between the static and dynamic Young's modulus relationships for soft rocks and hard rocks. He concluded that a correction is needed on the dynamic Young's moduli in order to use the data in engineering applications. Such a correction can be achieved by dividing the dynamic Young's modulus by a factor that ranges from 20 for very soft sands and 1.0 for very hard rocks.

4.7. RESULT AND DISCUSSION

4.7.1. ROCK MECHANICS

The principal goal of this part is to identify dynamic and static mechanical properties of the Khafji reservoir. Furthermore, calibrate dynamic into static mechanical properties. The summary of the test results is presented in Table 4.1.

Table 4.1 shows that static Young's modulus of rock samples varies between 1.13×10^6 psi and 1.91×10^6 psi and Poisson's ratio varies between 0.161 and 0.264.

TABLE 4.1. Summary of rock mechanics tests on rock samples obtained from
Zuluf-A well.

Sample #	Lithology*	Porosity %	Static	
			E (psi)	ν
C1-T20	Shaly sandstone	32.6	1.71E+06	0.184
C1-T17	Shaly sandstone	25.4	1.84E+06	0.255
C1-T13	Shaly sandstone	11.1	1.57E+06	0.228
C1-T3	Shaly sandstone	33.3	1.41E+06	0.210
C3-T23	Shaly sandstone	29.2	1.13E+06	0.150
C3-T20	Sandstone	34.8	1.38E+06	0.161
C3-T14	Shaly sandstone	29.9	1.54E+06	0.246
C3-T4	Sandy shale	14.0	1.91E+06	0.238

* Detailed lithology in Appendix B

Young's modulus and Poisson's ratio relationship with porosity are plotted in Figures 4.4 and 4.5. It was observed that a weak trend of increasing Young's modulus and decreasing Poisson's ratio with increasing porosity. Previous studies (Fahy and Guccione, 1979; Plumb et al., 1992) shown that strength generally decreases as porosity increases. This contradiction may be due to the limited number of samples used in this study.

4.7.2. BIOT'S CONSTANT

Biot's constant values were obtained through stress-strain data. Table 4.2 summarizes the data obtained. Static Biot's constant values are plotted against porosity of the samples. A trend of increasing Biot's constant with increasing porosity was observed (Figure 4.6).

4.7.3. CALIBRATION

The data required for a successful calibration of mechanical properties are acoustic logs (DTC and DTS), bulk density, static core values and depth shift. The missing DTS Zuluf-A was calculated using the DTS-DTC relationship of Zuluf-B the depth shift data is estimated by comparing the log bulk density and laboratory measured density.

Table 4.3 illustrates parameters used for calibration of mechanical properties by the three methods. Figure 4.7 shows the comparison of calibrated mechanical properties calculated using the three methods with dynamic measurements. While Figures 4.8 and 4.9 show the regression fit between both static and dynamic Young's modulus and Poisson's ratio.

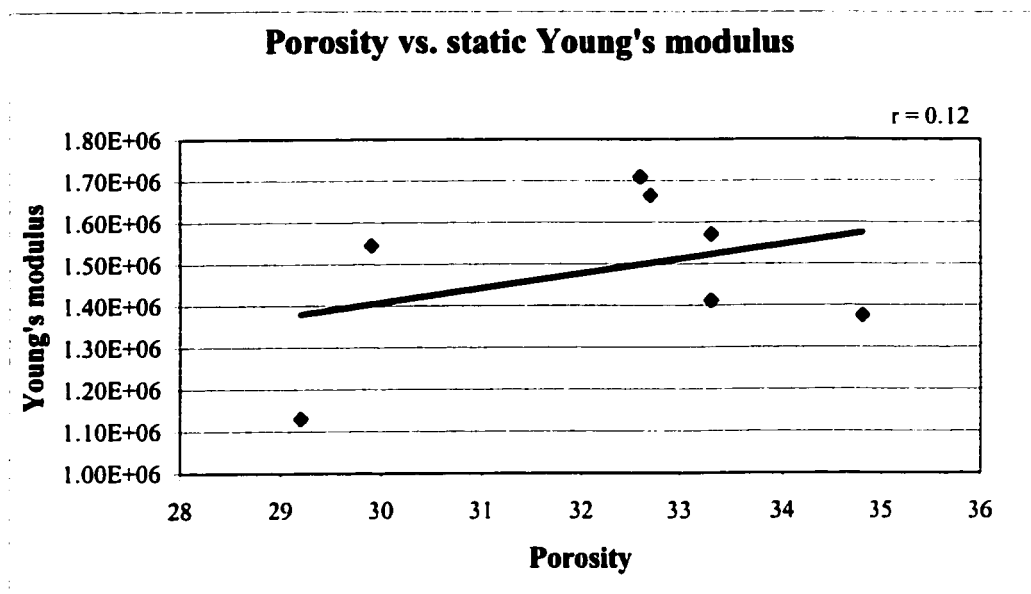


Figure 4.4. Variation of Young's modulus with porosity for the Khafji reservoir rock samples.

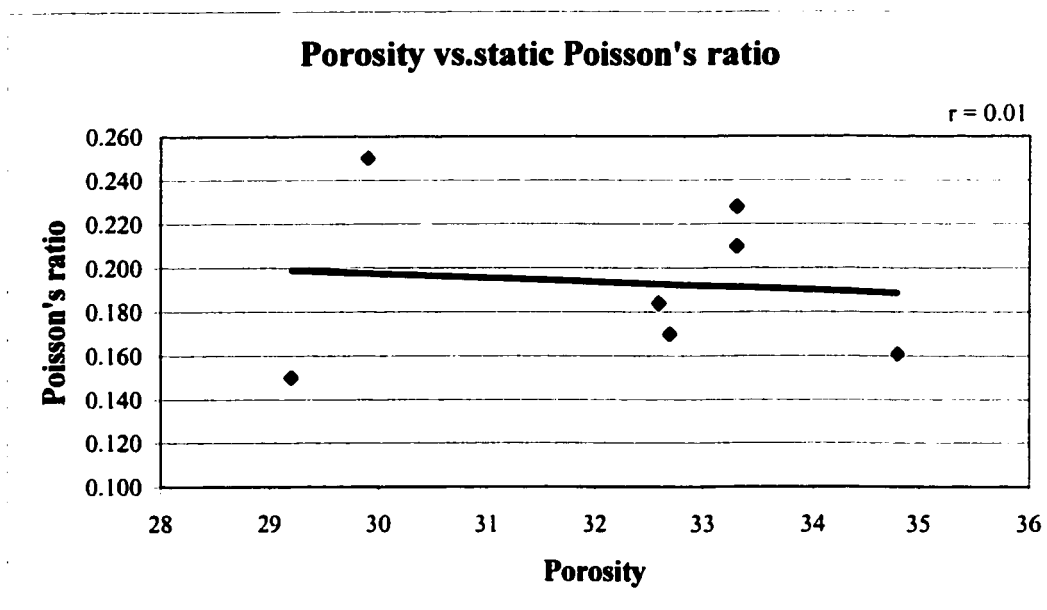


Figure 4.5. Variation of Poisson's ratio with porosity for the Khafji reservoir rock samples.

TABLE 4.2. Biot's constant values for Zuluf-A well samples.

Sample #	Static Poisson's ratio	K_{ma}	Biot's constant
C1-T20	0.184	6.21	0.86
C1-T17	0.255	0.62	0.81
C1-T13	0.228	6.62	0.85
C1-T3	0.21	5.58	0.87
C3-T23	0.15	3.70	0.91
C3-T20	0.161	4.67	0.89
C3-T14	0.246	6.96	0.84
C3-T9	0.16	3.61	0.92

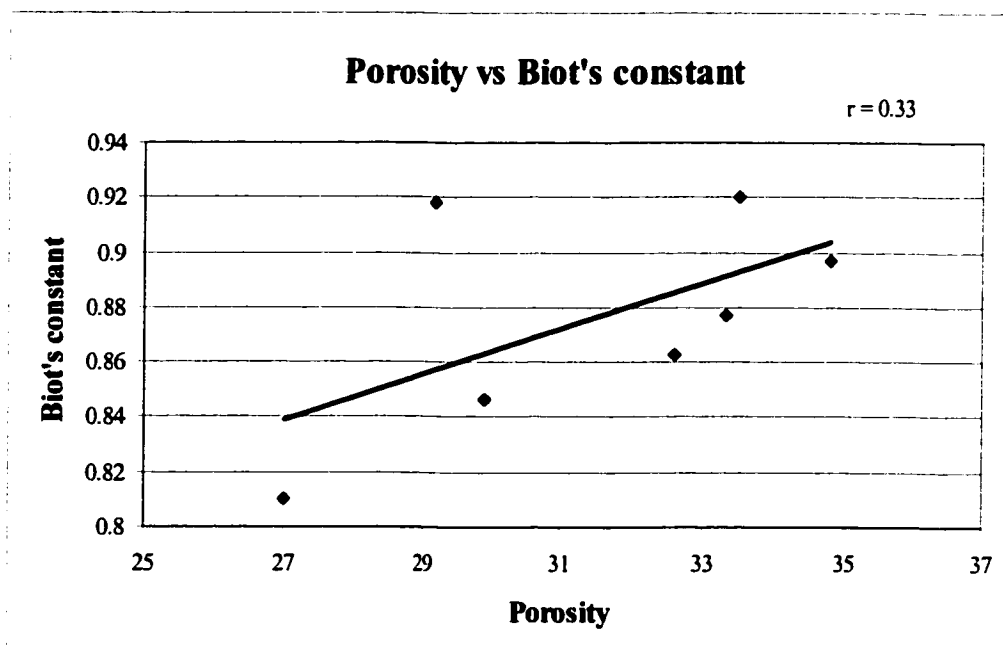


Figure 4.6. Variation of static Biot's constant with porosity.

TABLE 4.3. Parameters used for calibration of mechanical properties.

Young's modulus (Gpa)		Poisson's ratio		FORMEL parameters	
Regression	AUTOSCAN shift	Regression	AUTOSCAN shift	P	F
$Y=0.4141X+4.2908$	5.6118	$Y=-2.306X+0.9479$	0.1254	0.034	-0.042

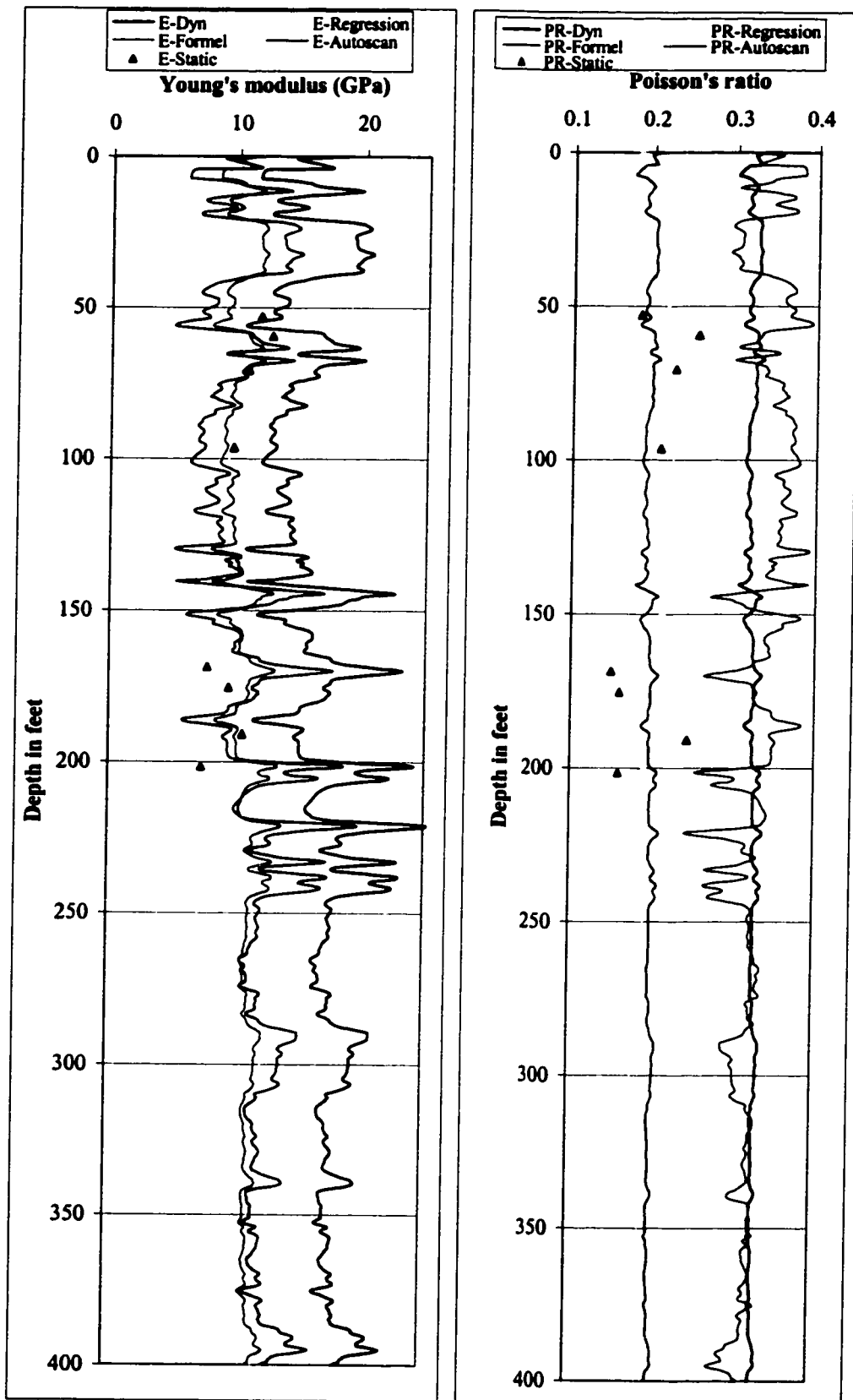


Figure 4.7. Comparison of calibrated and dynamic mechanical properties of the Khafji reservoir, Zuluf-A well.

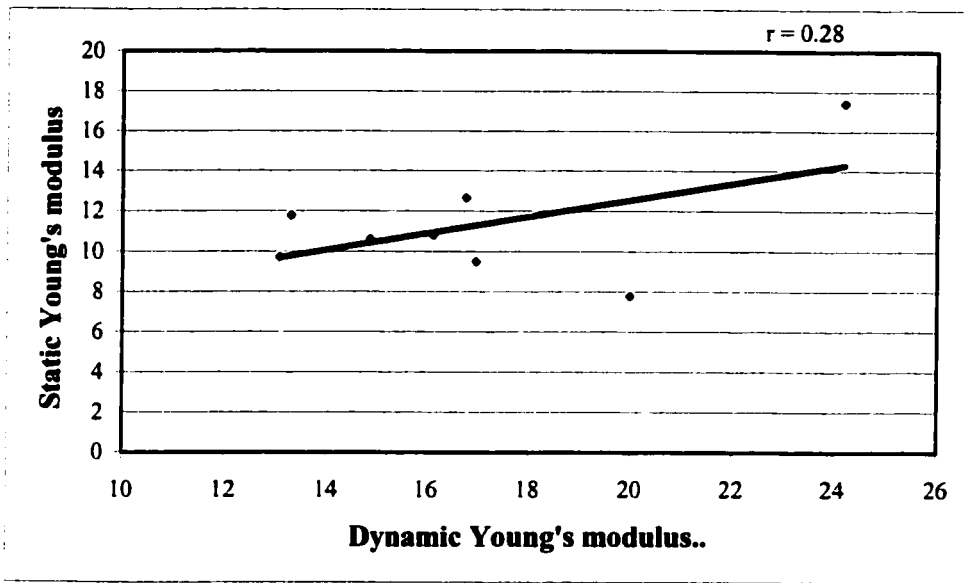


Figure 4.8. Linear regression between static and dynamic Young's modulus.

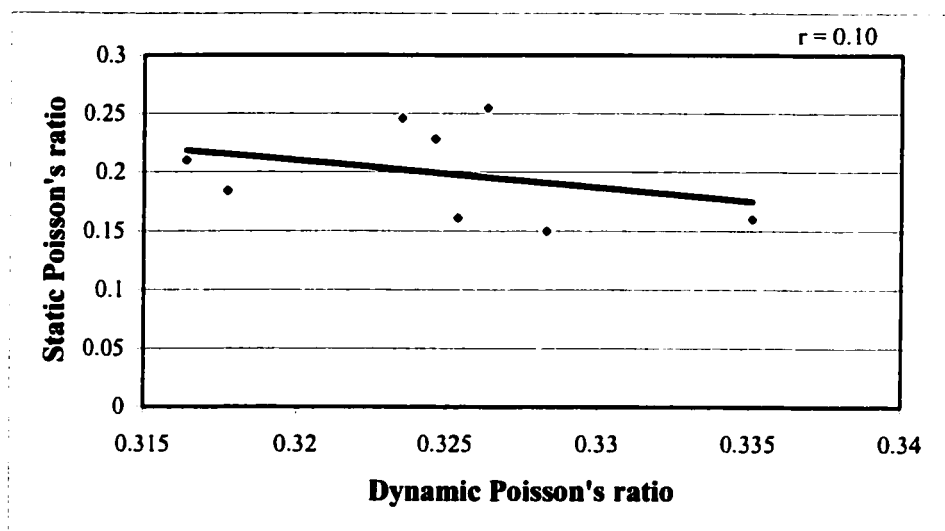


Figure 4.9. Linear regression between static and dynamic Poisson's ratio.

1. Regression method: For Young's modulus, the regression fits with low regression factor, which does not estimate the calibrated Young's modulus well (Figure 4.7). This is manifested by the failure of capturing the contrast of Young's modulus values of different layers in the Khafji reservoir as shown by log curve. However, if the regression coefficient value is good then the contrast is very well captured. The calibrated Young's modulus is always less than the log value.

The calibrated Poisson's ratio does not follow the log curve. Furthermore, the calibrated Poisson's ratio curve is different from the log value. This is may be due to the negative slope of the regression fit and hence it failed to give a good calibrated Poisson's ratio.

2. FORMEL method: For Young's modulus, it has successfully estimated the calibrated Young's modulus by approximately following the log curve. The variation in Young's modulus within the different layers in the section of interest is preserved by this method.

For Poisson's ratio, this method has failed to perform calibration between static and dynamic values successfully.

3. AUTOSCAN method: For Young's modulus, this method has successfully estimated the calibrated Young's modulus by approximately following the log curve. The variation in Young's modulus within the different layers in the reservoir is preserved by this method.

The AUTOSCAN method has performed the calibration of Poisson's ratio successfully in the well. The method preserved the variation in Poisson's ratio within different layers and considered the static measurements as well.

4.7.4. QUANTITATIVE COMPARISON

To compare the three methods of calibration quantitatively, the error between the calibrated values and the static values was calculated by using the following equation:

$$e^2 = \sum (X - Y)^2 / Y^2 \quad (4.25)$$

e^2 where is the error square, X is the calibrated values, and Y is the static values. Table 4.4 summarizes the error between the three methods used in this study.

The quantitative comparison shows that FORMEL method has the lowest error for calibrating Young's modulus with respect to other two methods. So, it calibrated Young's modulus successfully. However, the other two methods, linear regression and AUTOSCAN, still have low error and also calibrated Young's modulus successfully.

However, the linear regression method has the lowest error for Poisson's ratio calibration, it does not follow the log curve. This is may be due to the negative slope of the regression fit, therefore, it failed to give a good calibrated Poisson's ratio. Accordingly, AUTOSCAN method, due to its lower error and good similarity to the log curve, represents the best method for Poisson's ratio calibration.

4.7.5. LITHOLOGY CALIBRATION FACTOR

In Zuluf field, Khafji reservoir dynamic properties are systematically higher than static properties. Since the reservoir incorporates different lithologies, a lithology factor (static properties/dynamic properties) is calculated to find discrepancies between different lithologies static and dynamic mechanical properties.

Table 4.5. summarizes the average Young's modulus and Poisson's ratio lithology calibration factor for different lithology. The result shows that there is a discrepancy in lithology factor for the lithologies used in the analysis. The discrepancy

TABLE 4.4. Summary of error for different calibration methods.

	Linear	FORMEL	AUTOSCAN
Young's modulus (Gpa)	0.48	0.10	0.26
Poisson's ratio	0.26	3.44	1.25

TABLE 4.5. Lithology calibration factor for different lithologies.

Factors	Shaly sandstone	Sandstone
Young's modulus (GPa)	0.68	0.67
Poisson's ratio	0.65	0.54

is distinct specially for Poisson's ratio. Therefore, considering this discrepancy due to lithology effect in the calibration process will strengthen the result.

4.8 CONCLUSION

Static Young's modulus of rock samples varies between 1.13×10^6 psi and 1.91×10^6 psi and Poisson's ratio varies between 0.161 and 0.264. Biot's constant varies between 0.81 and 0.92. It was observed Biot's constant increases as porosity increases.

Qualitatively, the regression method calibrated Young's modulus and failed for Poisson's ratio. This may be due to the negative relationship between static and dynamic Poisson's ratio. On the other hand, FORMEL method calibrated Young's modulus successfully, while it failed for Poisson's ratio. Only AUTOSCAN method calibrated successfully both Young's modulus and Poisson's ratio.

The quantitative comparison among the three methods revealed that all of them are characterized by more or less low error for Young's modulus. So, they can calibrate Young's modulus successfully. However, only AUTOSCAN method has the lowest Poisson's ratio.

Different lithologies show discrepancies between static and dynamic mechanical properties. Consideration of lithology calibration factors in the calibration method will strengthen it.

CHAPTER FIVE

IN-SITU STRESS MODELING

5.1. INTRODUCTION

Stress is defined as force per unit area. It has the same units as pressure. However, stress is a much more complex quantity than pressure because it varies both with direction and with the surface it acts on. The types of stress are (Hatcher, 1990):

- 1. Compressive stress:** It is the stress that acts to shorten an object.
- 2. Tensile stress:** It is the stress that acts to lengthen an object.
- 3. Shear stress:** This stress acts parallel to a surface. It can cause one object to slide over another. It also tends to deform originally rectangular objects into parallelograms. The most general definition is that shear acts to change the angles in an object.

A knowledge of the orientation and magnitude of the in-situ horizontal stresses in a particular area is important in field-wide development plans, well design, wellbore stability analysis, wellbore completion strategy, hydraulic fracture design, and sand production prediction. More recent work has shown that accurate stress profile can be used to optimize fracturing of horizontal wells and designing multizone fracture treatment. Several techniques have been proposed to calculate in-situ stress profile (Blanton and Olson, 1997).

Differential stresses in basins can be an important factor in developing and maintaining an open fracture network. These fractures in turn can be influential in controlling fluid movement from source to reservoir and can enhance reservoir characteristics in potential reservoir rocks. In-situ stresses also influence fluid flow in producing reservoirs by controlling the direction of fracture permeability. Determining the magnitudes and directions of the in-situ stresses can therefore be a powerful predictive tool for evaluating both fluid movement within a basin and the development of fracture porosity and permeability in potential and producing reservoir rocks (Bell, 1990).

This chapter studies the in-situ stress in the Zuluf field. Leak-off test data is used in this study to estimate the minimum horizontal stress. The information compiled here includes specific in-situ stress measurement, specifically leak-off test, and interpretation of well logs. These data combine to give a coherent regional picture of principal stress orientations in the field.

The term in-situ stress is used to refer to the present-day active natural stresses within the field. In other words, how much and in what directions are the rocks being compressed at a specific location today? The stress regimes or paleostresses of the past are not of relevance here. The paleostresses might be indicated by permanent changes in rock fabric.

5.2. DETERMINATION OF IN-SITU STRESS

The unequal stresses around a wellbore are representative of regional stresses. Several methods are available to estimate the magnitude and direction of in-situ

stresses. These methods are (Prats, 1981; Warpinski et al., 1985; Brumley et al., 1994; Awal, 2002):

1. Leak-off test (LOT): Is often carried out while drilling exploration wells. It is run to measure the strength of rock units immediately below a casing shoe to indicate the formation pressure. Borehole fluid pressures are increased by pumping small quantity of water into the well. The water begins to leak off when a fracture is initiated in the borehole wall in the open interval below casing. Then, pumping is halted and borehole pressures are allowed to decay back. By plotting formation pressures and volume of water pumped into the borehole the value of shut-in pressure can be obtained. Shut-in pressure value represents a good estimate for the minimum principal stress.

2. Borehole extensometer: The extensometer measures the deformation of the wellbore before, during, and after hydraulic fracture initiation and propagation. These data are gathered and analyzed to obtain the in-situ stress direction, determine formation mechanical properties, and measure fracture closure pressure and fracture width.

3. Formation microscanner image (FMI): It measures the orientation of wellbore breakouts, which are unidirectional hole enlargements observed in the well.

4. Anelastic strain recovery (ASR): It is a core-based technique for determining the magnitudes and directions of the in-situ principal strains. This method is based on the theory that an oriented core relaxes or grows when the in-situ stresses are removed from it. During the process of relaxation, stress-relief microcracks are formed within the body of the core sample and the individual minerals and material components attempt to relax, which result in expansion. The presence of nonuniform confining stresses would result in a nonuniform expansion. The largest number of microcracks

would open perpendicular to the maximum stress, and least number of microcracks would open perpendicular to the minimum stress.

5. Borehole scanning record: Borehole acoustic/resistivity imaging is performed to determine the presence of any induced or natural fractures present on the wellbore.

This information provides the relative magnitude and the orientation of these fractures.

6. Multi-arm caliper log: Breakouts occur in the wellbore wall when the stress concentration at the cylindrical wellbore opening exceeds the compressive strength of the formation. Wellbore breakout is measured with an X-Y caliper tool. The wellbore tends to breakout in the direction parallel to the minimum horizontal stress.

7. Acoustic wave velocity: It is the most common method, where the equation that correlates the rock elastic property with the reservoir pressure and tectonics is used as given by the following relationship:

$$\sigma_h = \nu (\sigma_v - \alpha p) / (1 - \nu) + \alpha p + E (\epsilon_{\min} + \nu \epsilon_{\max}) / (1 - \nu^2) \quad (5.1)$$

where

σ_h = Minimum horizontal stress

ν = Poisson's ratio

σ_v = Overburden pressure

p = Pore pressure

α = Biot's constant

E = Young's modulus

ϵ_{\min} = Strain in the minimum horizontal stress direction

ϵ_{\max} = Strain in the maximum direction

5.3. APPLICATIONS OF IN-SITU STRESS INFORMATION

5.3.1. WELLBORE STABILITY

The orientation and magnitude of the in-situ stresses affect wellbore stability. The most stable wellbore will be achieved if the well is drilled parallel to the minimum horizontal stress. This minimizes the difference between the stresses acting on the wellbore wall (Woodland, 1988).

5.3.2. HYDRAULIC FRACTURE ORIENTATION

If the directions and relative magnitude of the principal stresses at the subsurface location are known, orientation of the induced hydraulic fractures can be predicted. This can be advantageous in a number of situations that arise during exploration and production program. If an exploration well has missed a small target such as a pinnacle reef, and the target's precise location is known, it is feasible to induce a fracture that will connect the well to the productive reservoir in the reef (Bell and Babcock, 1986). This is likely to be a cheaper option than directional drilling.

5.3.3. ENHANCE OIL RECOVERY

Both gas and oil production from tight reservoirs can be enhanced by inducing multiple fractures in a single well. If the hydrocarbon bearing section is thick and multi-fractured, inclined wells could be effective. However, the well must be drilled in a direction close to the maximum horizontal stress (Bell, 1990).

5.4. IN-SITU STRESS REGIMES

In-stress regimes cause bed-to-bed deformation and stress direction variations through the formations.

Five states of stress may be defined in terms of the principal stresses. The simplest case consists of all three principal stresses being equal. The second simplest case occurs in regions where the two horizontal stresses are equal and less than the vertical stress of the overburden (Whitehead et al., 1987).

For the remaining cases, the three principal stress magnitudes differ significantly. Unequal horizontal stresses can be attributed to tectonic forces or effects that result from the presence of geologic features. Depending on the ordering of the stresses, three cases are defined (Whitehead et al., 1987; Aleksandrowski et al., 1992):

1. Normal fault regime: σ_v is the maximum principal stress ($\sigma_v = \sigma_1$). Normal faults are dip-slip faults, in which the hanging wall has moved down relative to the footwall (Figure 5.1A).

2. Reverse fault regime: σ_v is the minimum principal stress ($\sigma_v = \sigma_3$). Reverse faults are dip-slip faults, in which the hanging wall has moved up relative to the footwall (Figure 5.1B).

3. Strike-slip fault regime: σ_v is the intermediate principal stress ($\sigma_v = \sigma_2$). In strike-slip faults the wall has moved horizontally (Figure 5.1C).

5.5. REGIONAL GEOTECTONICS

Tectonically, Saudi Arabia is part of the Arabian Plate. It consists of crystalline Precambrian basement overlain by low-dipping Phanerozoic sedimentary and volcanic rocks, which originated as a consequence of rifting along the line of the eventual Red

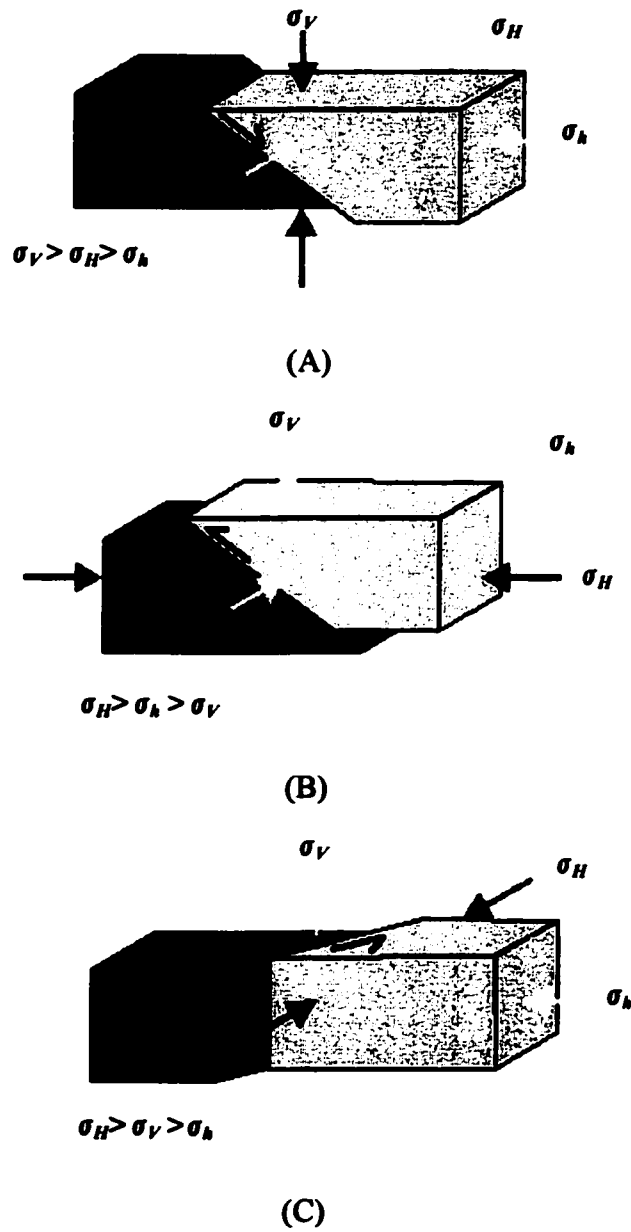


Figure 5.1. Relationships between principal stresses and types of faults (A: normal, B: reverse, and C: strike slip).

Sea and the Gulf of Aden. The plate moved north and collided with the Eurasian plate. Prior to rifting, the rocks of Saudi Arabia were contiguous with those of Northeast Africa, Figure 5.2 (Johnson, 1998).

The Phanerozoic geologic history of Saudi Arabia is marked by moderate degree of tectonism in the Precambrian basement and the formation of a succession arches, basins, and fault blocks. Coupled with the rise and fall of sea level in the flanking Tethys ocean and the epeirogenic effect of plate movements, these structures controlled sedimentation of the Phanerozoic rocks. Resulting in the development of unconformities, systematic sequence thickening and thinning, and facies migrations that characterize much of the Phanerozoic succession in Arabia (Johnson, 1998).

Previous studies of regional stress acting on the Arabian Plate in the area around the Arabian Gulf have identified two main stress regimes: the Oman stress, which was active during Paleozoic and Mesozoic time with peak activity during the Upper Cretaceous. And the Zagros stress, which was very active in Early Tertiary time and continues till the present day (Marzouk and Sattar, 1993). The principal horizontal stress for the Oman stress regime acted in the E-W direction, while the principal horizontal stress for the Zagros stress is NE-SW direction, perpendicular to the Zagros crush zone which marks the boundary between the Arabian Plate and the Central Iranian Plate. The Zagros crush zone lies on the Northeastern side of the main Zagros fold belt and is currently an area of compressional and dextral strike slip motion, Figure 5.2 (Jorgensen et al., 1994).

5.6. IN-SITU STRESSES CALCULATION

The state of the in-situ stress in earth can be described completely by three principal stresses that act perpendicular to each other: maximum principal stress,

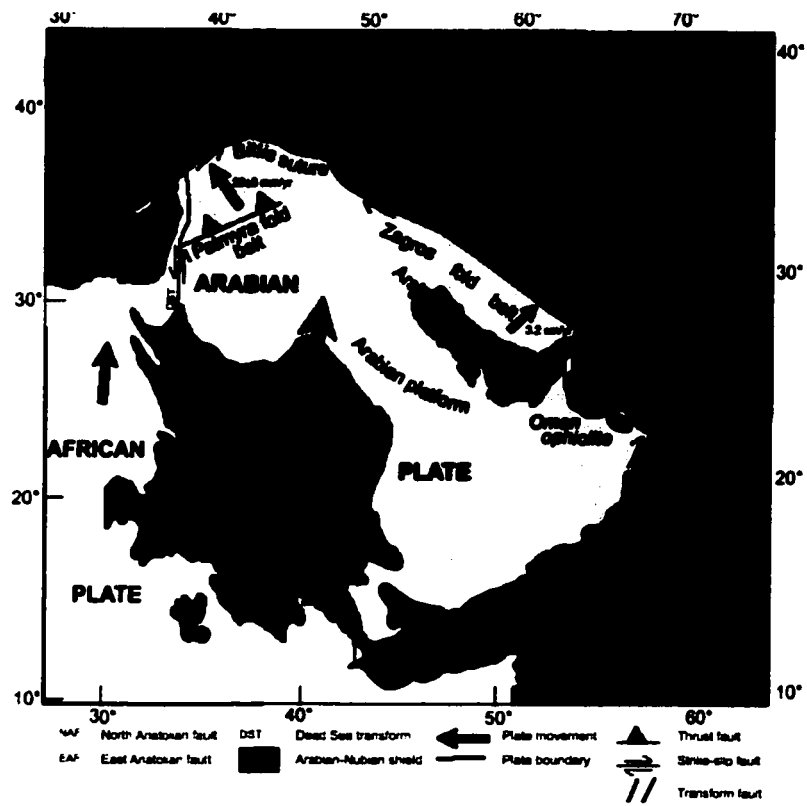


Figure 5.2. Tectonic features of Saudi Arabia and adjacent area
(after Johnson, 1998).

intermediate principal stress, and minimum principal stress. Because the principal stress directions are orthogonal, the direction of any two principal stresses automatically describes the direction of the third one.

A complete description of the state of in-situ stress is important because hydraulic fracture propagates perpendicular to the minimum principal stress. If the minimum principal stress is horizontal, a vertical fracture will be created; if the minimum principal stress is vertical, a horizontal fracture will be created; if the minimum principal stress is inclined, an inclined fracture normal to it will be created (Bell, 1990).

In this study the following methodology is used for determining the in-situ stress orientation and magnitude:

1. The orientation of σ_h is determined using FMI.
2. The value of σ_v is determined first, by integrating the density log over the depth.

$$\sigma_v = \int \rho_b dz. \quad (5.2)$$

3. The value of the minimum stress is calibrated to leak-off test value.
4. Then, the value of maximum horizontal stress is determined after the calculation of tectonic component stress.

5.7. IN-SITU STRESSES DETERMINATION FOR KHAFJI RESERVOIR

Several studies have been conducted to estimate the in-situ stress regime of Jauf and Khuff Formations in Ghawar field. These studies illustrated that those formations are under compressional tectonic stresses (Temeng et al., 1999; Al-Qahtani and Rahim, 2001).

5.7.1. IN-SITU STRESS ORIENTATION

The direction of the minimum horizontal stress in Zuluf field was determined from the analysis of FMI breakouts of Shu'aiba Formation, which underlies Khafji reservoir in Zuluf-C well. The FMI image (Figure 5.3) indicates the presence of breakouts. The rose diagram plot resulting from the interpretation of the FMI image is presented in Figure 5.4. Breakouts, and therefore the minimum horizontal stress, are oriented in N60°W direction and the maximum horizontal stress is normal to it (N30°E).

5.7.2. MAGNITUDE OF VERTICAL STRESS

The magnitude of vertical stress, σ_v , was determined by integrating bulk density, ρ_b , obtained from wireline logs over the depth, Z , of the formation.

$$\sigma_v = \int \rho_b dz. \quad (5.3)$$

Because Zuluf-A well does not have continuous density measurements to surface, a composite representative curve was created. For the Khafji reservoir, the vertical stress gradient is determined to be about 1.1 psi/ft.

5.7.3. MAGNITUDE OF HORIZONTAL STRESSES

The most common method to calculate minimum and maximum horizontal stresses is based on acoustic log, where the equations correlate the rock elastic properties with tectonics.

In this study the minimum and maximum horizontal stress values at every depth of the Khafji reservoir were computed from equations 5.4 and 5.5:

$$\sigma_h = \nu (\sigma_v - \alpha p) / (1 - \nu) + \alpha p + E (\epsilon_{min} + \nu \epsilon_{max}) / (1 - \nu^2) \quad (5.4)$$

$$\sigma_H = \nu (\sigma_v - \alpha p) / (1 - \nu) + \alpha p + E (\epsilon_{max} + \nu \epsilon_{min}) / (1 - \nu^2) \quad (5.5)$$

ϵ_{min} is the strain in the minimum stress direction, ϵ_{max} is the strain in the minimum

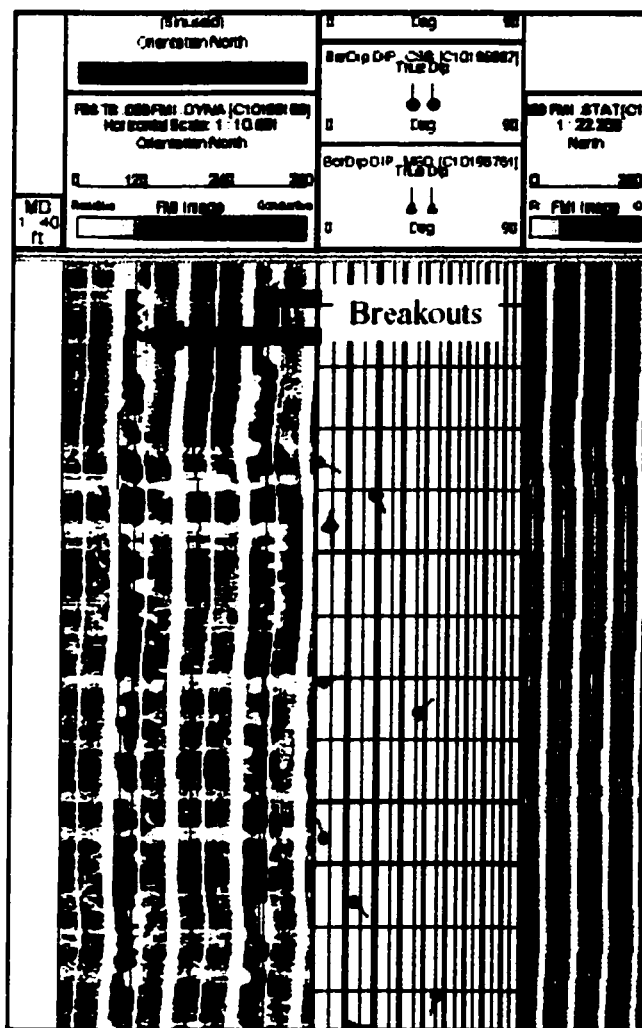


Figure 5.3. Zuluf-C FMI illustrating the breakout directions.

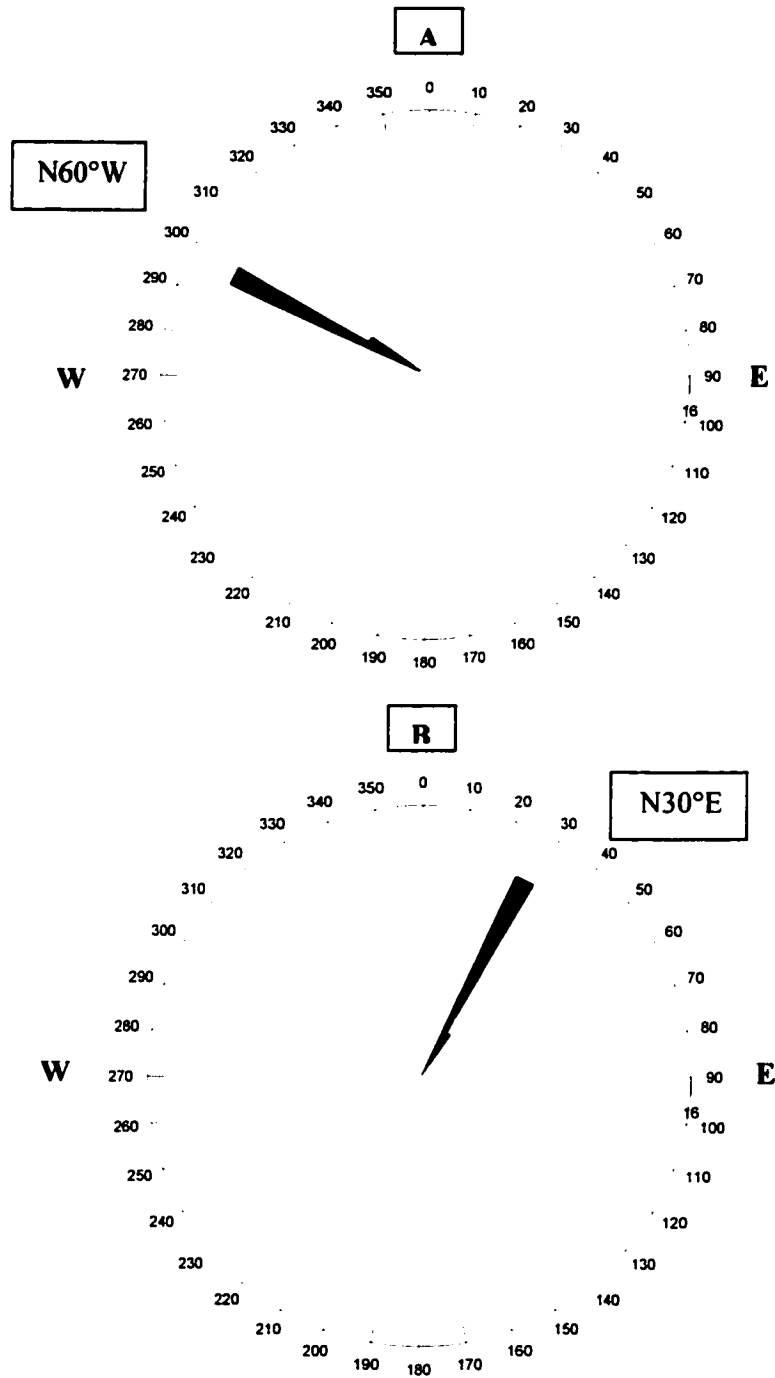


Figure 5.4. (A) Minimum and (B) maximum horizontal stress directions for Zuluf field.

stress direction, $E (\varepsilon_{min} + \nu \varepsilon_{max}) / (1-\nu^2)$ represents the tectonic stress component. RFT (Repeat Formation Test) was conducted on Zuluf field and a value of 0.45 was taken as constant for pore pressure. For ease of calculation, ε_{min} was set to zero.

A leak-off test (LOT) was conducted in the Khafji reservoir. Nine injection cycles using sea water were performed. Consequently, the reservoir pressure increased at each cycle (Figure 5.5). Decrease in the reservoir pressure indicates opening of the fractures. The shut-in pressure value represents the minimum horizontal stress. A value of 0.72 psi/ft is used as the minimum horizontal stress.

To calculate the maximum horizontal stress, ε_{max} value is calculated from equation (5.4) and substituted in equation (5.5). Using the calibrated values of Young's modulus and Poisson's ratio, curves for minimum and maximum horizontal stresses were generated (Figure 5.6).

5.8. CONCLUSION

The Khafji reservoir in Zuluf field appears to be tectonically stressed. The azimuths of the minimum and maximum horizontal stress are approximately northwest and northeast, respectively.

Typical values of minimum and maximum horizontal stress gradients are 0.82 psi/ft and 0.9 psi/ft, respectively. The vertical stress (σ_v) gradient is approximately 1.1 psi/ft. For the Khafji reservoir, the maximum principal stress is the vertical stress (σ_v), the intermediate principal stress is the maximum horizontal stress (σ_H), and the minimum horizontal (σ_h) stress represents the minimum principal stress. The relationship between the magnitudes of the three principal stresses ($\sigma_v > \sigma_H > \sigma_h$) suggests a normal fault regime. It appears that Zagros stress regime does not have the major effect in the field.

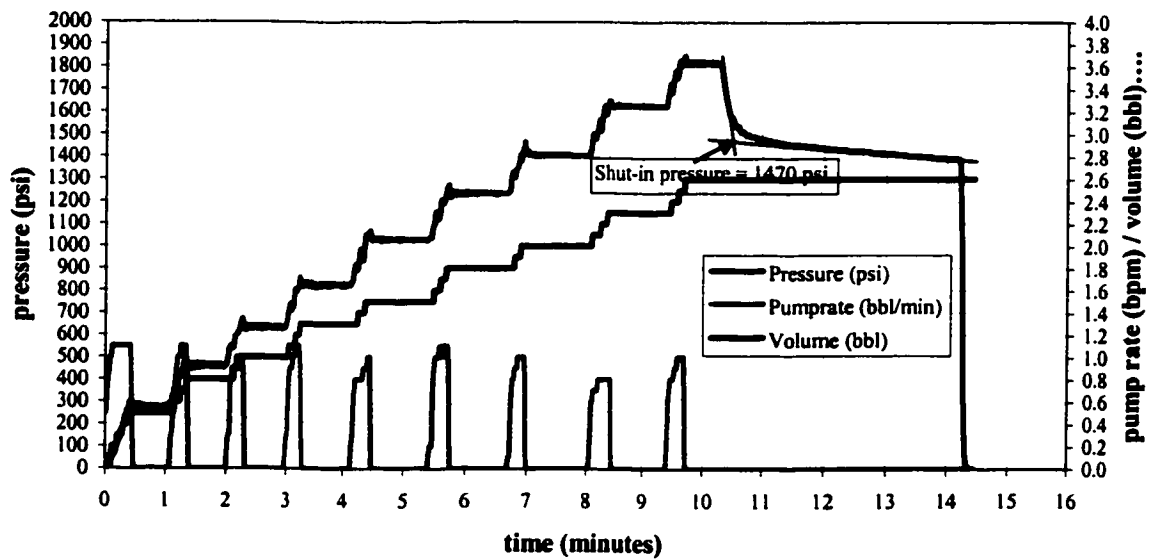
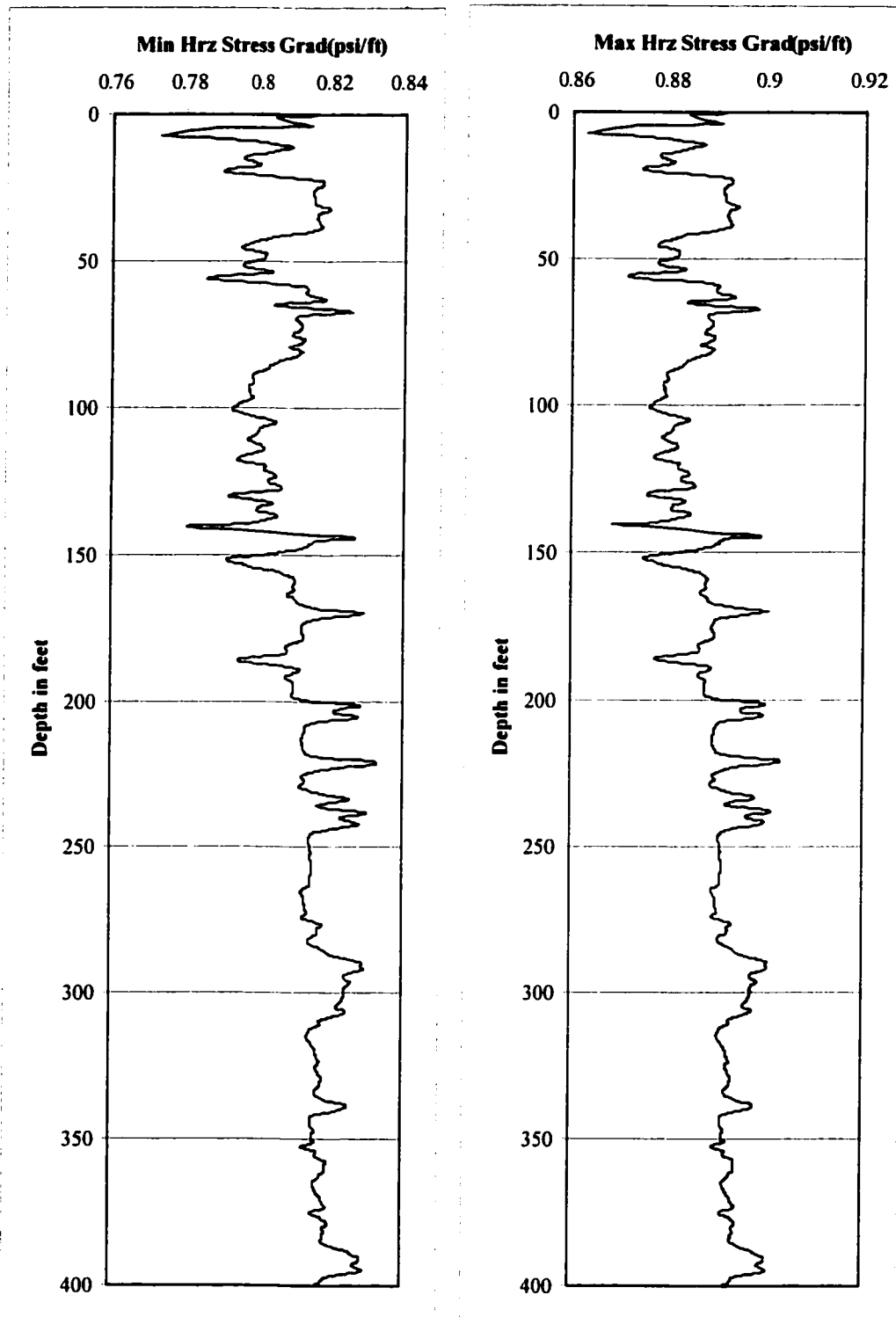


Figure 5.5. Leak-off test data from Zuluf-D well.



(A)

(B)

Figure 5.6. Minimum and maximum horizontal stress gradient for well Zuluf-A.

The stress orientations are useful for predicting the orientations of hydraulic fractures. In case of Khafji reservoir, hydraulic fractures will propagate northeast (parallel to the maximum horizontal stress). This information is also helpful for planning secondary recovery programs.

When planning a directional well, the stability of the wellbore can be different depending on the alignment of the wellbore with the principal stresses. The wellbore is easily stabilized if the principal stresses acting on the wellbore sides are as similar as possible. If a horizontal well is to be drilled in a normally stressed area, then drilling in the direction of σ_h would give σ_v and σ_H acting on the wellbore. Difference between the acting stresses = $\sigma_v - \sigma_H$. Drilling in the direction of σ_H would give σ_v and σ_h acting on the wellbore. Difference between the acting stresses = $\sigma_v - \sigma_h$.

$$(\sigma_v - \sigma_H) < (\sigma_v - \sigma_h)$$

As a conclusion, stable horizontal wellbore is achieved if the well is drilled parallel to the minimum horizontal stress to minimize the differences between the stresses acting on the wellbore. So, in such normal stress fault regime acting on Zuluf field, the horizontal wells toward northeast will be less stable than horizontal wells toward northwest.

CHAPTER SIX

CONCLUSIONS AND RECOMMENDATIONS

6.1. CONCLUSIONS

Since rocks are the host of oil and gas, their mechanical behavior and factors such as in-situ stress are important in both exploration and development processes of a reservoir.

The objectives of the study were to investigate the relationships between the geological parameters and the mechanical properties through the study of compositional and textural elements of the Khafji reservoir, Zuluf field, offshore Saudi Arabia. The study also made an attempt to establish a relationship between static and dynamic elastic moduli and to model the in-situ stress affecting the field.

Sieve analysis was done to characterize the grain size distribution of the reservoir samples. The relationships between grain size parameters and mechanical properties were quantified by a comprehensive bivariate statistical evaluation. The correlation was made between grain median, mean, sorting, skewness, and kurtosis and Young's modulus and Poisson's ratio. The study showed that the relationships were not significant.

The Khafji reservoir sandstone consists mainly of quartz and low percentages of feldspar and clay. On the basis of (QFL) classification, the main sand reservoir studied samples are classified as quartz arenite. While the stringer sand reservoir

samples are dominated by quartz wacke. The XRD study revealed that kaolinite is the main clay mineral in the samples. The EDS of samples showed that most of the samples are rich in silica, which indicates quartz enrichment. The relatively high content of Al indicates the presence of kaolinite that appeared in XRD test.

It is believed that due to compaction and burial the porosity decreases and rock strength increases with depth. However, the later processes such as diagenesis affect this relationship. Petrographic study was conducted to identify both the mineralogical composition and grain contacts percentage. The relationships between petrographic characteristics and mechanical properties were quantified by a comprehensive bivariate statistical evaluation. It was observed that the relationships between percentages of quartz and grain contacts with Young's modulus were not significant whilst it was significant with Poisson's ratio. The correlation coefficient with percentages of quartz and grain contacts suggested a tendency for Poisson's ratio to increase as the percentages of quartz and grain contacts decrease. The good relationships between Poisson's ratio and petrographic characteristics were attributed to thin sections direction. Petrographic characteristics parallel to the direction of lateral strain showed a better correlation with Poisson's ratio.

The effect of confining pressure on the mechanical properties was also investigated. In this study, it was observed that the value of Young's modulus increases with increase in confining pressure. However, this behavior was not exhibited by Poisson's ratio.

To investigate the effect of the depositional environment on mechanical properties, the approach suggested by Moiola and Weiser (1968) was used to classify Khafji reservoir samples. According to them, samples were categorized into beach

sand and river sand. It was found that samples representing beach sand had the lowest average Young's modulus and Poisson's ratio.

For the same purpose, factor analysis was used and three factors were identified. Factor 2 is highly truncated distribution sandstone, Factor 3 is highly truncated shaly sandstone, and Factor 1 is sandstone population with small amount of shale. Each factor represents specific type of depositional environment. Factor 2 represents beach environment, Factor 3 represents gravitational settling environment, and Factor 1 represents current energy environment. It was observed that beach environment has lower values of Young's modulus and Poisson's ratio relative to gravitational settling environment.

A sequence stratigraphic model was interpreted for the Khafji reservoir in well Zuluf-A. The model was constructed based on gamma ray and resistivity logs. Another model was interpreted for Zuluf-AA for confirmation purpose. The main sand and the upper stringer sand represent a (LST) and succeeding (TST). It was observed that the (LST) has the highest Young's modulus and Poisson's ratio relative to the (TST).

Static Young's modulus for Zuluf-A well varies between 1.13×10^6 psi and 1.91×10^6 psi. While, the Poisson's ratio varies among 0.161 and 0.264. Biot's constant values range between 0.81 and 0.92. It was observed that Biot's constant increases with increases in porosity.

Three methods were used for calibration of dynamic rock mechanical properties using static values. They are: linear regression, FORMEL, and AUTOSCAN. Only, AUTOSCAN method calibrated successfully both Young's modulus and Poisson's ratio.

Quantitatively, the comparison among the three methods revealed that they can be used successfully for calibration of Young's modulus with relatively low error. However, only AUTOSCAN method has the lowest error for Poisson's ratio. Therefore, it is the best method for calibration.

It was demonstrated that data gathered through logging and leak-off and microfrac tests can be used to estimate principal in-situ stress magnitudes and orientations in the field. It was found that the Khafji reservoir in Zuluf field appears to be tectonically stressed. FMI record was analyzed for indication of horizontal principal stress orientation. The azimuths of the minimum and maximum horizontal stresses are approximately northwest and northeast, respectively.

Typical values of minimum and maximum horizontal stress gradients are 0.82 psi/ft and 0.9 psi/ft, respectively. The vertical stress gradient is approximately 1.1 psi/ft. The maximum principal stress is the vertical stress and the intermediate principal stress is the maximum horizontal stress, while the minimum horizontal stress represents the minimum principal stress. The relationship among the magnitudes of the three principal stresses ($\sigma_v > \sigma_H > \sigma_h$) suggests a normal fault regime and demonstrates that Zagros stress regime does not have the major effect in the field.

6.2. RECOMMENDATIONS

Additional textural, compositional, and mechanical properties of samples from other wells in the Zuluf field may be analyzed to extend and/or reinforce the findings of this study. Model can then be constructed to predict the rock mechanical properties from textural and compositional properties.

No explicit relationship based on a sound theory exists in converting static and dynamic properties of reservoir rocks. When comparing dynamic to static properties,

the two types of properties should be measured at the same condition (pressure, saturation, etc). Therefore, preservation of the cores directly after their extraction from wellbore shipping them quickly to the laboratory will provide a better empirical relationship.

An almost universal feature of rock formation in sedimentary basins is that they tend to be heterogeneous. This heterogeneity includes variation in lithology, porosity, and pore fluid properties. Consequently, lithology calibration factor will provide a better utility for dynamic static properties conversion. So, development of a new calibration method utilizing it would be of great value.

Unfortunately, there is no universal relationship between dynamic and static mechanical properties for all reservoir rocks. Because rocks vary greatly from reservoir to reservoir in terms of pore pressure, mineralogy, etc. Therefore, it is recommended to establish local or regional empirical relationship between dynamic and static mechanical properties for a given field.

An alternative method for determining the in-situ stress orientation may be used to compare the results of the present study.

APPENDIX A

THIN SECTION PHOTOMICROGRAPHS

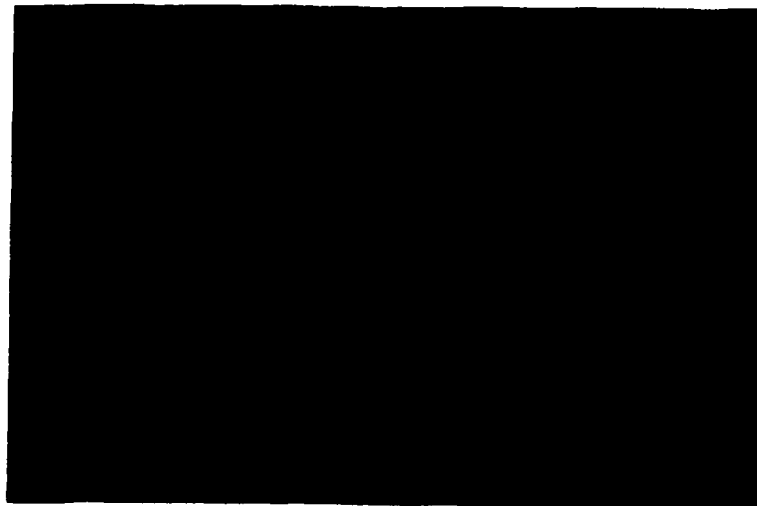


Figure A.1. Thin section photomicrograph, X10 under plane and cross-polarized light, for sample C1-T20.

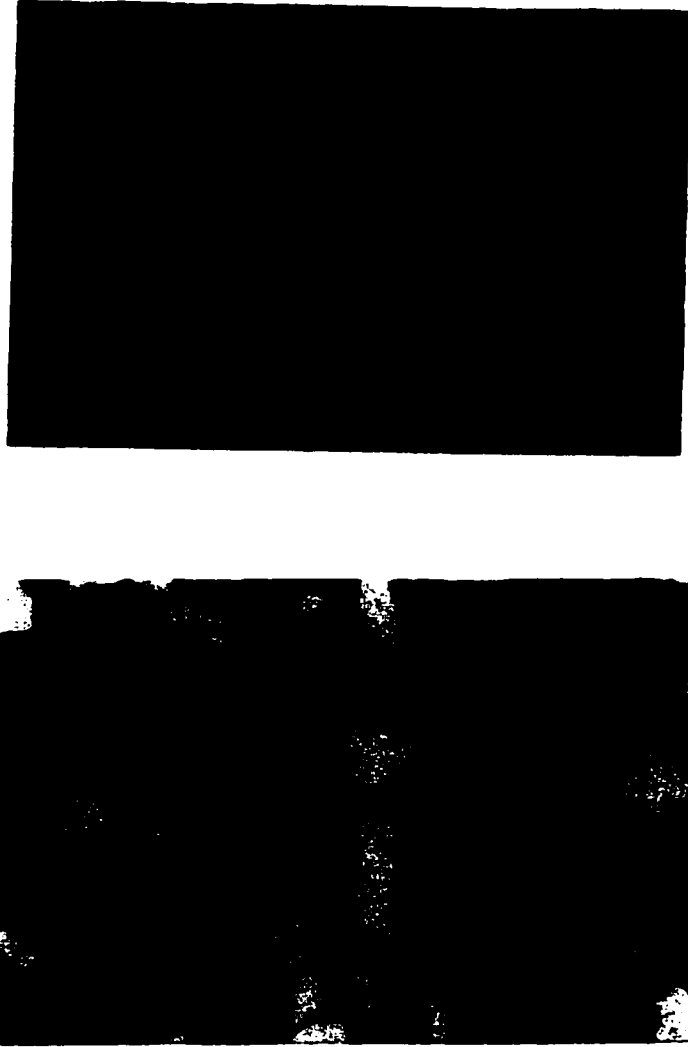


Figure A.2. Thin section photomicrograph, X10 under plane and cross-polarized light, for sample C1-T13.

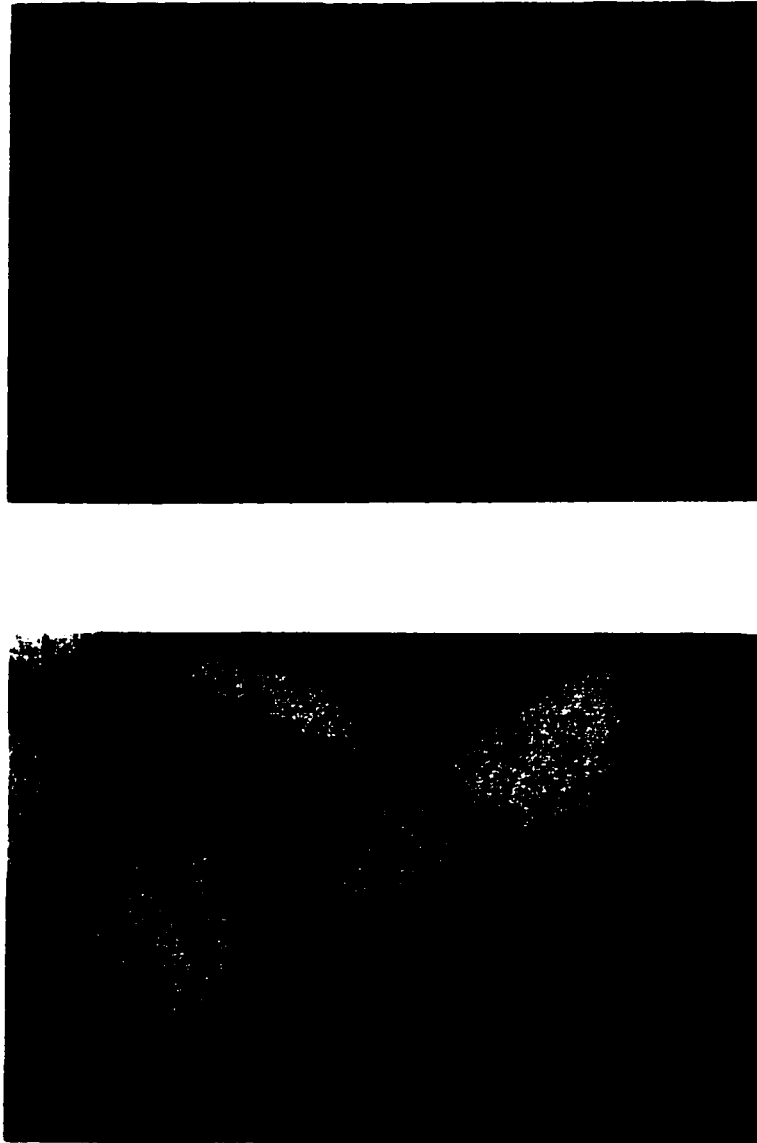


Figure A.3. Thin section photomicrograph, X10 under plane and cross-polarized light, for sample C1-T6.

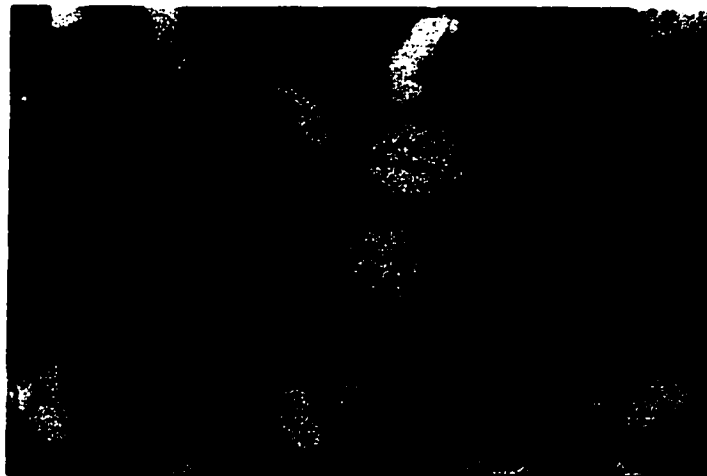
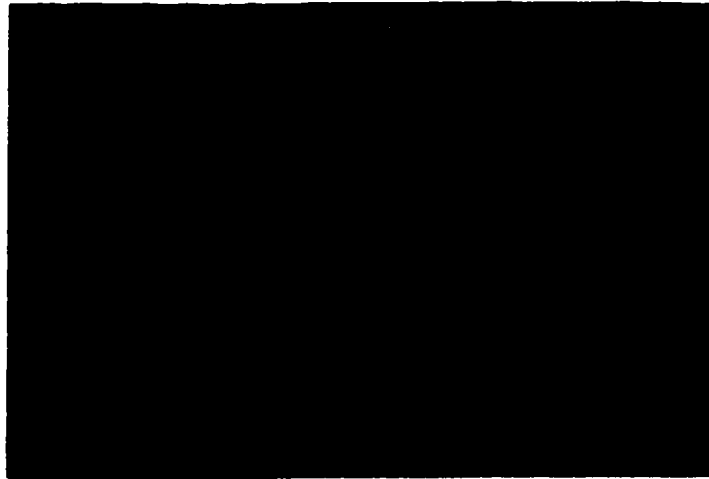


Figure A.4. Thin section photomicrograph, X10 under plane and cross-polarized light, for sample C1-T3.

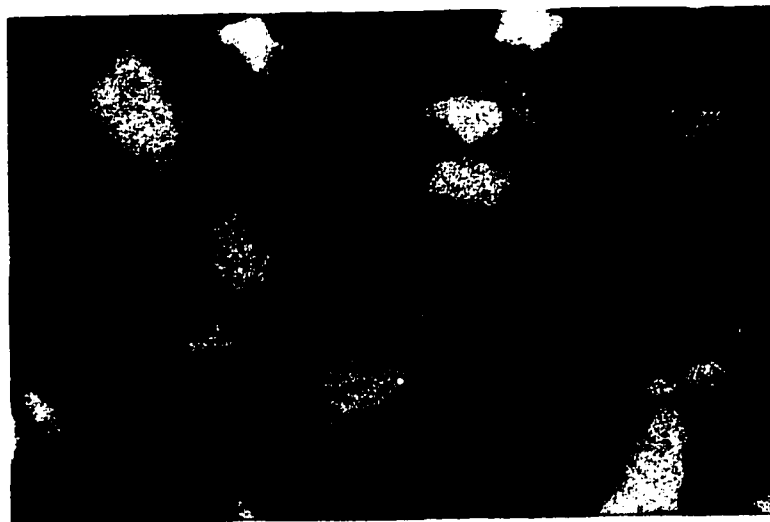


Figure A.5. Thin section photomicrograph, X10 under plane and cross-polarized light, for sample C2-T21.



Figure A.6. Thin section photomicrograph, X10 under plane and cross-polarized light, for sample C2-T11.

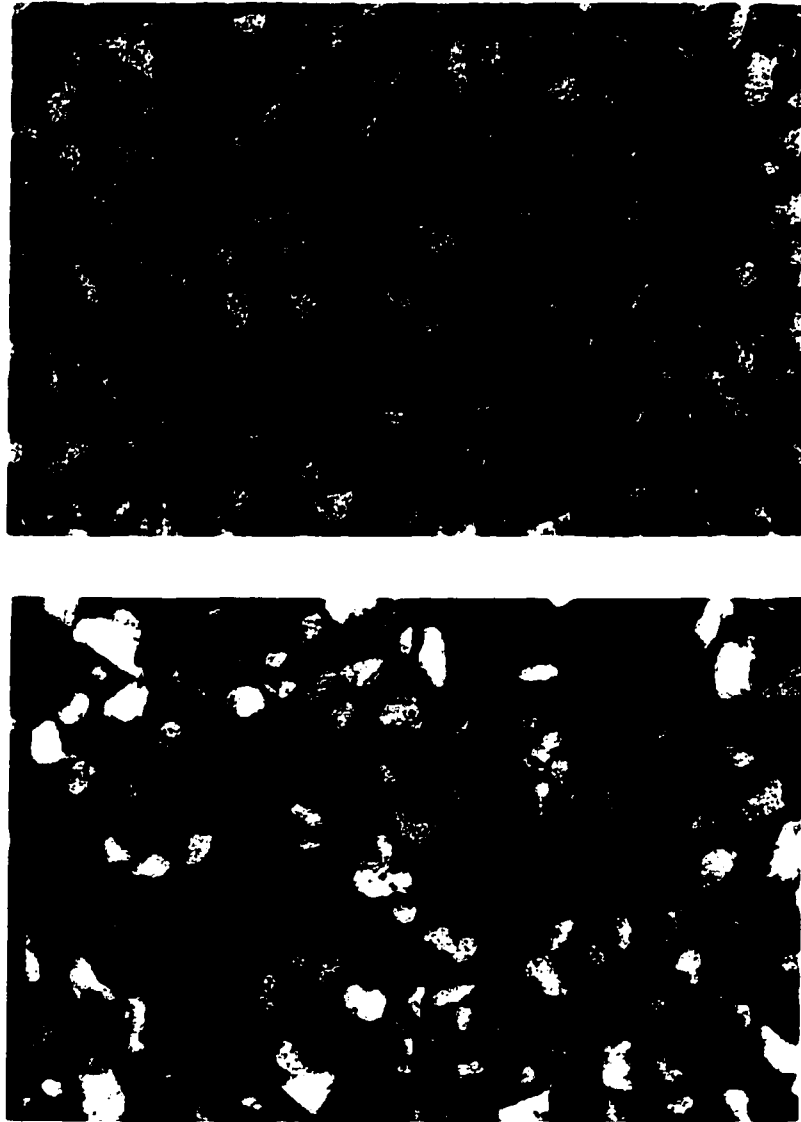


Figure A.7. Thin section photomicrograph, X10 under plane and cross-polarized light, for sample C2-T8.

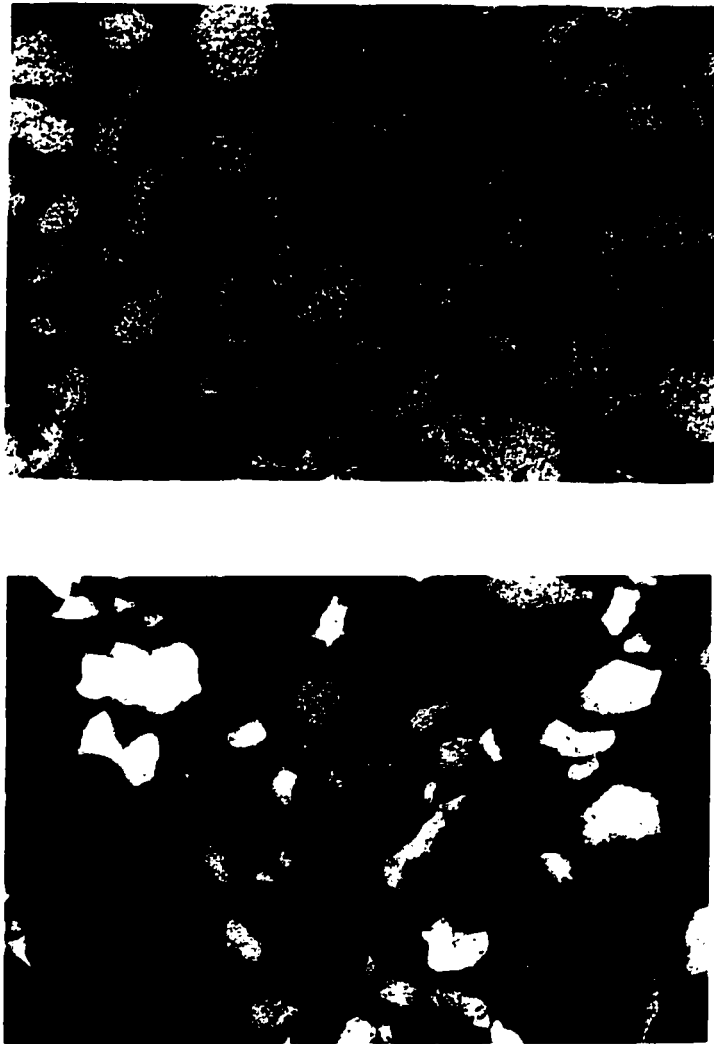


Figure A.8. Thin section photomicrograph, X10 under plane and cross-polarized light, for sample C2-T1.

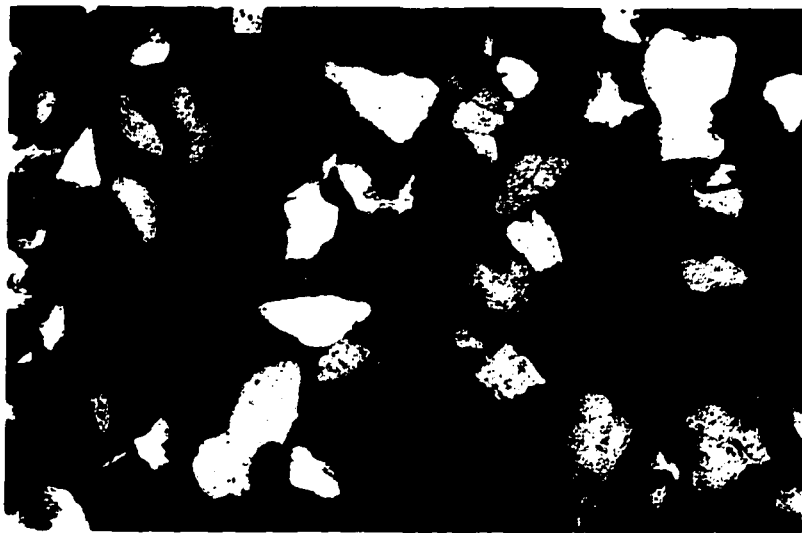


Figure A.9. Thin section photomicrograph, X10 under cross-polarized light, for sample C3-T23.



Figure A.10. Thin section photomicrograph, X10 under plane and cross-polarized light, for sample C3-T20.

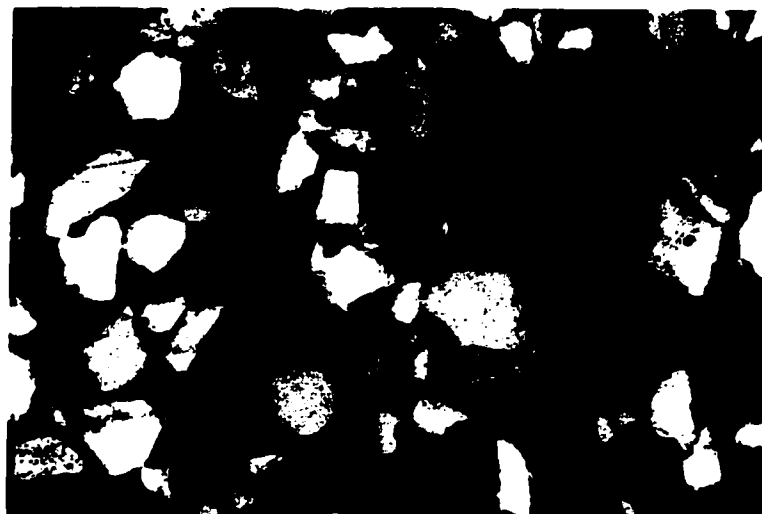
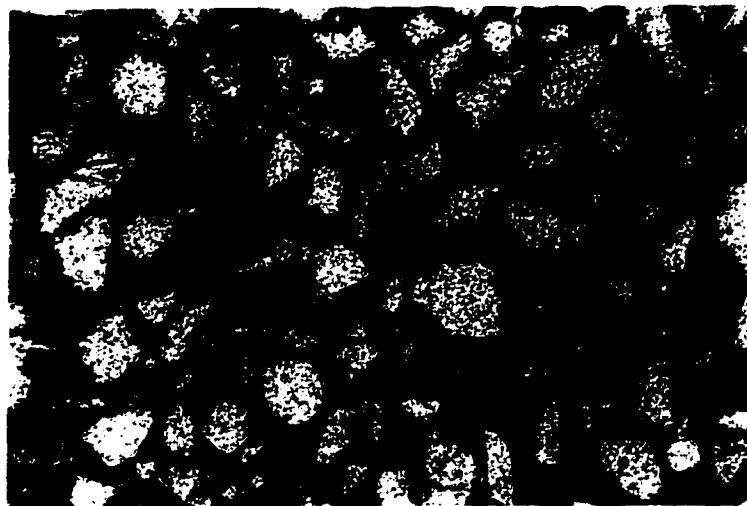


Figure A.11. Thin section photomicrograph, X10 under plane and cross-polarized light, for sample C3-T14.

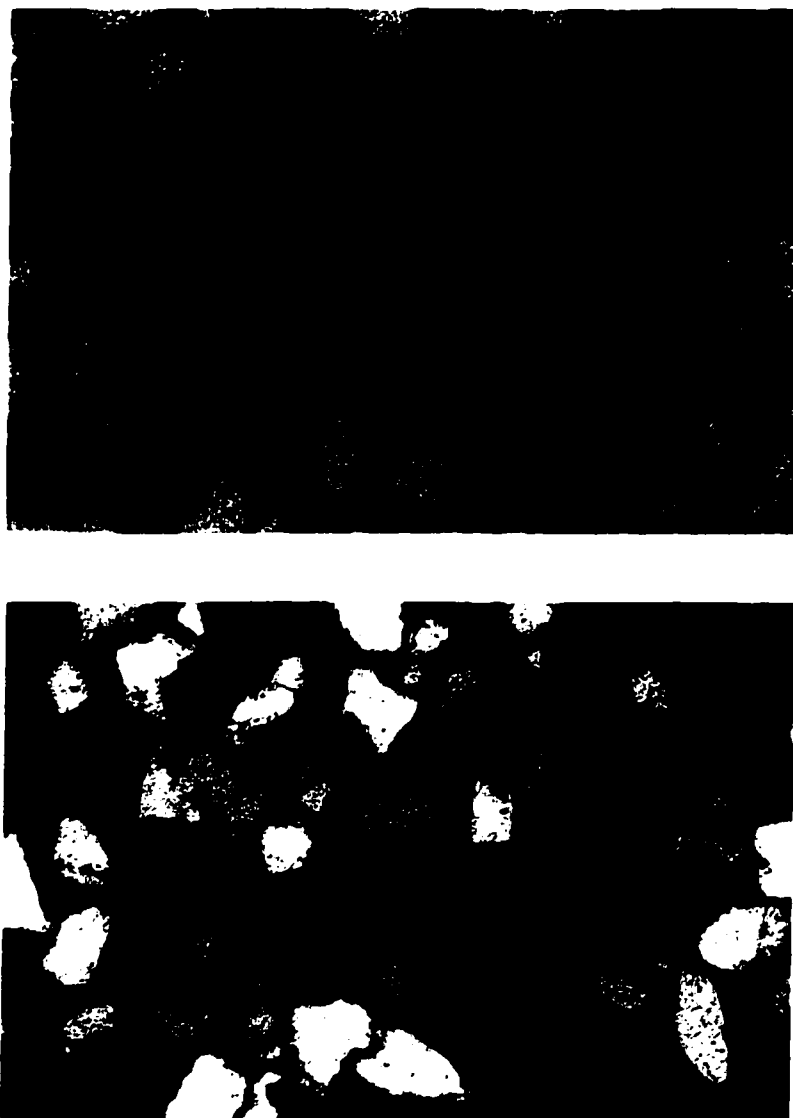


Figure A.12. Thin section photomicrograph, X10 under plane and cross-polarized light, for sample C4-T23.

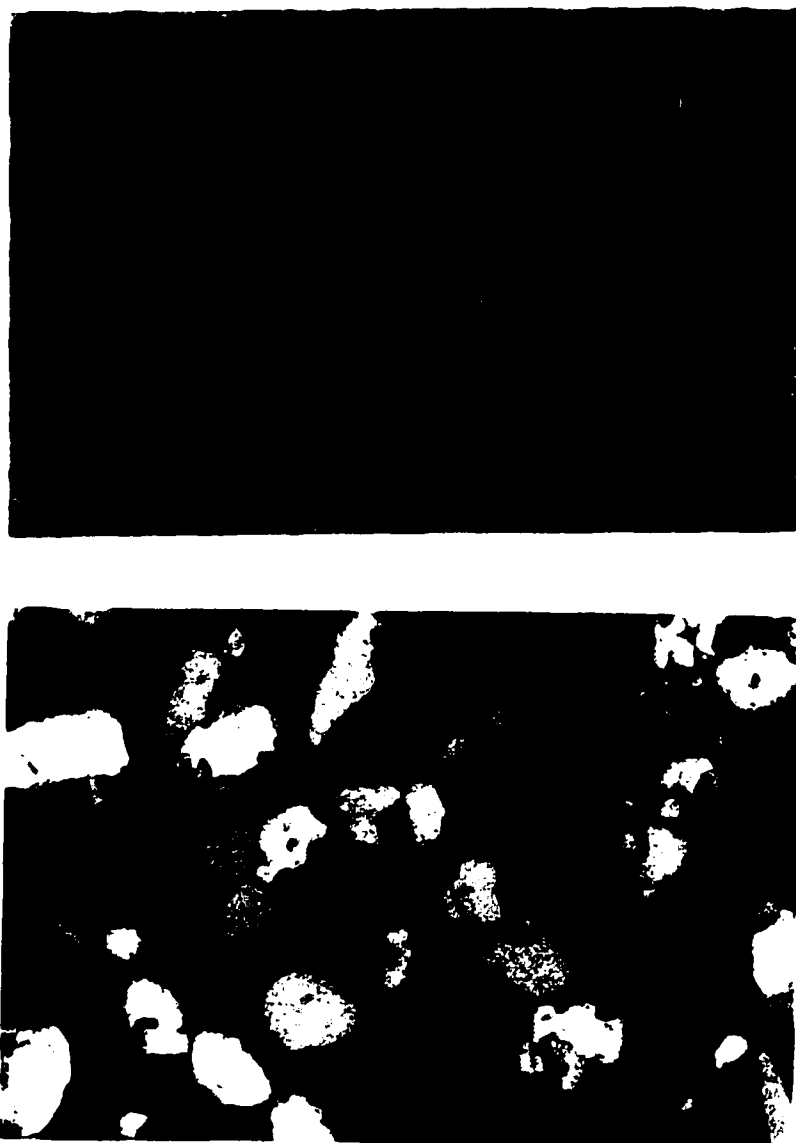


Figure A.13. Thin section photomicrograph, X10 under plane and cross-polarized light, for sample C4-T11.



Figure A.14. Thin section photomicrograph, X10 under plane and cross-polarized light, for sample C4-T7.

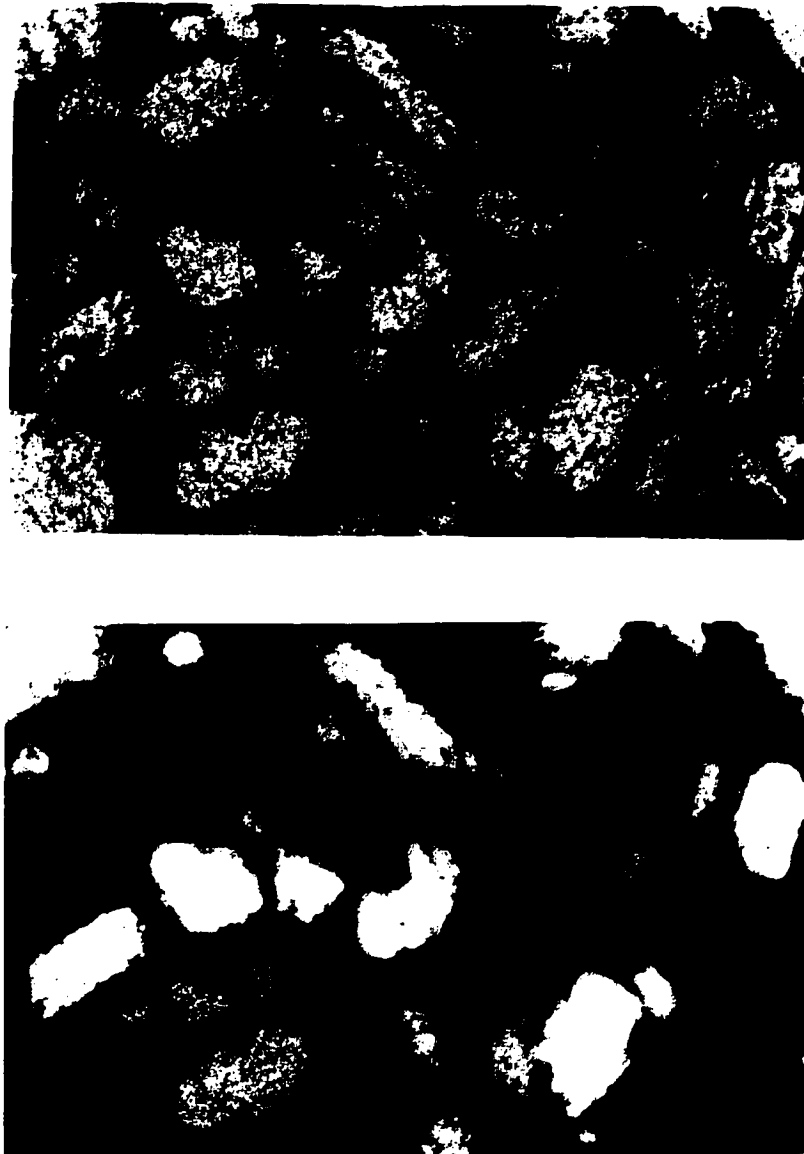


Figure A.15. Thin section photomicrograph, X10 under plane and cross-polarized light, for sample C4-T1.

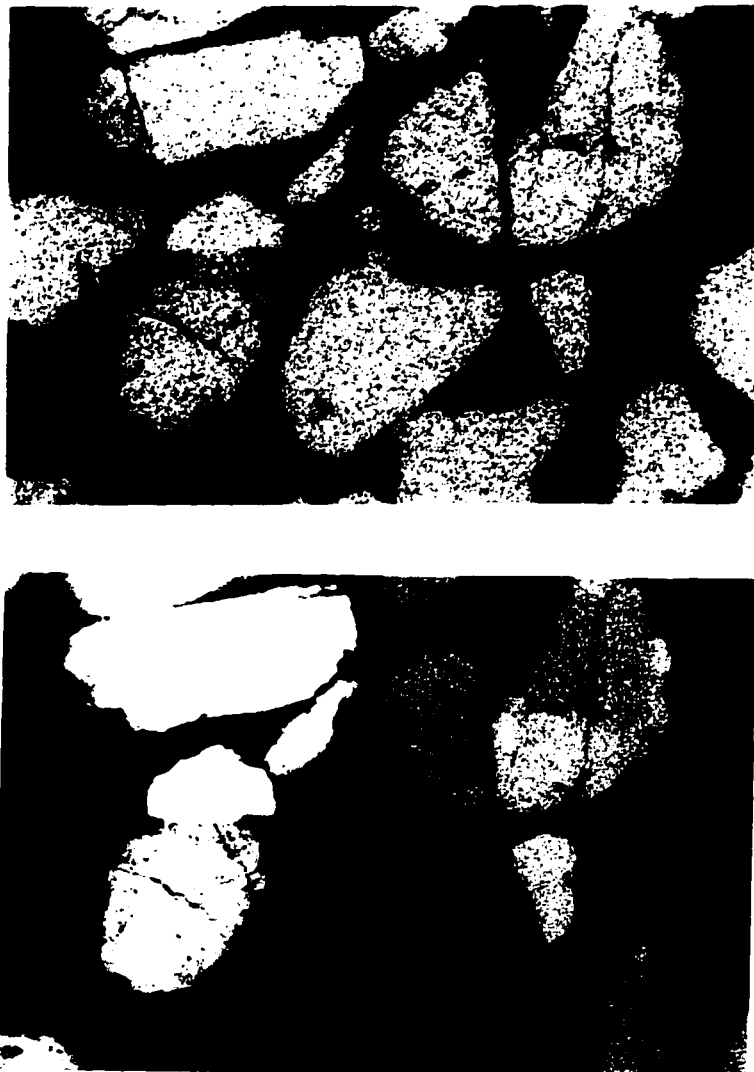


Figure A.16. Thin section photomicrograph, X10 under plane and cross-polarized light, for sample C5-T10.

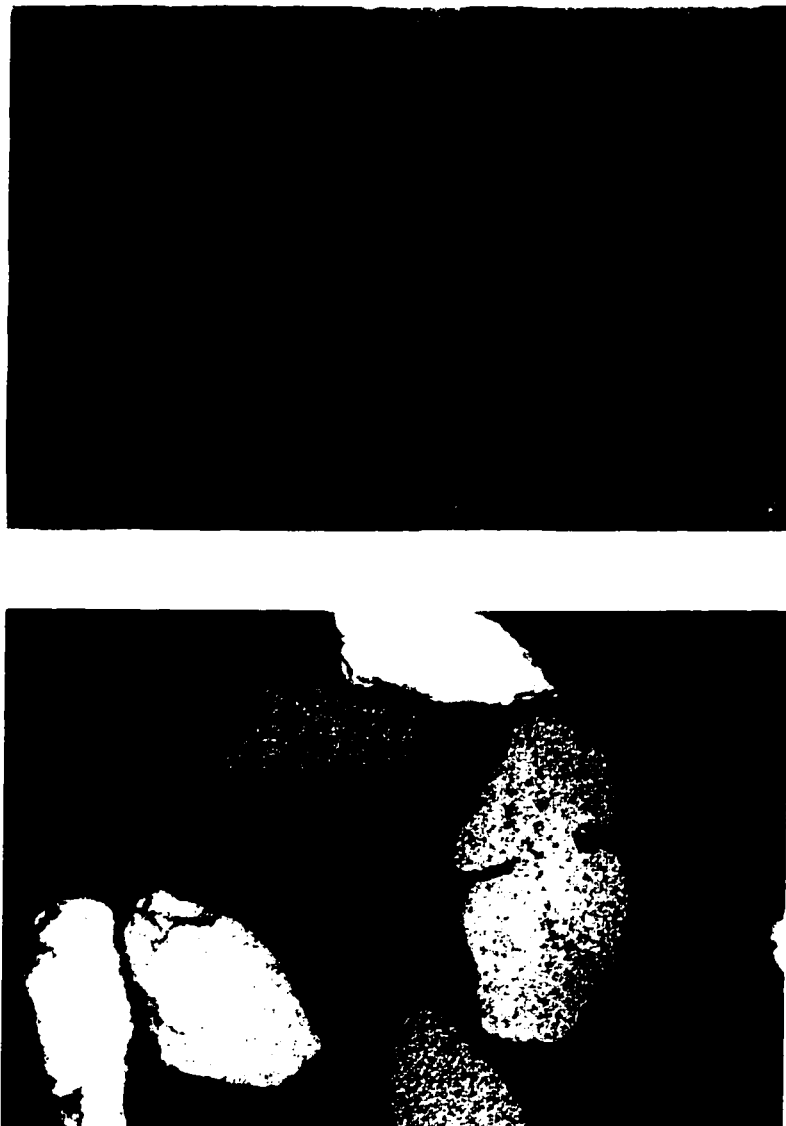


Figure A.17. Thin section photomicrograph, X10 under plane and cross-polarized light, for sample C5-T3.

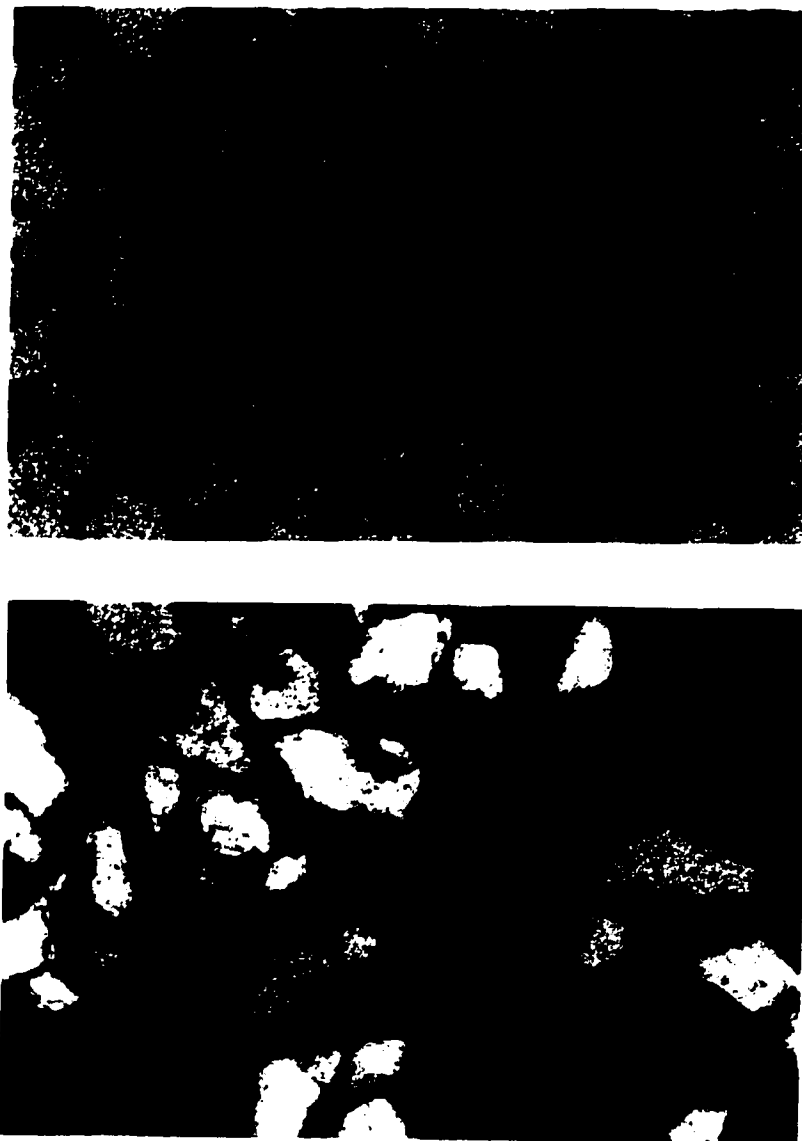


Figure A.18: Thin section photomicrograph, X10 under plane and cross-polarized light, for sample C6-T20.

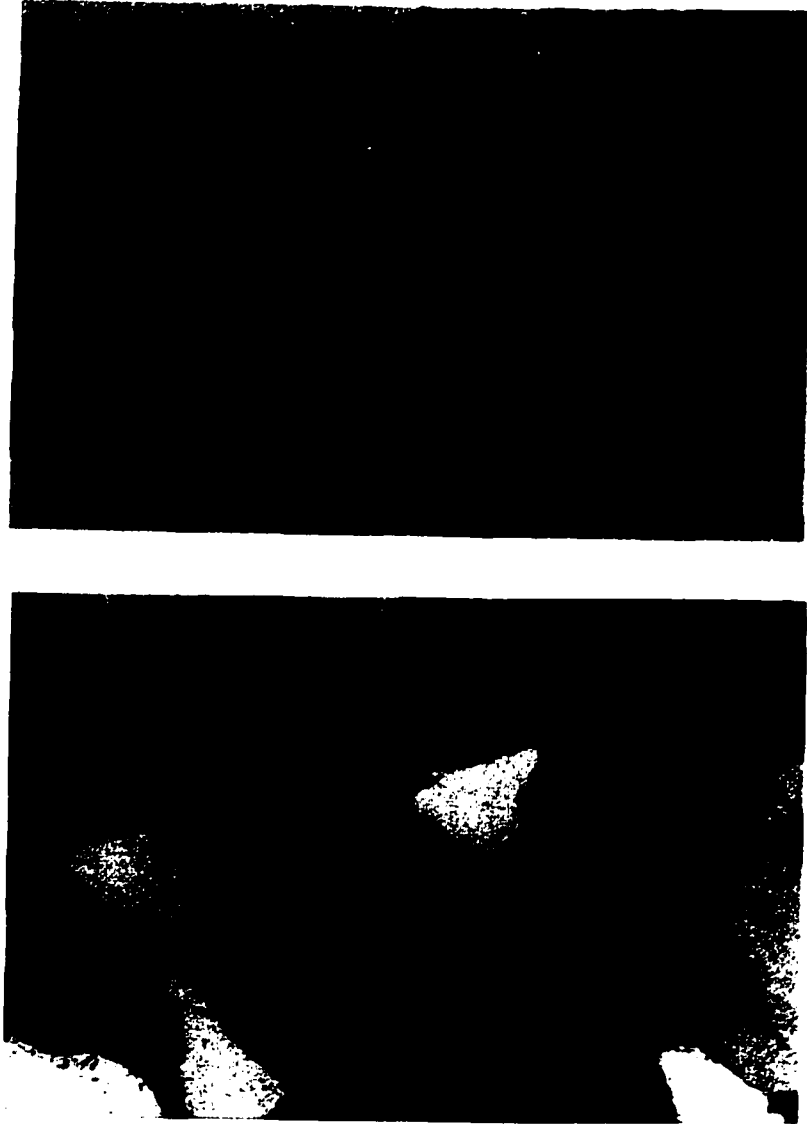


Figure A.19. Thin section photomicrograph, X10 under plane and cross-polarized light, for sample C6-T4.

APPENDIX B

**LITHOLOGICAL DESCRIPTION OF RESERVOIR
ROCK SAMPLES**

Sample	Description
C1-T20	Yellow, well sorted, subangular to subrounded, fine laminated shaly sandstone
C1-T17	Yellow, well sorted, subangular to subrounded, fine laminated shaly sandstone
C1-T13	Yellow, well sorted, subangular to subrounded, fine laminated shaly sandstone
C1-T6	Yellow, well sorted, subangular to subrounded, medium friable laminated shaly sandstone
C1-T3	Yellow, well sorted, subangular to subrounded, fine friable laminated shaly sandstone
C2-21	Yellow, well sorted, subangular to subrounded, fine laminated shaly sandstone
C2-T11	Yellow, moderately sorted, subangular to subrounded, fine to medium clean sandstone
C2-T8	Brown, moderately sorted, subangular to subrounded, very fine laminated shaly sandstone
C2-T1	Brown, poorly sorted, subangular to subrounded, very fine to fine shaly sandstone
C3-T23	Yellow, poorly sorted, subangular to subrounded, fine laminated shaly sandstone.
C3-T20	Yellow, poorly sorted, subangular to subrounded, very fine to fine sandstone
C3-T14	Yellow, well sorted, subangular to subrounded, very fine to fine shaly sandstone
C3-T4	Grey, poorly sorted, subangular to subrounded, very fine to fine laminated sandy shale
C4-T23	Yellow, poorly sorted, subangular to subrounded, fine sandstone
C4-T11	Yellow, moderately sorted, subangular to subrounded, very fine to fine laminated shaly sandstone
C4-T7	Yellow, moderately sorted, subangular to subrounded, very fine

	to fine laminated shaly sandstone
C4-T1	Yellow, poorly sorted, subangular to subrounded, fine to medium laminated shaly sandstone
C5-T10	Yellow, moderately sorted, subangular to subrounded, coarse sandstone
C5-T3	Yellow, moderately sorted, subangular to subrounded, coarse sandstone
C6-T20	Yellow, Poorly sorted, subangular to subrounded, medium to coarse to laminated shaly sandstone
C6-T4	Yellow, poorly sorted, subangular to subrounded, medium to coarse sandstone

NOMENCLATURE

static = Static elastic property

dynamic = Dynamic elastic property

α = Biot's constant

p = Pore pressure

σ = Stress

σ' = Effective stress

σ_p = Hydrostatic stress

σ_v = Vertical stress

σ_h = Maximum horizontal stress

σ_H = Minimum horizontal stress

ε = Strain

ε_v = Volumetric strain

δ = Kronecker delta

ν = Poisson's ratio

E = Young's modulus

E_d = Dynamic Young's modulus

ϕ = Phi size

S = Grain size in millimeters

M_d = Median

M_z = Mean

σ_1 = Sorting

Sk_1 = Skewness

K_G = Kurtosis

EDS = Energy dispersive x-ray

SEM = Scanning electron microscope

XRD = X-Ray Diffraction

ρ_b = Bulk density

V = Velocity

V_s = Velocity of propagation of a S-wave

V_p = Velocity of propagation of a P-wave

G = Shear modulus

K = Bulk modulus

K_d = Dynamic bulk modulus

Δt_s and Δt_c = S-wave and P-wave travel times, respectively

λ = Wavelength

f = Frequency

S = stand-off

β = ratio of mud velocity to formation velocity

D = Depth of alteration

K_s = adiabatic bulk modulus

K_T = isothermal bulk modulus

τ = Coefficient of thermal expansion (K^{-1})

T = Temperature (K)

Q = Specific volume ($m^3 kg^{-1}$)

C_p = Specific heat at constant pressure ($J kg^{-1} K^{-1}$)

α = Biot's constant

K_b = Bulk (grains and pores) compressibility

K_{ma} = Matrix compressibility

FORMEL = FORMation MEchanical Logging

REFERENCES

- Ahmed, U., M.E. Markley, and S.F. Crary.** 1991. *Enhanced in-situ stress profiling with microfracture, core and sonic logging data.* SPE 19004, SPE Formation Evaluation, June 1991. pp. 243-251.
- Al-Ghamdi, A.H., R.M. Al-Zayer, I.A. Al-Samin, and A.A. Al-Gattan.** 2001. *Interpretational complexities and operation complication affecting pressure transient analysis in Zuluf field, Saudi Arabia.* SPE 71576 paper presented at SPE Annual Technical Conference and Exhibition held in New Orleans, 30 September-3 October 2001.
- Aleksandrowski, P., O.H. Inderhaug, and B. Knapstad.** 1992. *Tectonic structures and wellbore breakout orientation.* Proceedings of the 33rd U. S. Symposium on Rock Mechanics, Santa Re, New Mexico, U.S.A.
- Al-Fares, A., M. Bauman, and P. Jeans.** 1998. *A new look at the Middle to Lower Cretaceous stratigraphy, offshore Kuwait.* GeoArabia. v. 3. no. 4. pp. 543-560.
- Al-Qahtani, M.Y., and Z. Rahim.** 2001. *A mathematical algorithm for modeling geomechanical rock properties of the Khuff and pre-Khuff reservoirs in Ghawar field.* SPE 68194 paper presented at the 2001 SPE Middle East Oil Show held in Bahrain, 17-20 March 2001.
- Al-Sabti, H.M.** 1991. *Lithology determination of clastic reservoir facies from well logs, Saudi Arabia.* SPE 214557 paper presented at the SPE Middle East Oil Show held in Bahrain, 16-19 November 1991.
- Alsharhan, A.S., and A.E.M. Nairn.** 1986. *A Review of the Cretaceous Formations in the Arabian Peninsula and Gulf: Part I. Lower Cretaceous (Thamama Group) stratigraphy and paleogeography.* Journal of Petroleum Geology. v. 9. pp. 365 – 392.
- Avasthi, J.M., H.E. Goodman, and R.P. Jansson.** 2000. *Acquisition, calibration and use of the in situ stress data for oil and gas well construction and production.* SPE 60320 paper presented at the SPE Rocky Mountain Regional Meeting/Low permeability reservoirs symposium, Denver, Colorado, 12-15 March 2000.
- Awal, M.R.** 2002. *In-situ stresses. Rock mechanics for petroleum engineers.* Short course notes. King Fahd University of Petroleum and Minerals.
- Azeemuddin, M., Jr. T.E. Scott, M.M. Zaman, and J.C. Roegiers.** 2001. *Stress-dependent Biot's constant through dynamic measurements on Ekofisk Chalk.* In Elsworth, Tinucci and Heasley (eds). Proc. 38th U.S. Rock Mechanics Symposium, in Rock Mechanics in the National Interest. The Netherlands.

- Banthia, B.S., M.S. King, and I. Fatt.** 1965. *Ultrasonic shear-wave velocities in rocks subjected to simulated overburden pressure and internal pore pressure.* Geophysics. pp. 117-121.
- Basu, A., S.W. Young, L.J. Suttner, W.C. James, and G.H. Mack.** 1975. *Reevaluation of the use of undulatory extinction and polycrystallinity in detrital quartz for provenance interpretation.* Journal of Sedimentary Petrology. v. 45. pp. 873-882.
- Bell, F.G.** 1978. *The physical and mechanical properties of the Fell Sandstone, Northumberland, England.* Engineering Geology. v. 12. pp. 1-29.
- Bell, F.G., and P. Lindsay.** 1999. *The petrographic and geomechanical properties of some sandstones from Newspaper Member of the Natal Group near Durban, South Africa.* Engineering Geology. v. 53. pp. 57-81.
- Bell, J.S., and E.A. Babcock.** 1986. *The stress regime of the Western Canadian Basins and implications for hydrocarbon production.* Bulletin of Canadian Petroleum Geology. v. 34. pp. 364-378.
- Bell, J.S.** 1990. *Investigation stress regimes in sedimentary basins using information from oil industry wireline logs and drilling records.* In Hurst, Lovell, and Morton (eds). Geological applications of wireline logs. Geological Society Special Publication No. 48. pp. 305-325.
- Biot, M.A., and D.G. Willis.** 1957. *The elastic theory of consolidation.* Journal of Applied Mechanics. v. 24. pp. 594-601.
- Bjorlykke, K.** 2001. *Mechanical and chemical compaction of sand and sandstones: Implication for reservoir quality and compressibility.* Abstract posted on www.gfz-potsdam.de.
- Blanton, T.L., and J.E. Olson.** 1997. *Stress magnitudes from logs: effects of tectonic Strains and temperature.* SPE 38719 paper presented at the 1997 SPE Annual Technical Conference and Exhibition, San Antonio, Texas, 5-8 October 1997.
- Blatt, H., G.V. Middleton, and R. Murray.** 1980. *Original of sedimentary rocks.* Second Edition. Prentice Hall. 782 p.
- Boggs, S.J.** 1995. *Principles of sedimentology and stratigraphy.* Prentice Hall. 773 p.
- Brace, W.F.** 1961. *Dependence of fracture strength of rocks on grain size.* Proceedings of Fourth Symposium on Rock Mechanics. Pennsylvania State University.
- Brown, L.F., and W.L. Fisher.** 1977. *Seismic stratigraphic interpretation of depositional systems: examples from Brazil rift and pull-apart basins.* In Payton

- (ed.). *Seismic Stratigraphy Applications to Hydrocarbon Exploration*. AAPG memoir 26. pp. 213-248.
- Brumley, J., R. Kuhlman, H. Abbas, C. Christiansen, and L. Nydahl.** 1994. *In-situ stress field determination and formation characterization-Offshore Qatar case history*. Proceedings of Rock Mechanics in Petroleum Engineering. pp. 905-919.
- Carroll, M.M.** 1979. *An effective stress law for anisotropic elastic deformation*. Journal of Geophysical Research. v. 84. pp. 7510-7512.
- Chatterjee, R., and M. Mukhopadhyay.** 2001. *Petrophysical and geomechanical properties of rocks from the oilfields of the Krishna-Godvari and Cauvery basins, India*. Bulletin of Engineering Geology and Environment. v. 61. pp. 169-178.
- Cheng, A.H.D., Y. Abousleiman, and J.C. Roegiers** .1993. *Review of some poroelastic effects in rock mechanics*. International Journal of Rock Mechanics, Mineral Sciences and Geomechanical Abstracts. v. 30. no. 7. p. 1119-1126.
- Cipolla, C.L., D. Liu, and D.G. Kyte.** 1994. *Practical application of in-situ stress profiles*. SPE 28607 paper presented at the 69th SPE Annual Technical Conference and Exhibition held in New Orleans, USA.
- Cooper, M.R.** 1977. *Eustatic during the Cretaceous: Its applications and importance*. Paleogeog., Paleoclimatol., Paleoecol. v. 22. pp. 1-60.
- Christian, L.** 1997. *Cretaceous subsurface geology of the Middle East region*. GeoArabia. v. 2. no. 2. p. 239-256.
- Davies, R.B, D.M. Casey, A.D. Horbury, P.R. Sharland, and M.D. Simmons.** 2002. *Early to mid-Cretaceous mixed carbonate-clastic shelfal systems: example, issues, and models from the Arabian Plate*. GeoArabia. v. 7. no.3. pp. 541-598.
- Donath, F.A., and L.S. Fruth.** 1971. *Dependence of strain-rate effects on deformational mechanism and rock type*. Journal of Geology. v. 79. pp. 347-371.
- Dott, R.H.** 1960. *Wacke, greywacke, and matrix – what approach to immature sandstone classification*. Journal of Sedimentary Petrology. v. 34. pp. 625-632.
- Economides, M. J. and K.G. Nolte.** 2000. *Reservoir Stimulation*. Third edition. John Wiley and Sons. 640 p.
- Edgell, H.S.** 1992. *Basement tectonics of Saudi Arabia as related to oil field structures*. In: Rickard et al. (eds.), *Basement Tectonics 9*. Kluwer Academic Publisher. Dordrecht. pp. 169-193.

- Edlmann, K., J.M. Somerville, B.G.D. Smart, S.A. Hamilton, and B.R. Crawford** .1998. *Predicting rock mechanical properties from wireline porosities*. SPE 47344 paper presented at the SPE/ISRM Eurock '98, Trondheim, Norway.
- Eissa, E.A., and A. Kazi.** 1988. *Relation between static and dynamic Young's modulus of rocks*. International Journal of Rock Mechanics, Mineral Sciences and Geomechanical Abstracts. v. 25. no. 6. pp. 479-482.
- Enstminger, L.D.** 1981. *Sedimentary response to tectonic and eustatic changes: An example from the Mid-Cretaceous Wasia Formation, Saudi Arabia*. SPE 9592 paper presented in at the Middle East Oil Technical Conference of the SPE held in Bahrain, 9-12 March 1981.
- Fabre, D., and J. Gustkiewicz.** 1997. *Poroelastic properties of limestones and sandstones under hydrostatic conditions*. Technical Note. International Journal of Rock Mechanics, Mineral Sciences and Geomechanical Abstracts. v. 34. no. 1. pp. 127-134.
- Fahy, M.P., and M.J. Guccione.** 1979. *Estimating strength of coal measure sandstone using petrographic thin section data*. Bulletin of Association of Engineering Geologist. v. 16. pp. 467-486.
- Farquhar, R.A., J.M. Somerville, and B.G.D. Smart.** 1994. *Porosity as mechanical indicator: an application of core and log data and rock mechanics*. SPE 28853 paper presented at the European Petroleum Conference, London, U.K. 25-27 October 1994.
- Fjaer, E., R.M. Holt, P. Horsrud, A.M. Raaen, and R. Risnes.** 1992. *Petroleum related rock mechanics*. Elsevier. 338 p.
- Folk, R.L.** 1974. *Petrology of sedimentary rocks*. Hemphill's Book Store, 182 p.
- Franquet, J.A., and H.H. Abass.** 1999. *Experimental evaluation of Biot's poroelastic parameter – three different methods*. In Amadei et al. (eds.). Rock Mechanics for Industry. Rotterdam. pp. 349-355.
- Friedman, G.M.** 1961. *Distinction between dune, beach, and river sands from their textural characteristics*. Journal of Sedimentary Petrology. v. 37. pp. 514-529.
- Gattens, J.M., C.W. Harrison, D.E. Lancaster, and F.K. Guidry.** 1990. *In-situ stress tests and acoustic logs determine mechanical properties and stress profiles in the Devonian Shales*. SPE Formation Evaluation, September 1990. pp. 248-254.
- Geertsma, J.** 1957. *The effect of fluid pressure decline on volumetric changes of porous rock*. Trans., AIME. pp. 331-339.

- Glover, P.** 2002. *The acoustic log*. Petrophysics MSc Course Notes. University of Aberdeen.
- Grant, C.W. and F.A. Al-Humam.** 1994. *Integrating geologic data into geostatistical modeling: An example from the Khaffi reservoir, northern offshore area, Saudi Arabia*. In Al-Husseini (ed.). The Middle East Petroleum Geosciences GEO '94. v. II. pp. 433-446.
- Haq, B.U., J. Hardenbol, and P.R. Vail.** 1988. *Mesozoic and Cenozoic chronostratigraphy and cycles of sea level changes*. In Wilugs et al. (eds). *Sea level changes: an integrated approach*. Society of Economic and Paleontologists and Mineralogists Special Publication 42. pp. 71-108.
- Hatcher, R.D.** 1990. *Structural geology*. Merrill Publishing Company. 531 p.
- Hoshino, K, H. Koide, K. Inami, S. Iwamura, and S. Mitsui.** 1972. *Mechanical properties of Japanese Tertiary sedimentary rocks under high confining pressure*. Geological Survey of Japan. 200 p.
- Johnson, P.R.** 1998. *Tectonic map of Saudi Arabia and adjacent areas*. Ministry of Petroleum and Mineral Resources, Deputy Ministry for Mineral Resources. Technical report.
- Jorgensen, L.N., A.A. Brown, and G.E. Redekop.** 1994. *Stress field orientation and fault trends offshore Qatar*. In Al-Husseini (ed.). The Middle East Petroleum Geosciences GEO '94. v. II. pp. 561-570.
- King, M.S.** 1969. *Static and dynamic elastic moduli of rocks under pressure*. In Somerton, W.H.(ed). *Rock Mechanics – Theory and Practice*. University of California, Berkeley. pp. 329-351.
- Klimentos, T., A. Harouka, B. Mtawaa, and S. Saner.** 1998. *Experimental determination of the Biot's elastic constant: Applications in formation evaluation (Sonic Porosity, Rock strength, Earth Stresses, and Sanding Predictions)*. SPE Reservoir Evaluation and Engineering, pp. 57-63.
- Klovan, J.E.** 1966. *The use of factor analysis in determining depositional environments from grain size distributions*. *Journal of Sedimentary Petrology*. v. 36. pp. 115-125.
- Kokesh, F.P., and R.B. Blizard.** 1959. *Geometrical factor in sonic logging*. *Geophysics*. v. 24. no. 1. pp. 64-76.
- Kokesh, F.P., R.J. Schwartz, W.B. Wall, and R.L. Morris.** 1965. *A new approach to sonic logging and other acoustic measurements*. *Journal of Petroleum Technology*. pp. 282-286.

- Krief, M., J. Garat, J. Stellingwerff, and J. Ventre.** 1990. *A petrophysical interpretation using the velocities of P and S waves (Full-Wave Form Sonic)*. In Wang and Nur (eds). *Seismic and Acoustic Velocities in Reservoir Rocks*. Geophysical Reprint Series no. 19. pp. 384-401.
- Krumbein, W.C.** 1934. *Size frequency distribution of sediments*. *Journal of Sedimentary Petrology*. v. 4. pp. 65-77.
- Larsen, I., E. Fjaer, and L. Renlie.** 2000. *Static and dynamic Poisson's ratio of weak sandstone*. In Liebman et al. (eds). *Pacific Rocks 2000*. pp. 77-82.
- Lo, T.W., K.B. Coyner, and M.N. Toksoz.** 1986. *Experimental determination of elastic anisotropy of Berea Sandstone, Chicope Shale, and Chelmsford Granite*. *Geophysics*. v. 51. no. 1. pp. 164-171.
- Manificat, G., and Y. Gueguen.** 1998. *What does control V_p/V_s in granular rocks?* *Geophysical Research Letter*. v. 25. pp. 381-384.
- Marion, D., and D. Jizba.** 1992. *Acoustic properties and their dependence on porosity, mineralogy, and saturation: Application to field-scale measurements*. *Advances in Core Evaluation III -Reservoir Management*. pp. 43-61.
- Marzouk, I.M., and M.A. Sattar.** 1993. *Indications of wrench tectonics on hydrocarbon reservoirs*. SPE 25608 paper presented at the SPE Middle East Oil Technical Conference and Exhibition held in Bahrain, 3-6 April 1993.
- McLaren, P.** 1981. *An interpretation of trends in grain size measures*. *Journal of Sedimentary Petrology*. v. 51. pp. 611-624.
- Meehan, D.N.** 1994. *Rock mechanics issues in petroleum engineering*. In Nelson and Laubach (eds.) *Rock Mechanics*. Balkema. pp. 3-17.
- Mitchum, R.M.** 1977. *Seismic stratigraphy and global changes of sea level, Part 1: Glossary of terms used in seismic stratigraphy*. In Payton (ed.). *Seismic Stratigraphy Applications to Hydrocarbon Exploration*. AAPG Memoir 26. pp. 205-212.
- Moiola, R.J., and D. Weiser.** 1968. *Textural parameters: an evaluation*. *Journal of Sedimentary Petrology*. v. 38. pp. 45-53.
- Montmayeur, H., and R.M. Graves.** 1985. *Prediction of static elastic/mechanical properties of consolidated and unconsolidated sands from acoustic measurements*. SPE 14159 paper presented at the 60th Annual Technical Conference and Exhibition of the SPE held in Las Vegas, 22-25 September 1985.
- Moshrif, M.A.** 1978. *Stratigraphy, sedimentation, and paleoenvironments of Middle Cretaceous rocks of central Saudi Arabia (abstract)*. *AAPG Bulletin*. v. 62. pp. 546-547.

- Moshrif, M.A.** 1980. *Recognition of fluvial environments in Biyadh-Wasia sandstones (Lower-Middle Cretaceous) central Saudi Arabia as revealed by textural analysis.* Journal of Sedimentary Petrology. v. 50. pp. 603 – 612.
- Moshrif, M.A., and G. Kelling.** 1984. *Stratigraphy and sedimentary history of Upper-Lower and Middle Cretaceous rocks, central Saudi Arabia.* Saudi Arabian Deputy Ministry for Mineral Resources, Jiddah, Mineral Resources Bulletin 28. 28 p.
- Morris, R.J.** 1980. *Middle east: stratigraphic evolution and oil habitat.* AAPG. v. 64. no. 5. pp. 597-618.
- Nur, A., and J.D. Byerlee.** 1971. *An exact effective stress law for deformation of rock with fluids.* Journal of Geophysical Research. v. 76. p. 6414-6419.
- Onaisi, A. J. Locane, and R. Razimbaud.** 2000. *Stress-related wellbore instability problems in deep wells in ABK field.* ADIPEC-0936. ADIPEC-0936 paper presented at the 9th Abu Dhabi International Petroleum Exhibition and Conference, Abu Dhabi, UAE, 15-18 October 2000.
- Page, J.H., P. Sheng, H.P. Schriemer, I. Jones, X. Jing, and D.A. Weitz.** 1996. *Group velocity in strongly scattering media.* Science. v. 271. pp. 634-637.
- Perkins, T.K., and J.A. Gonzalez.** 1984. *Changes in earth stresses around a wellbore caused by radially symmetrical pressure and temperature gradients.* SPE 10080. SPE Journal. pp. 129-140.
- Plat, H.** 1992. *Sedimentary petrology.* Freeman and Company. 514 p.
- Plumb, R.A., S.L. Herron, and M.P. Olsen.** 1992. *Influence of composition and texture on compressive strength variations in the Travis Peak Formation.* SPE 24758 paper presented at the 67th Annual Technical Conference and Exhibition of the SPE held in Washington, 4-7 October 1992.
- Plumb, R.A.** 1994. *Influence of composition and texture on the failure properties of clastic rocks.* Proceedings of Rock Mechanics in Petroleum Engineering. Balkema. pp. 13-20.
- Powers, R.W., L.F. Ramirez, C.D. Redmond, and E.L. Elberg.** 1966. *Sedimentary Geology of Saudi Arabia.* USGS Professional Paper, 560-D. 147 p.
- Powers, R.W.** 1968. *Lexique Stratigraphique Internationale.* Asie, III, Fasc. 10 b 1. Arabie Saudite, Centre National de La Recherche Scientifique, Paris. 147 p.
- Prats, M.** 1981. *Effect of burial history on the subsurface horizontal stresses of formations having different material properties.* SPE 9017. SPE Journal. v. 21. no. 6. pp. 658-662.

- Prensky, S.** 1992. *Borehole breakouts and in-situ stress... a review*. The Log Analyst. v. 33. no. 3. pp. 304-312.
- Raaen, A.M., K.A. Hovem, H. Joranson, and E. Fjaer.** 1996. *FORMEL: A step forward in strength logging*. SPE 36533 paper presented at the SPE Annual Technical Conference and Exhibition, Denver, 1996.
- Rahim, Z., and M. Y. Al-Qahtani.** 2001. *Sensitivity study on geomechanical properties to determine their impact on fracture dimensions and gas production in the Khuff and Pre-Khuff formations using a layered reservoir system approach, Ghawar reservoir, Saudi Arabia*. SPE 72142 paper presented at the SPE Asia Pacific Improved Oil Recovery Conference held in Kuala Lumpur, Malaysia, 8-9 October 2001.
- Rider, M.H.** 1986. *The geological interpretation of well logs*. Balckie Halsted Press. 175 p.
- Reineck, H.E., and I.B. Singh.** 1980. *Depositional sedimentary environments*. Springer-Verlag. 549 p.
- Salamy, S.P., and T. Finkbeiner.** 2000. *A poroelastic analysis to address the impact of depletion rate on wellbore stability in openhole horizontal completion*. ADIPEC 10-86 paper presented at the 10th Abu Dhabi International Petroleum Exhibition and Conference held in Abu Dhabi , UAE, 13-16 October 2002.
- Santarelli, F.J.** 1994. *Rock mechanics characterization of deep formations: A technico-economical overview*. Proceedings of Rock Mechanics in Petroleum Engineering. Balkema. pp. 3-12.
- Sarda, J.P., N. Kessler, E. Wiequart, K. Hannaford, and J.P. Deflandre.** 1993. *Use of porosity as strength indicator for sand production evaluation*. SPE 26454 paper presented at the 68th Annual Technical Conference and Exhibition of the SPE held in Huston, Texas, 3-6 October 1993.
- Schlumberger.** 1991. *Log interpretation principles/applications*. Schlumberger Educational Services. 13-19 p.
- Senalp, M., S. Al-Akeel, and F. Jones.** 1988. *Khaffi reservoir multi-layer geologic and GEOSET modeling, Marjan area, volume 1, geologic model*. In-house report for Aramco Geological Department Exploitation Division. Field and Reservoir Study Report Number 119.
- Serra, O.** 1984. *Fundamentals of well-log interpretation*. Elsevier, Amsterdam. 423 p.
- Shakoor, A., and R.E. Bonelli.** 1991. *Relationship between petrographic characteristics, engineering index properties, and mechanical properties of selected sandstones*. Bulletin of Association of Engineering Geologist. v. 28. pp. 55-71.

- Sharief, F.A., K. Magara, and H.M. Abdullah.** 1989. *Depositional system and reservoir potential of the Middle Cretaceous Wasia Formation in the central – Eastern Arabia.* Journal of Marine and Petroleum Geology, v. 6, pp. 303–315.
- Siggins, A.F.** 1993. *Dynamic elastic tests for rock engineering.* In Hudson et al. (eds). Comprehensive Rock Engineering. Pergamon Press. UK.
- Steneike, M., R.A. Bramkamp, and N.J. Sander.** 1958. *Stratigraphic relations of Arabian Jurassic Oil.* AAPG Symposium, Tulsa, USA. pp. 1294 –1329.
- Suarez-Rivera, R.S., L. Nakagawa, and R. Myer.** 1997. *Determination of rock elastic properties from acoustic measurements of rock fragments.* International Journal of Rock Mechanics, Mineral Sciences and Geomechanical Abstracts. v. 34. pp. 3-4.
- Taylor, J.M.** 1950. *Pore-space reduction in sandstones.* AAPG. v. 34. pp. 701-716.
- Temeng, K.O., M.O. Al-Amoudi, and O. Chardac.** 1999. *Magnitude and Orientation of In-situ Stresses in the Ghawar Khuff Reservoirs.* SPE 56511 paper presented at the 1999 SPE Annual Technical Conference and Exhibition, Houston, 3-6 October 1999.
- TerraTek.** 2001. *The difference between static and dynamic mechanical properties.* Assay posted in www.terratek.com/geomech/gm_acoys.htm.
- Thiercelin, M.J., and R.A. Plumb.** 1991. *A core based prediction of lithologic stress contrasts in east Texas formations.* SPE 21847 paper presented at the Rocky Mountain Regional Meeting and Low-Permeability Reservoirs Symposium, Denver, 15-17 April 1991.
- Thurber, C.H.** 1957. *Velocity survey aid in seismic interpretation.* World Oil. v. 146. pp. 78-82.
- Tokle, K., P. Horsrud, and R.K. Bratli.** 1986. *Predicting uniaxial compressive strength from log parameters.* SPE 36533 paper presented at 61st Annual Technical Conference and Exhibition of the SPE held in New Orleans, 5-8 October 1986.
- Tutuncu, A.N., and M.M. Sharma.** 1992. *Relating static and ultrasonic laboratory measurements to acoustic log measurements in tight gas sands.* SPE 24689 paper presented at the 67th SPE Annual Technical Conference and Exhibition, Washington, U.S.A.
- Ulusay, R. K. Tureli, and M.H. Ider.** 1994. *Prediction of engineering properties of selected litharenite sandstone from its petrographical characteristics using correlation and multivariate statistical techniques.* Engineering Geology. v. 37. pp. 135-157.

- USC sequence stratigraphy web.** 2002. *The use of well logs to make sequence stratigraphic models of the subsurface.* <http://strata.geol.sc.edu/ss-well-log.html>.
- Van Eck, M.** 1985. *Sirhan-Turayf phosphate project. Lithostratigraphy of the Aruma Formation.* Saudi Arabian Deputy Ministry for Mineral Resources, Jeddah, Open File RF-OF-05-23. 26 p.
- Van Wagoner, J.C.** 1985. *Reservoir facies distribution as controlled by sea level changes.* Abstract, Society of Economic and Paleontologists and Mineralogists. Mid year meeting, Colorado. pp. 91-92.
- Van Wagoner, J.C., H.W. Posamentier, R.M. Mitchum, P.R. Vail, J.F. Sarg, T.S. Loutit, and J. Hardenbol.** 1988. *An overview of sequence stratigraphy and key definitions.* In Wilgus et al. (eds). *Sea Level Changes: An Integrated Approach.* Society of Economic and Paleontologists and Mineralogists Special Publication 42. pp. 39-45.
- Van Wagoner, J.C., R.M. Mitchum, K.M. Campion, and V.D. Rahmanian.** 1990. *Siliciclastic sequence stratigraphy in well logs, cores, and outcrops.* AAPG methods in exploration series No 7. 55 p.
- Vaslet, D., C. Pellaton, J. Manivit, Y. M. Le Nindre, J. M. Brosse, and J. Fourguet.** 1985. *Geologic map of Al Sulaiyyimah quadrangle, sheet 21H, Kingdom of Saudi Arabia (with text).* Saudi Arabian Deputy Ministry for Mineral Resources, Jeddah. Geoscience Map GM – 100A.
- Visher, G.S.** 1965. *Use of vertical profile in environmental reconstruction.* AAPG. v. 49. pp. 41-61.
- Wallace, C.A., S.M. Dini, and A.A. Farassani.** 1997. *Geologic map of Al Jawf quadrangle (sheet 29D), Kingdom of Saudi Arabia.* Saudi Arabian Deputy Ministry of Mineral Resources. Geologic Map GM-128, Scale 1:250,000.
- Wang, Z.** 2000. *Dynamic versus static elastic properties of reservoir rocks.* In Wang and Nur (eds). *Seismic and Acoustic Velocities in Reservoir Rocks.* Geophysical Reprint Series. pp.531- 539.
- Walsh, J.B.** 1965. *The effect of cracks on the compressibility of rocks.* Journal of Geophysical Research. v. 70. pp. 381-389.
- Warpinski, N.R.** 1992. *Rock mechanics issues in completion and stimulation operations.* In Tillerson and Wawersik (eds). *Rock Mechanics.* Balkema. pp. 375-386.
- Warpinski, N.R., P. Branagan, and R. Wilmer.** 1985. *In-situ stress measurements at U.S./DOE's multiwell experiment site, Mesaverde Group, Rifle, Colorado.* HPT. v. 37. pp. 110-132.

- Warpinski, N.R., and L.W. Teufel.** 1992. *Determination of the effective stress law for permeability and deformation in low permeability rocks.* SPE 20572. SPE Formation Evaluation. pp. 123-131.
- Warpinski, N.R., R.E. Peterson, P.T. Branagan, B.P. Engler, and S.L. Wolhart.** 1998. *In-situ stress and moduli: Comparison of values derived from multiple techniques.* SPE 49190 paper presented at the SPE Annual Technical Conference and Exhibition, New Orleans, 1998.
- Whitehead, W.S., E.R. Hunt, and S.A. Holditch.** 1987. *The effect of lithology and reservoir pressure on the in-situ stress in the Waskom (Travis Peak) field.* SPE 16403 paper presented at the SPE/DOE Low Permeability Reservoirs Symposium, Colorado, U.S.A.
- Woodland, D.C.** 1988. *Borehole instability in the Western Canadian overthrust belt.* SPE 17508 paper presented at the SPE Rocky Mountain Regional Meeting held in Casper WY, 11-13 May 1988.
- Yale, D.P., and W.H. Jamieson.** 1994. *Static and dynamic mechanical properties of carbonates.* Rock mechanics. Balkema. pp. 463-471.
- Ziegler, M.A.** 2001. *Late Permian to Holocene paleofacies evolution of the Arabian Plate and its Hydrocarbon occurrences.* GeoArabia. v.6 no.3. pp. 445-504.

VITAE

■ Mr. Waleed Mohamed El Hassan, earned B. Sc. (Honours) in Geology from University of Khartoum, Sudan.

■ He worked as a Teaching Assistant at the same university he graduated from.

■ He jointed Earth Sciences Department, King Fahd University of Petroleum and Minerals as a Research Assistant in February, 2000.